UNIVERSITÀ DEGLI STUDI DI PADOVA

Dipartimento di Fisica e Astronomia "Galileo Galilei"

Master Degree in Physics

Final Dissertation

The effect of Delayed Dynamics on the Stability of Ecosystems

Thesis supervisor

Prof. Samir Suweis

Thesis co-supervisor

Prof. Sandro Azaele

Candidate

Damiano Sgarbossa

Academic Year 2019/2020

Alla mia famiglia.

Abstract

Differential Equations and random matrix theory have found applications in many fields, ranging from physics, number theory and ecology. Fifty years ago, in a seminal article entitled "Will a Large Complex System be Stable?", Robert May showed that increasingly large or complex ecological networks have negligibly small probability to be stable. However, from field studies in ecology experimental evidences point on the opposite direction: large and complex ecosystems seem to be stable. This apparent contradiction is known as the Complexity-Stability paradox. May and other scientists analyzed large networks in which species interact at random and studied analytically the asymptotic stability of such systems as a function of the number of species and the number of interactions through the use of random matrix theory. This master thesis is aimed to critically review these results and show how the introduction of delay in ecosystem population dynamics may have a strong impact on ecosystem dynamics and change important aspects of the Complexity-Stability paradox.

Contents

INTRODUCTION

The study of population dynamics and its application to describe the time evolution and the stability of ecosystems is experiencing an important growth in the last decades [18], [4]. The main reason for this increasing attention from the scientific community is clearly the global warming and the disruptive effects that the human activities have on nature. Indeed there is little doubt that Earth biodiversity is decreasing faster than the past centuries with a frightening ever-growing rate [2].
One of the principal goals of all these studies is to comprehend how natural ecosystems respond to the enormous stresses generated by human activities or by their indirect influence. This indeed causes considerable changes on the food webs and on the infra-species interactions, leading to high rates of extinctions and invasions [1]. Such relevant changes call for a quantitative study on how the diversity (also called complexity) and the structure of the ecosystems are related to their stability, defined as the ability of the system to recover from small perturbations around its equilibrium point [14].

In this context, 50 years ago, Robert May published his famous article entitled: "Will a Large Complex System be Stable?" [13]. There he showed that, modelling the ecosystem dynamics around a given equilibrium as a linear system where interactions among species are described by a random matrix, increasingly large or complex ecological communities have negligibly small probability to be (linearly) stable. This unexpected theoretical result raised many discussions as it points the opposite direction of many empirical evidences, which support the idea that large complex ecosystems are, generally, the most stable ones. This presumed contradiction is known as the Complexity-Stability paradox and gave rise to the Complexity-Stability debate [14].
As of today we still do not have an exhaustive explanation for such paradoxical relationship. However, in the last decades many ecologists proposed different studies suggesting that moving beyond the linear random matrix approach, also theoretically, in some cases, diversity is able to increase the stability of an ecosystem. Some of these possible explanations have been reviewed by McCann [14].

The purpose of this Thesis is to include a novel perspective on the Complexity-Stability debate: the effect of a time delayed dynamics on the mathematical description of the ecosystem. Indeed, until now, the relation between complexity and stability has been investigated only for systems described by simple Ordinary Differential equations. Here we will study how the Complexity-Stability relationship changes when the ecosystem is described by a Delayed Differential equation (DDE) with a fixed time-delay T. The DDEs which we will use in this work are simple ODEs with the substantial difference that the variation $\dot{x}(t)$ depends not only on the solution $x(t)$ at the same time but also on the solution $x(t-T)$ at a previous time [22].
First of all, we are going to analyze the effect of the insertion of delayed terms on simple one or few-species systems, like the Logistic equation and the Lotka-Volterra system. Then we will study how the delay changes the behavior of the solutions and the characteristics of the oscillations near the equilibrium. Furthermore we will present some useful techniques that can be implemented to characterize the chaotic region of the solutions and distinguish between normal and chaotic oscillations.
Next we are going to characterize the effect of the delay on complex multi-species ecosystems, with really large species interaction networks, which we describe by sampling the entrances from a probability distribution and using techniques of the Random Matrix Theory. We will show indeed how the stability, the distribution of eigenvalues and the scaling of the rightmost (real part) eigenvalue changes when the system also depends on a delayed term.
Finally we will show one of the possible explanations of the Complexity-Stability paradox through the application of such time delays.

CHAPTER 1

DISCRETE DYNAMICAL SYSTEMS

In this chapter, as a starting point for our discussion on the effect which delays have on the dynamics and stability of ecosystems, we will consider the classic models of one species population dynamics. Starting from these models we observe how the introduction of delayed terms on the equations of dynamics affects the behavior of their solutions. Finally we analyze the famous Lotka-Volterra system of equations for two species dynamics and we introduce in it some delayed terms to see how the stability of the solutions is modified.

1.1 Introduction to Population dynamics

The first evidences we have on the mathematical description of ecosystems and the time evolution of their population can be traced back to Leonardo Fibonacci which, long before the introduction of the concept of derivative, tried to model the growth of a colony of rabbits based on some idealized assumptions on their mating habits [21]. Supposing that the number of new individuals born in each generation is equal to the sum of the total population of the 2 previous generations, one obtains the well known Fibonacci sequence:

$$N_{t+2} = N_{t+1} + N_t \qquad \text{with:} \quad N_0 = 0,\ N_1 = 1.$$

A more rigorous study of population dynamics begun with the introduction of a single-species model for the description of demographic growth by Thomas Malthus [12]. Such model consisted in an ordinary differential equation of the form:

$$\dot{N}(t) = f(N, t) \qquad \text{with:} \quad N(t = 0) = N_0.$$

Supposing that $f(N)$ is a linear function of the population N, e.g. $f(N) = rN$ where r is called growth rate, he obtained the famous Exponential law of population growth.

Indeed in this case the solution of the equation is an exponential function (which is exactly the asymptotic behavior of the Fibonacci sequence in the limit $t \to \infty$).
However Malthus approach was fairly unrealistic for the description of single-species population dynamics. Indeed, even though it was able to describe exactly the population growth in the first generations, in real ecosystems the growth rate of the population must decrease at a certain point, because of multiple environmental reasons and resource constraints.
In 1838, Pierre-François Verhulst figured out that the only way to have a more realistic description of the time evolution of a species population, is to allow for the growth rate r to depend on the population (instead of being a constant) [25]. Indeed, he argued that the rate of reproduction must depend on the available resources which cannot be the same when the population of consumers increases. Therefore he supposed that the growth rate should decrease linearly with N proportionally to a parameter K which he called carrying capacity. He thus obtained a non-linear differential equation, which is the well known Logistic equation:

$$\dot{N}(t) \;=\; rN(t)\big[1 \;-\; N(t)\big] \qquad \text{the growth rate now is:} \quad r \longrightarrow r\big[1 - N(t)\big].$$

The solution can be computed analytically and it is the so called Logistic function:

$$N(t) = \frac{K}{1 + (K/N_0 - 1)e^{-rt}} \qquad \text{where} \quad \lim_{t\to\infty} N(t) = K. \tag{1.1}$$

The next straightforward improvement is the generalization of the population dynamics to multi-species ecosystems. This can be achieved through the introduction of first-order non-linear systems of coupled differential equations. Indeed the coupling between the time evolution equations of different populations is necessary to capture the interaction between different species in the ecosystem and obtain a more realistic description.
The first approach on this direction is the famous Lotka-Volterra predator-prey equations [10] which are able to describe the oscillatory time evolution of a 2-species ecosystem of predators and preys:

$$\begin{cases} \dot{x}(t) = \alpha x - \beta xy \\ \dot{y}(t) = \delta xy - \gamma y \end{cases} \qquad \text{where} \quad \alpha, \beta, \delta, \gamma > 0 \qquad \text{and} \quad \begin{cases} x = \text{preys} \\ y = \text{predators.} \end{cases}$$

This system can be further developed by inserting a larger number of species (and thus equations) obtaining the so called Generalized Lotka–Volterra equations:

$$\dot{\vec{X}} \;=\; diag\big[\vec{f}\,(\vec{X}, t)\big] \cdot \vec{X}(t) \qquad \text{with} \quad \vec{f} \;=\; \vec{r} \;+\; A\vec{X} \qquad A = \text{ Community matrix.}$$

Finally the Lotka-Volterra model can be extended further by adding functional responses and generalized growth rates obtaining the so called Rosenzweig–MacArthur model [11]. However we will not study this last model because it is far too complex for the aim of our work.

Instead, in this chapter we will study the effect of the delay on the discretized forms of the Logistic equation and the Lotka-Volterra equations. Our focus on the dynamical maps, instead of the continuous equations, can be easily explained by the fact that the first ones are a lot more straightforward to study numerically and in addition they maintain the same phenomenology and complexity of the continuous time models.
For instance the Logistic map presents a really complex phenomenology in terms of variability of the solutions, even more complex than its continuous analogous (which is always solved by a simple logistic function). Indeed its solutions are not only converging to the equilibrium, they can also display stable limit cycles with fixed periodicity or even chaotic cycles which are a-periodic.

1.2 Delayed Logistic equation

To begin our investigation on the effect of the delay on the description of ecosystems dynamics and stability, we start with from the logistic equation for the demographic growth of one species. As we explained in the previous section, this particular relation describes the time evolution of a single species in which the growth rate decreases when the population approaches the carrying capacity K.
Both the logistic equation without delay and with it have already been deeply studied in the literature: [8],[15],[16],[22]. Here, we are going to review the main results and techniques which are useful not only in these particular cases but also to tackle more complex and larger ecological systems.
The delayed Logistic equation in its adimensional form (i.e., $N/K \to N$) has the following formulation:

$$\dot{N}(t) \;=\; rN(t)\big[1 \;-\; N(t-T)\big], \tag{1.2}$$

where r is the growth rate, and T is the delay.

1.2.1 Analytical results

We start now by studying equation (1.2) from the analytical point of view, in particular our objective is to study the stability of the solutions and the bifurcation point, which demarcates the instability region. There are two main paths that we can choose to study the logistic equation: we can use the continuous time formalism (1.2) or we consider discrete time steps and we study the analogue, but discrete dynamical system given by (1.5). The techniques used on both cases in this section are explained with detail in chapters 1 & 2 of [15].

Stability and bifurcation of the continuous time Logisitic equation.

For the continuous time Logisitic equation given by (1.2), it is possible to characterize both the stability and the presence of bifurcations of the equilibria by making use of the Linear Stability Analysis as shown in [16].
First of all, we observe that the only non-trivial (N^*=0) equilibrium of (1.2) is $N^* = 1$

(here we set $K = 1$), therefore we can linearize the system near this equilibrium by changing the variable into $N = y + N^*$ and considering only the terms which are linear in y. We obtain then the linear equation:

$$\dot{y}(t) \;=\; -ry(t-T), \tag{1.3}$$

where r and T has been defined above. By hypothesizing a solution of the form $y = ve^{\lambda T}$ we apply the Linear Stability Analysis to the linearized equation obtaining the correspondent characteristic equation for the eigenvalue $\lambda = \mu + i\omega$:

$$\lambda = -re^{-\lambda T} \qquad \longrightarrow \qquad \begin{cases} R[\lambda] = \mu = -re^{-\mu T}\cos(\omega T) \\ I[\lambda] \;= \omega = \;\; re^{-\mu T}\sin(\omega T). \end{cases} \tag{1.4}$$

We can thus solve each of the two parts of Eq. (1.4), by using the following method. First we notice that both ω and $-\omega$ can be solutions of our system, so we can consider only the solutions with $\omega > 0$.
Then, to describe the stability we need to find all the solutions having the eigenvalue with negative real part. Therefore using the constraint $\mu < 0$ we get the condition:

$$\cos(\omega T) > 0 \qquad \rightarrow \qquad \omega T < \pi/2.$$

Here we are not interested on the periodicity of the conditions because we need the first and smallest value of T in which the equilibrium bifurcates. In addition, to find the bifurcating point we will consider the case $\mu = 0$ obtaining:

$$\begin{cases} \cos(\omega T) = 0 \\ \omega = \;\; re^{-\mu T}\sin(\omega T) \end{cases} \longrightarrow \begin{cases} T = \dfrac{\pi}{2r} \\ \omega = r \end{cases} \longrightarrow \quad T^* = \frac{\pi}{2r}.$$

Therefore we conclude that the equilibrium $N^* = 1$ is stable when the delay of the system is in the range $T \in [0, T^*)$, where T^* is the so called bifurcation point of the equilibrium.

Stability and bifurcation of the discrete time Logistic equation

By changing parameters and rewriting the time derivative using the Euler formulation: $\dot{a}(t) = (a_{n+1} - a_n)/dt$ we are able to transform the continuous time delayed logistic equation (1.2) into its discretized form, i.e. the Logistic (delayed) map:

$$\begin{cases} 1 + r\ dt \to r \\ T/dt \to T \end{cases} \qquad N^{(n+1)} \;=\; rN^{(n)}\Big[\; 1 \;-\; N^{(n-T)} \;\Big]. \tag{1.5}$$

As before, the non-null equilibrium can be found easily by taking $N^{(n+1)} = N^{(n)} = N^{(n-T)} = N^* = (r-1)/r$.
We are thus able to linearize the equation near the equilibrium by using the same change of variables of before, $N = y + N^*$, and, by taking only the terms which are

linear in y, we obtain the recursive equation:

$$y^{(n+1)} \; - \; y^{(n)} \; + \; (r-1)y^{(n-T)} \; = \; 0. \tag{1.6}$$

Next, by using the Linear Stability Analysis, we hypothesize solutions in the form $y^{(n)} = z^n$ where $z \in \mathbb{C}$, obtaining the characteristic equation (1.7). The solutions near the equilibrium N^* are stable only if they have absolute value less than 1. Indeed this constraint clearly implies that the solutions converge to zero in the limit $n \to \infty$:

$$z^{T+1} - z^T + (r-1) = 0 \qquad \text{with:} \qquad |z| < 1. \tag{1.7}$$

The analytical technique performed to solve this polynomial equation on the complex plane is explained with greater detail in section 1.3, where it is extensively used. In here, we avoid giving the details, also because in the following subsection we will present exclusively the numerical analysis.

1.2.2 Numerical results

We now want to explore the differences in the solutions between the generic Logistic map and the delayed Logistic map. Indeed, we aim at understanding what is the effect on the behavior of the solutions when adding a delayed term into the population dynamics. We will use here the discretized formulation (1.5) for the delayed case, which in the limit $T \to 0$ converges to the non-delayed.
In figure (1.1) we show the comparison between some solutions of the non-delayed and the delayed logistic map. It is clear that the delay has a strong influence on the dynamics of the population.

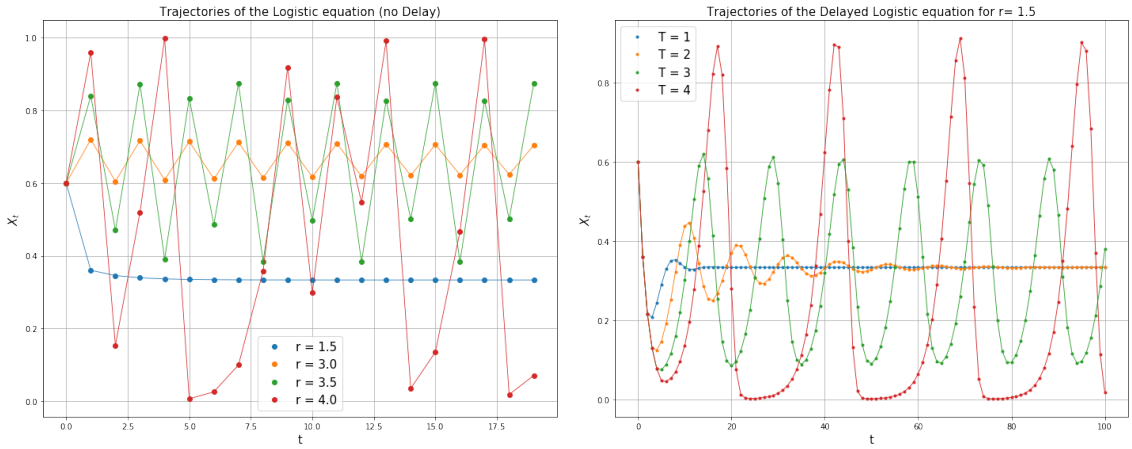

Figure 1.1: *Some examples of the trajectories of the two different Logistic maps. For the standard logistic map (which has no delayed term) we computed the solutions for different values of the parameter r (different colors). For the delayed Logistic map, instead, we have chosen a fixed value of r and computed the trajectories for different time delays T (corresponding to the different colors).*

The main difference between the two types of solutions is that the non-delayed ones display stable cycles of oscillations around the equilibrium , i.e. the population assumes only some fixed values with an integer periodicity, which depends on the

parameter r (at least below the chaotic threshold). On the other hand, the solutions of the delayed equation are not stable cycles anymore, because the values of the population are not periodically the same (as in a stable cycle), rather they slightly change each time. Nevertheless, also the delayed solution presents a periodic behavior with a non-integer periodicity. Therefore, the presence of the delayed term increases somehow the variability of the solutions generating more complex oscillations, which actually better describe the empirical time evolution of populations in ecosystems.

Furthermore, we can better appreciate the change that the insertion of the delay term incorporates into the variability of the solutions of the system, by observing the differences between the corresponding bifurcation diagrams.
In figure (1.2) we show the bifurcation plot of the non-delayed Logistic map: this is the famous bifurcation diagram obtained by Feigenbaum [6] and we can observe how the behavior of the solutions changes when the parameter r increases.

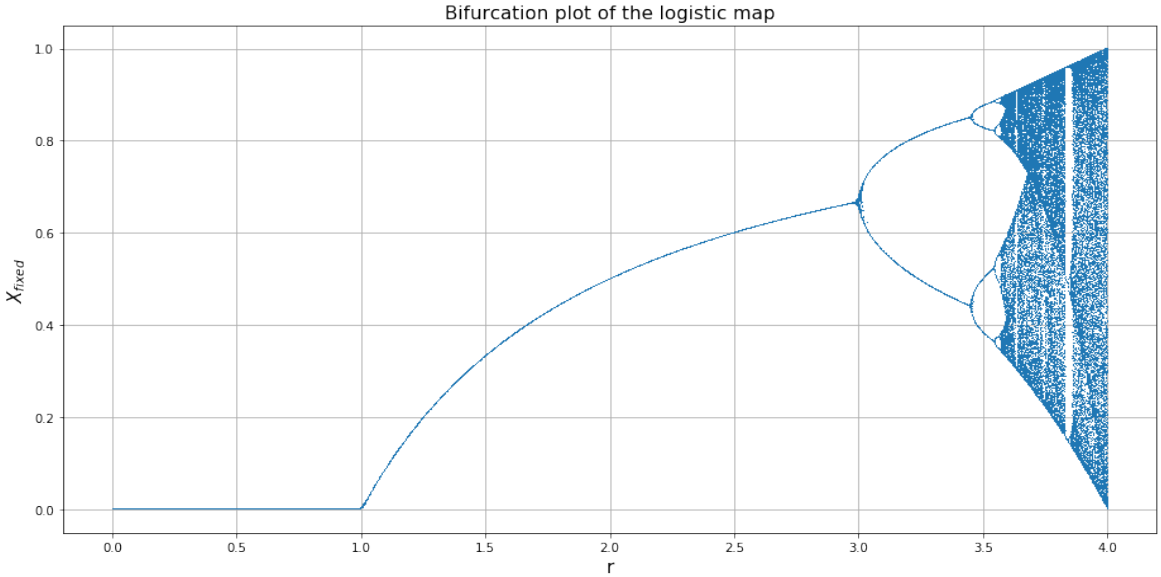

Figure 1.2: *Bifurcation diagram of the standard Logistic map (no delay).*

In particular, at $r < 1$ all the solutions die out, while for $1 < r < 3$ the solutions converge to the equilibrium $N^* = (r-1)/r$; then when $r > 3$ the diagram starts to bifurcate and the periodicity of the solutions doubles, each time in a smaller interval, creating limit cycles of period $2, 4, 8, \ldots 2^\infty$. In his article [6] Feigenbaum shows that the ratios between the lengths of successive period-doubling intervals approach the Feigenbaum constant $\delta = 4.66920$. At $r > 3.56995$ the oscillations become completely chaotic and there are no more limit cycles. However, even if most values of r beyond this limit give a chaotic behavior, there exist still certain isolated ranges of values of r in which the solutions exhibit a non-chaotic behavior like, for instance, at $r = 1 + \sqrt{8}$, where there are period-3 limit cycles. Finally at $r > 4$ the solutions are not stable anymore and for almost all initial conditions they diverge to infinity.

Next, in figure (1.3) we show the bifurcation diagrams of the delayed Logistic map for different values of the delay T.

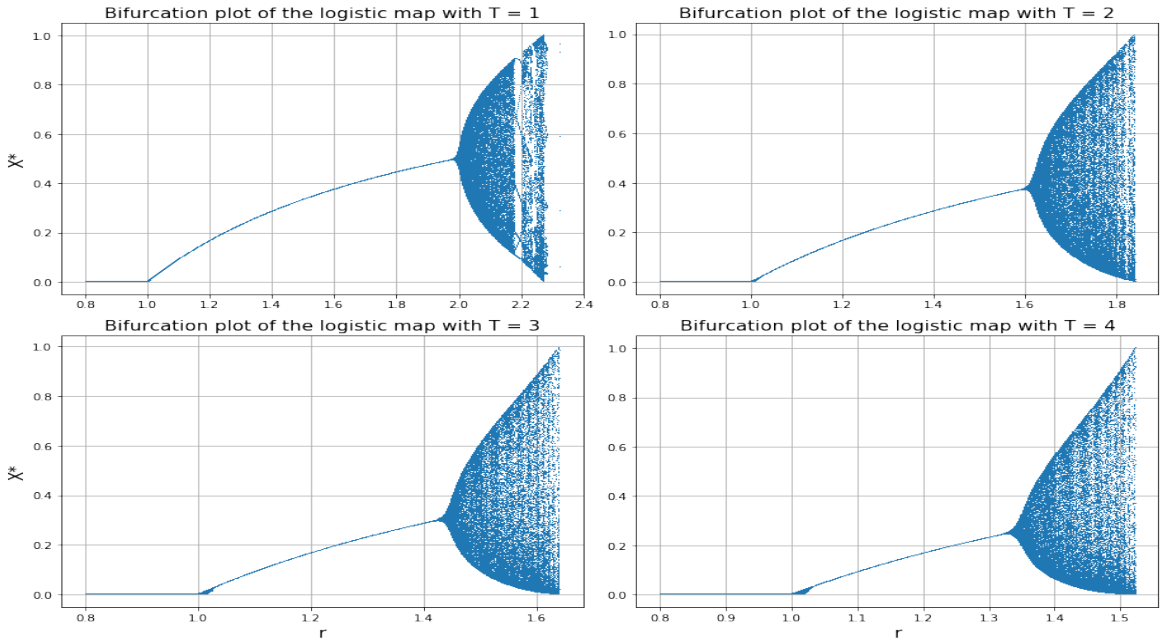

Figure 1.3: *Bifurcation diagrams of the delayed Logistic map for different values of the delay.*

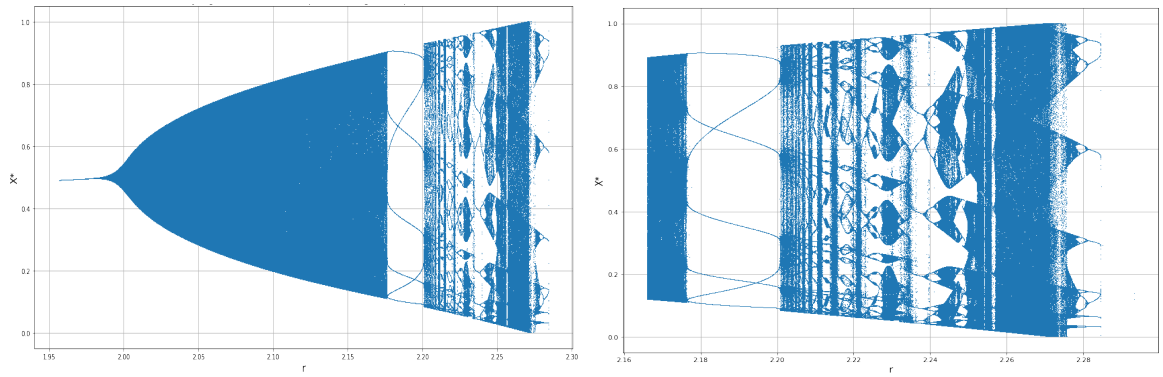

Figure 1.4: *Magnifications of the bifurcation diagram of the delayed Logistic map with* $T = 1$.

We highlight how the bifurcation diagrams are divided into two main areas, one where the solutions converge first to zero and then to the equilibrium $N^* = (r-1)/r$ and one where they oscillate around it. We also note that the limit value of r, after which the solutions diverge to infinity, decreases for increasing delays. Similarly, the r value under which the solutions converge to the equilibrium also decreases for increasing T. Figure (1.6) shows how both of these intervals scale with the time delay. In the same figure we also plot the limits of the stable range predicted by our theoretical results given by Eq. (1.7) in section 1.2.1 (however, we cannot calculate the limit of the oscillating range analytically).
Moreover we observe that, while the region in which the solutions go to zero or converge to the equilibrium has the same behavior as the non-delayed case, the interval in which the solutions are sustained oscillations have a completely different behavior with respect to the non-delayed case. Indeed there we do not have any limit cycle, where the population oscillates between a fixed (by the value of r) number of values, but instead the solution assumes any value inside a certain interval $[a, b] \in \mathbb{R}$, with $0 < a, b < 1$. This fact does not mean that the solution is chaotic. In fact, there

is still some order in it, for example the periodicity of the auto-correlation or the simple distribution of the values assumed by N_t. Finally this periodicity is clearer if we also observe the time evolution of the solutions in figure (1.1). In fact, there we can see that the trajectories generally are a sort of "continuous and derivable" oscillations with periodic behavior.

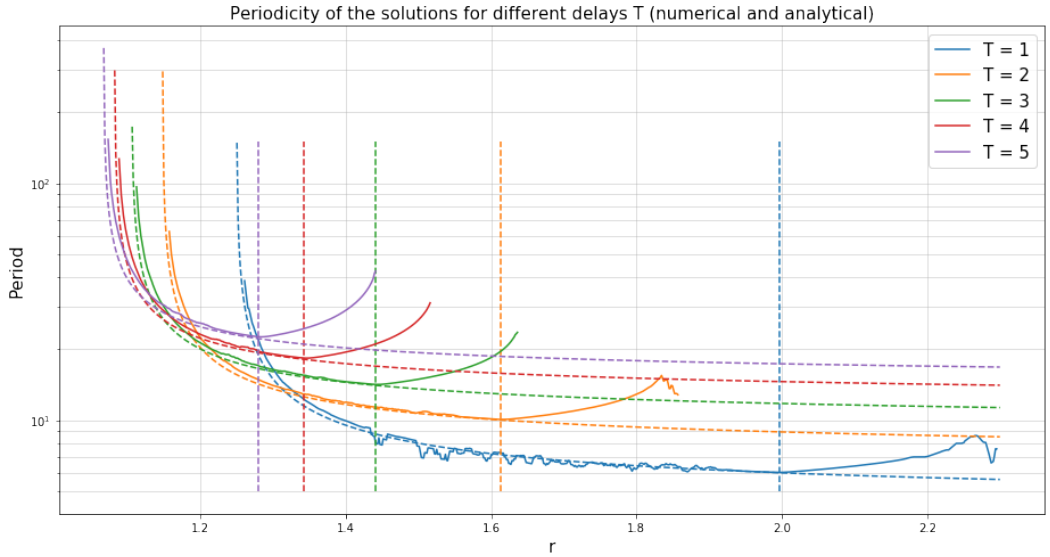

Figure 1.5: *Periodicity of the solutions of the delayed Logistic map as a function of the parameter r for different values of delay T. The values have been computed numerically by taking the average of 10 solutions with different initial conditions, then to smooth the plot we also have taken the moving average of the results (5 values in total). The vertical dashed lines represent, for each value of the delay, the limit of the stable (converging) range, while the other dashed lines represent the analytical prediction for the periodicity of the solutions as a function of the parameter r.*

In figure (1.5) we compute numerically the periodicity of the solutions as a function of r. We can clearly observe that the period of the oscillations is well predicted by the analytical results only in the converging range, i.e. where the solution converges to the equilibrium. Then, after that point, the solutions start to oscillate in a sustained way, the period therefore starts to increase and cannot be predicted anymore until it reaches the diverging point, where it cannot even be computed. The period that we have obtained analytically is computed simply as $2\pi/\theta(r)$, where $\theta(r)$ is the phase of the solution z of (1.7), which obviously depends on r.

Finally, we notice that the presence of sustained non-chaotic oscillations (instead of the typical limit cycles) does not mean that the insertion of the delay eliminates the intrinsic chaoticity of the Logistic map. In fact, there are also many exceptions to such an oscillating behavior. For instance, particularly for small delays (for example at $T = 1$), there exist some regions in which the solutions return to limit cycles and chaotic oscillations. In these regions the bifurcation diagram remembers vaguely the non-delayed one. In figure (1.4), for example, we show some magnifications of the oscillatory region of the bifurcation diagram with $T = 1$, in which we observe this particular behavior.

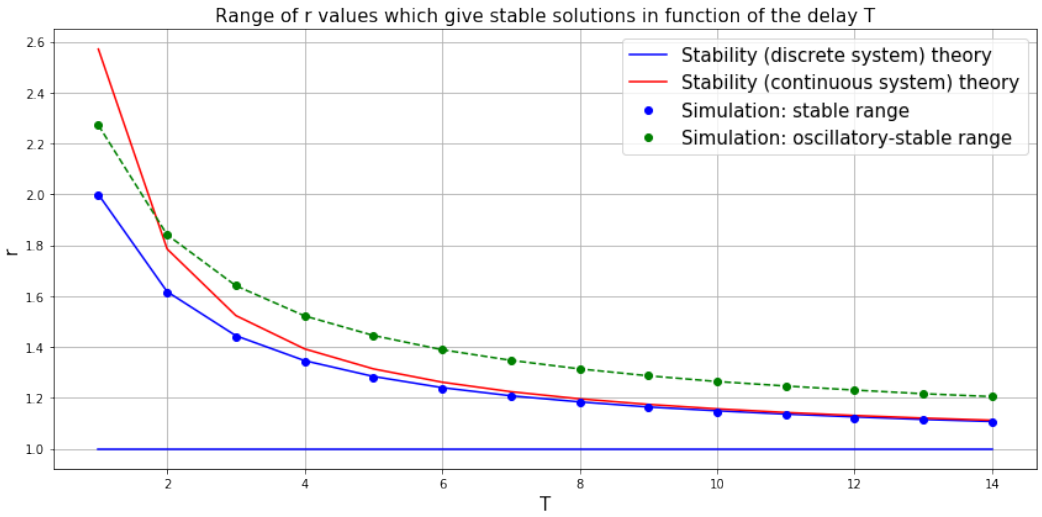

Figure 1.6: *Ranges of r values which give stability or sustained oscillations on the delayed Logistic map as a function of the delay T. The two solid lines are the analytical predictions (using the continuous ODE or the discretized system), while the points are the numerical results.*

1.3 Delayed Lotka-Volterra equations

The main objective of this section is to study the effect of the delay on ecosystems dynamics which, differently from the previous one, includes more than one species. This can be characterized through the Lotka-Volterra equations. A generalized Lotka-Volterra system with Verhulst's saturation term, in absence of delay is described by the set of equations:

$$\dot{N}_i(t) \;=\; \Big[\; k_i \;+\; \sum_{j=1}^{S} a_{i,j} N_j(t) \;\Big] N_i(t) \quad \text{with:} \quad i = 1 \dots S, \tag{1.8}$$

where $a_{i,j}$ is the so called community matrix.
We introduce the delay in the most simple way, which is the one proposed by Montroll in [16]. Indeed, here we want to show that even the most simple delayed differential equation (DDE) can produce a variety of solutions, which have a lot more complexity with respect to the original non-delayed ODEs.
We introduce then the delay parameter by choosing a fixed value denoted as T and inserting it into the variables of (1.8), which describe the total growth rate of the species in the same way as we did for the delayed Logistic equation in section 1.2. We thus obtain the following system:

$$\dot{N}_i(t) \;=\; \Big[\; k_i \;+\; \sum_{j=1}^{S} a_{i,j} N_j(t-T) \;\Big] N_i(t). \tag{1.9}$$

Here the index i is the species index; k_i describes the growth (for $k > 0$) or death (for $k < 0$) rate of species i, while $a_{i,i}$ describes the self interaction of each species and it is the so called Verhulst's saturation term, setting a limit in the maximal population N_i. Finally the coefficients of the community matrix $a_{i,j}$ describe the interaction between the species (i, j): a positive $a_{i,j}$ indicates a positive contribution

to the growth of N_i, while a negative $a_{i,j}$ quantify how rapidly the encounters between the two species lead to a decrease in N_i. Finally $a_{i,j} = 0$ means that there is no interaction between the two species.

In general, to obtain a meaningful ecological description, we impose $a_{i,i} < 0$ as in this way there is an effective saturation of each species. Next we can choose the off-diagonal coefficients $a_{i,j}$ to describe different types of interactions: if both $a_{i,j}$ and $a_{j,i}$ have the same sign, then the i-th and j-th species are cooperating or competing with each other for the resources. On the other hand, if the two entries have opposite signs, then we are in a predator-prey type of system.

As a final remark we observe that the choice of non-zero self-interaction terms $a_{i,i} \neq 0$ limits strongly the variability of the solutions of the non-delayed system. Indeed this "dampening" term is generally strong enough to oppose the sustained oscillations and transform them into converging solutions (overdampening). As we will now see, this choice does not affect significantly the Delayed system, which is still able to exhibit a wide range of configurations, from simple converging solutions, to more chaotic oscillating ones.

1.3.1 Analytical results

In this subsection we study analytically the equation (1.9) and we characterize both the stability of the solutions and the presence of Höpf bifurcations in terms of the delay parameter T.

There are two substantially different ways we can choose to treat the equation. The first method is to apply the analytical tools of standard continuous DDEs, while in the second one we will start with a discretization of the equation, using Euler formula, and then study the discretized system using different analytical tools. The two final results will be similar, but the ones obtained with the second method will give results in line with the computational simulations. We highlight that the presence of the delay changes the behavior of the solutions and this does not depend on the chosen discretization method.

Stability of the Continuous System

We start by adimensionalizing Eq. (1.9), by applying the following change of variables and obtaining the new system (which has $b_{i,i} = -1$ by definition) on the adimensional variable $\vec{x}$. The latter is a sort of population density (even though, because of the total population is not fixed, this is not the real density). In particular:

$$\begin{cases} x_i = -a_{i,i}N_i/k_i \\ b_{i,j} = -(a_{i,j}k_j)/(a_{j,j}k_i) \end{cases} \qquad \dot{x}_i(t) \;=\; k_i x_i(t)\Big[\; 1 \;+\; \sum_{j=1}^{S} b_{i,j}x_j(t-T) \;\Big]. \tag{1.10}$$

Starting from Eq. (1.10), we are able to compute the equilibria of the new system by imposing $\dot{x}_i = 0 \ \ \forall i$ obtaining then the equation:

$$q_i \Big[\ 1 \ + \ \sum_{j=1}^{S} b_{i,j} q_j \ \Big] = 0 \quad \Rightarrow \quad \vec{q} = -B^{-1}\vec{1} \rightarrow q_i = -\sum_{j=1}^{S} (b^{-1})_{i,j}.$$

In the previous equation we select only the non-null solutions, in fact there are also other $(2^S - 1)$ different equilibria in which at least one, or even all, species have zero population, which means that they become extinct. We obviously cannot accept those cases because we consider the system to be stable only if none of the species goes extinct, i.e. we impose the constraint $q_i \neq 0 \ \ \forall i$.
Furthermore, to have meaningful solutions from an ecological point of view, we must have feasible equilibria and consider also the constraint: $q_i > 0 \ \ \forall i$, because the variable x_i describes the population of a species and it must be undoubtedly positive.

Then, to study the stability of the equilibrium, we can make the following change of variables: $x_i(t) = q_i + u_i(t)$. We thus rewrite the linearized system by approximating at the first order of $u_i(t)$ obtaining:

$$\dot{u}_i(t) \ = \ k_i q_i \sum_{j=1}^{S} b_{i,j} u_j(t-T) \ = \ -\sum_{j=1}^{S} c_{i,j} u_j(t-T) \quad \text{with:} \quad c_{i,j} = -k_i q_i b_{i,j}. \tag{1.11}$$

Finally, we just need to compute the solutions of the equation $\quad \dot{\vec{u}}(t) = -C\vec{u}(t-T) \quad$. We are able to compute the solutions by performing the Linear Stability Analysis and by searching for solutions of the type: $\vec{u} = \vec{v}e^{\lambda t}$ obtaining the characteristic equation

$$det\big(\lambda e^{\lambda T} + C\big) = 0 \quad \longrightarrow \quad \prod_i \big(\lambda e^{\lambda T} + eig_i(C)\big) = 0, \tag{1.12}$$

where $eig_i(C)$ denotes the i-th eigenvalue of matrix C.

This characteristic equation is the product of terms in the form $\ ze^z + \gamma = 0$ where γ is a complex number. As shown in Appendix D of the work of Montroll and colleagues [16], if we consider $eig_i(C) = \rho_i e^{i\theta_i}$, then we are able to derive a condition under which all the solutions of the characteristic equation have negative real parts, i.e. the equilibrium is stable. This condition can be written in the following way:

$$Re[\lambda] < 0 \quad \Longleftrightarrow \quad \frac{\pi}{2} - |\theta_i| > \rho_i T \quad \cap \quad Re[eig_i(C)] < 0 \qquad \forall i = 1 \dots S \tag{1.13}$$

Höpf bifurcation in the continuous system

Given the stability condition, we now aim at investigating if any Höpf bifurcation emerges in our system dynamics by increasing the delay parameter T. As we know, an Höpf bifurcation on a certain parameter is defined when, by slowly changing the parameter (increasing or decreasing it), the real part of one of the eigenvalues of the linearized system changes sign, passing through a bifurcation value which is a purely imaginary number.

Again, the characteristic equation of the linearized system $\dot{\vec{u}}(t) = -C\vec{u}(t-T)$ (with the notation: $\gamma_i = eig_i(C)$) is the following:

$$det\big(\lambda e^{\lambda T} + C\big) = 0 \quad \longrightarrow \quad \prod_i \big(\lambda e^{\lambda T} + \gamma_i\big) = 0.$$

To study the bifurcation we apply the method presented in [26]. First of all, we consider that all the eigenvalues are functions of the delay T, i.e. $\lambda = \lambda(T)$; then we compute their derivative by differentiating the characteristic equation with respect to T, obtaining

$$\sum_i \big[e^{\lambda T}(\dot{\lambda} + T\lambda\dot{\lambda} + \lambda^2) + \gamma_i\big] \prod_{j\neq i} \big(\lambda e^{\lambda T} + \gamma_j\big) = 0. \tag{1.14}$$

Finally, to find the bifurcation point we solve the characteristic equation by imposing that the solution is a purely imaginary eigenvalue, i.e. we look for the value T^* for which $\lambda = i\omega$. We thus obtain:

$$\prod_i \big(i\omega e^{i\omega T} + \gamma_i\big) = \prod_i \big(-\omega\sin(\omega T) + i\omega\cos(\omega T) + R(\gamma_i) + iI(\gamma_i)\big) = 0 \tag{1.15}$$

We want now to find all the possible couples (ω, T) which solve equation (1.15) by taking both the real and the imaginary part of the expression and equating them to zero. For each eigenvalue index i we thus get the following system for the solutions:

$$\begin{cases} \omega\sin(\omega T) = R(\gamma_i) \\ \omega\cos(\omega T) = -I(\gamma_i) \end{cases} \longrightarrow \begin{cases} \tan(\omega T) = -\dfrac{R(\gamma_i)}{I(\gamma_i)} \\ \pm\dfrac{\omega\tan(\omega T)}{\sqrt{1+\tan^2(\omega T)}} = R(\gamma_i) \end{cases} \longrightarrow \begin{cases} \omega T = k\pi - \arctan\Big[\dfrac{R(\gamma_i)}{I(\gamma_i)}\Big] \\ \omega = \pm|\gamma_i|. \end{cases}$$

Finally, solving such systems of equations, we get:

$$T_i^{(k)} = \pm\frac{1}{|\gamma_i|}\Big(\arctan\Big[\frac{R(\gamma_i)}{I(\gamma_i)}\Big] + k\pi\Big) \qquad \text{and} \qquad \omega_i = \pm|\gamma_i|. \tag{1.16}$$

All the different couples $(\omega_i, T_i^{(k)})$ are possible bifurcation points of the system. We are interested only on the first positive one, which is the one with the smaller delay. Indeed the negative ones are not meaningful for our case and also, after passing the first bifurcation point, the system has at least one eigenvalue with positive real part and it becomes undoubtedly unstable.
Given that, we define the bifurcation parameter (and its correspondent ω value) as

$$T^* = \min_{i,k}(T_i^{(k)}) \qquad \text{with the associated} \qquad \omega^* = \omega_{i^*}. \tag{1.17}$$

Furthermore we compute also $\dot{\lambda}(T^*)$, the derivative of the eigenvalue with respect to the delay at the bifurcation point, using (1.14). If we neglect all the negligible terms $i \neq i^*$ we obtain the following approximated relation:

$$e^{\lambda T^*}(\dot{\lambda} + T^*\lambda\dot{\lambda} + \lambda^2) + \gamma_{i^*} = 0 \quad \longrightarrow \quad \dot{\lambda}\big|_{T^*} = \frac{(\omega^*)^2 - \gamma_{i^*}e^{-i\omega^* T^*}}{1 + i\omega^* T^*}.$$

In addition, using the following identities which we derived from the real and imaginary part of the starting equation: (1.15):

$$\begin{cases} R(\gamma_{i^*})\cos(\omega^* T^*) + I(\gamma_{i^*})\sin(\omega^* T^*) = 0 \\ (I(\gamma_{i^*})\cos(\omega^* T^*) - R(\gamma_{i^*})\sin(\omega^* T^*))\omega^* = -(R(\gamma_{i^*})^2 + I(\gamma_{i^*})^2) = -|\gamma_{i^*}|^2, \end{cases}$$

we can simplify even further the expression for the derivative. Eventually, we find that the derivative of the system's eigenvalue, with respect to the delay, in the bifurcation point is always positive. This means that the real part of the eigenvalue goes across the bifurcation point $R(\lambda) = 0$ from left to right and becomes positive for increasing values of T, i.e.

$$\frac{d}{dT}\Big[R(\lambda)\Big]_{T^*} = \frac{(\omega^*)^2 + T^*|\gamma_{i^*}|^2}{1 + (\omega^* T^*)^2} > 0$$

Therefore, in conclusion, we proved that the system is stable for delays $T \in [0, T^*)$ and it reaches an Höpf bifurcation at the value $T = T^*$ defined in (1.17).

Stability of the Discrete System

Starting from the generalized delayed Lotka-Volterra equation (1.9) we can rewrite the time derivative using the Euler formula $\dot{a}(t) \sim (a_{n+1} - a_n)/dt$, obtaining a discretized first order form of the Lotka-Volterra equations:

$$N_i^{(n+1)} \;\sim\; N_i^{(n)}\Big[\;(1 + dt \cdot k_i) \;+\; \sum_{j=1}^{S} dt \cdot a_{i,j} N_j^{(n-T/dt)}\;\Big].$$

Then we perform the following change of variables

$$\begin{cases} 1 + dt \cdot k_i \to k_i \\ dt \cdot a_{i,j} \to a_{i,j} \\ T/dt \to T \end{cases} \qquad N_i^{(n+1)} \;\approx\; N_i^{(n)}\Big[\;k_i \;+\; \sum_{j=1}^{S} a_{i,j} N_j^{(n-T)}\;\Big],$$

to obtain again a discretized dynamical system of equations similar to Eq. (1.9). Finally, using the same substitutions of the continuous case give by Eq. (1.10), we rewrite the system in an adimensional form (with $b_{i,i} = -1$), i.e.

$$x_i^{(n+1)} \;=\; k_i x_i^{(n)}\Big[\;1 \;+\; \sum_{j=1}^{S} b_{i,j} x_j^{(n-T)}\;\Big]. \tag{1.18}$$

In the expression above we have used the equivalence sign because our aim is to study the dynamical system associated to (1.9) and not just an approximation of (1.9). Indeed these two systems have a similar behavior, but one is not the approximation of the other.
Given the discretized system (1.18) we find its equilibria by imposing the condition:

$x_i^{n+1} = x_i^n = x_i^{n-T} = q_i \ \ \forall i$ obtaining the equation:

$$q_i k_i \Big[\ 1 \ + \ \sum_{j=1}^{S} b_{i,j} q_j \ \Big] = q_i \quad \Rightarrow \quad \vec{q} = B^{-1} \frac{\vec{1} - \vec{k}}{\vec{k}} \quad \rightarrow \quad q_i = \sum_{j=1}^{S} (b^{-1})_{i,j} \frac{1 - k_j}{k_j}.$$

Using the same arguments presented for the continuous case, we again conclude that these solutions are valid only in the stable case where we do not observe any population going extinct. Therefore we impose the constraint $q_i \neq 0 \ \ \forall i$; moreover to have feasible equilibria we also request $q_i > 0 \ \ \forall i$.

To examine the stability of the equilibria we perform the change of variables $x_i^n = q_i + u_i^n$ and rewrite the linear system by considering only the first order terms of u_i^n, obtaining:

$$u_i^{(n+1)} \ = \ u_i^{(n)} + q_i k_i \sum_{j=1}^{S} b_{i,j} u_j^{(n-T)} \ = \ u_i^{(n)} - \sum_{j=1}^{S} c_{i,j} u_j^{(n-T)} \quad \text{with:} \quad c_{i,j} = -k_i q_i b_{i,j}. \tag{1.19}$$

In summary, we obtain the following system of equations: $\vec{u}^{n+1} = \vec{u}^n - C\vec{u}^{n-T}$.

We now study the stability of this particular system by hypothesizing a solution in the form: $\vec{u}^n = \vec{v} z^n$, where $z \in \mathbb{C}$. Then, by substituting it into the equation above, we obtain

$$\vec{v} z^{n+1} = \vec{v} z^n - C\vec{v} z^{n-T} \quad \longrightarrow \quad \big(\mathbb{1}(z^{T+1} - z^T) + C\big)\vec{v} = 0 \quad \longrightarrow \quad det\big[\mathbb{1}(z^{T+1} - z^T) + C\big] = 0.$$

By using the well known properties of the eigenvalues, solving the above equation, we obtain the characteristic equation (1.20) that is valid for each eigenvalue $\gamma_i = eig_i(C)$ of the matrix C.
In order to have a stable equilibria, all the solutions $z \in \mathbb{C}$ of Eq. (1.20) must have an absolute value smaller than one. Otherwise the solutions will not converge to the equilibrium as $n \to \infty$:

$$z^{T+1} - z^T + \gamma_i = 0 \qquad \text{each solution with:} \quad |z| < 1 \qquad \forall i = 1 \dots S. \tag{1.20}$$

Neimark-Sacker bifurcation in the discrete system

Now we intend to verify that in the discrete dynamical system there is a Neimark-Sacker bifurcation (as a function of the delay parameter T), which is the analog of the Höpf bifurcation of the continuous case. The main difference in this case is that the transition to an unstable state occurs when one of the eigenvalues of the linearized system changes its absolute value from $|z| < 1$ to $|z| > 1$, as in the latter case the solution diverges when $n \to \infty$.

As we have seen above, the characteristic equation associated to the linearized system $\vec{u}^{(n+1)} = \vec{u}^{(n)} - C\vec{u}^{(n-T)}$ (with $\gamma_i = eig_i(C)$) is

$$det\big(\mathbb{1}(z^{T+1}-z^T)+C\big)=0 \quad \longrightarrow \quad \prod_i \big(z^{T+1}-z^T+\gamma_i\big)=0. \tag{1.21}$$

First of all, we consider that all the eigenvalues are functions of the delay T: $z=z(T)$ then, like in the continuous case, we compute their derivative by differentiating with respect to T the characteristic equation. We thus obtain

$$\dot{z}\big[(T+1)z^T-Tz^{T-1}\big]+\ln(z)\big[z^{T+1}-z^T\big]=0 \quad \to \quad \dot{z}(T)=\frac{z(1-z)\ln(z)}{(T+1)z-T}, \tag{1.22}$$

where the derivative of the squared modulus for $z=e^{i\omega}$ is given by

$$\frac{d}{dT}|z|^2=z^*\frac{dz}{dT}+z\frac{dz^*}{dT} \quad \to \quad \frac{d}{dT}\Big[|z|^2\Big]_{z=e^{i\omega}}=\frac{2\omega\sin(\omega)}{1+2T(T+1)[1-\cos(\omega)]}. \tag{1.23}$$

We can then solve the characteristic equation for $z=e^{i\omega}$, which is the bifurcation point (it has unitary modulus), finding the values of the parameters (ω, T^*) at the bifurcation:

$$\prod_i \big(e^{i\omega(T+1)}-e^{i\omega T}+\gamma_i\big)=\prod_i \big(\cos(\omega(T+1))-\cos(\omega T)+i\sin(\omega(T+1))-i\sin(\omega T)+R(\gamma_i)+iI(\gamma_i)\big)=0.$$

Next, taking both the real and the imaginary part of the expression and equating them to zero for each eigenvalue index i, we find the following system for the bifurcation parameters:

$$\begin{cases} \cos\big(\omega(T+1)\big)-\cos\big(\omega T\big)=-2\sin\big(\omega/2\big)\sin\big(\omega(T+1/2)\big)=-R(\gamma_i) \\ \sin\big(\omega(T+1)\big)-\sin\big(\omega T\big) \;=\; 2\sin\big(\omega/2\big)\cos\big(\omega(T+1/2)\big)=-I(\gamma_i) \end{cases}$$

$$\begin{cases} \tan\big(\omega(T+1/2)\big)=-\dfrac{R(\gamma_i)}{I(\gamma_i)} \\ \dfrac{2\sin\big(\omega/2\big)}{\sqrt{1+\tan^2\big(\omega(T+1/2)\big)}}=-I(\gamma_i) \end{cases} \longrightarrow \begin{cases} \omega(T+1/2)=-\arctan\Big[\dfrac{R(\gamma_i)}{I(\gamma_i)}\Big]+k\pi \\ \\ 2\sin\big(\omega/2\big)=\pm\sqrt{R(\gamma_i)^2+I(\gamma_i)^2}=\pm|\gamma_i|. \end{cases}$$

Finally, we solve the above system of equations, finding all the possible couples of the two parameters giving a bifurcation for each eigenvalue γ_i, i.e.:

$$T_i^{(k)}=-\frac{1}{2}\pm\frac{\arctan\Big[\dfrac{R(\gamma_i)}{I(\gamma_i)}\Big]+k\pi}{2\arcsin\big[|\gamma_i|/2\big]} \qquad \text{and} \qquad \omega_i=\pm 2\arcsin\big[|\gamma_i|/2\big]. \tag{1.24}$$

Furthermore, like for the continuous case, the solutions $(\omega_i, T_i^{(k)})$ give all the possible bifurcation points of the system. Obviously we are interested only on the first one, which is the one with smaller positive delay, as already explained before.
Therefore, defining

$$T^*=\min_{i,k}(T_i^{(k)}) \qquad \text{with the associated} \qquad \omega^* \tag{1.25}$$

we compute the derivative, with respect to the delay, of the square modulus of the eigenvalue in the bifurcation point (ω^*, T^*). This value, as before, is always positive, i.e. the modulus of the eigenvalue passes the bifurcation point at $|z| = 1$ and becomes larger than one for increasing delays T.

$$\frac{d}{dT}\Big[|z|^2\Big]_{T^*} = \frac{2\omega^* \sin(\omega^*)}{1 + 2T^*(T^*+1)[1-\cos(\omega^*)]} = \frac{2|\gamma_i| \arcsin\left[|\gamma_i|/2\right]\sqrt{4-|\gamma_i|^2}}{1+T^*(T^*+1)|\gamma_i|^2} > 0.$$

Therefore, we conclude that the system is stable for delays $T \in [0, T^*)$ and it reaches a Neimark-Sacker Bifurcation at $T = T^*$ (as defined in1.25).

1.3.2 Numerical results

To explore the effect of the Delay on the discretized adimensional Lotka-Volterra system presented in (1.18), we start by identifying the range of parameters giving feasible equilibria and solutions. In figure (1.7) we consider a two species system with fixed species interactions given by the matrix A, displaying three different types of interactions: predator-prey $(+\ -)$, cooperative $(+\ +)$ and competitive $(-\ -)$. There we show, for the non-delayed case, which values of the growth vector $\vec{k}$ give a feasible equilibrium ($\vec{q} > 0$) and which values give a stable equilibrium. The stability is evaluated by computing the solutions z of the "discrete characteristic equation" (1.20) for $T = 0$ and verifying if all satisfy the condition $|z| < 1$.

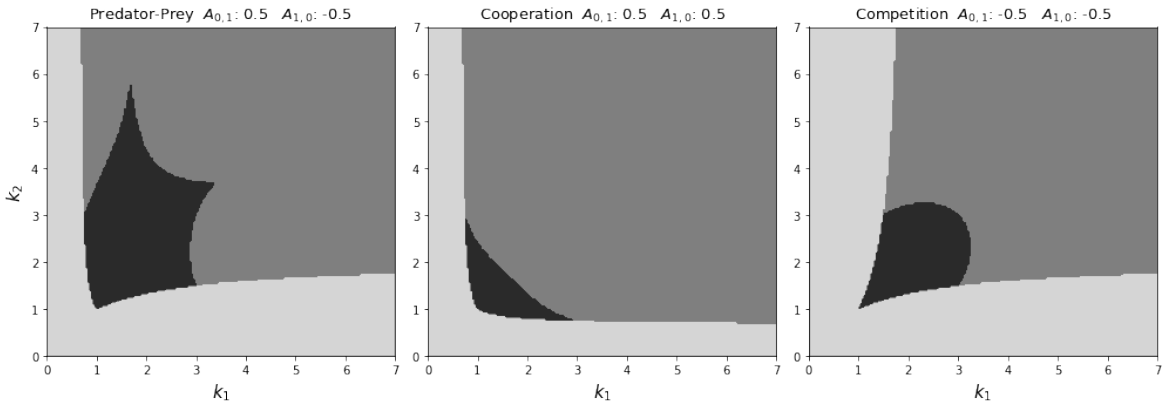

Figure 1.7: *Range of $\vec{k}$ values which give a Feasible (positive) equilibrium (grey + black area) or a Stable one in the non-delayed case (only black area). Here we used the 3 different types of community matrices with representative values of the parameters.*

A first result that we can conclude from such analysis is that, as expected, the types of species interactions influence the shape of the "Stability-Surface" diagram in the parameter-space. Also, we observe that the predator-prey system, is the most stable (corresponding to the black area). On the contrary, cooperative ecological systems are the most unstable. These results are in agreement with previous studies [17], [20]. We also find that relative changes of the magnitude of the entries of A affect only slightly the stability region.

We notice that the parameters giving the stable equilibria in the non-delayed case are only small subset of the ones giving feasible equilibria (which approximately all

lie in the first quadrant). Therefore, according to Eq. (1.20), if delay stabilizes the ecosystem dynamics, we should observe an increase of the stability region (given by the black area). On the contrary, delay destabilizes the system, as shown in figure (1.8). In fact we observe that the presence of the delay decreases the area in which the equilibria are stable. We see then a contraction of the available area for stable solutions when the delay T increases. We thus conclude that, at least from the analytical perspective, the presence of the delay is destabilizing because it diminishes the range of values of the parameters giving stable solutions (we verified that this happens in the same way also for a larger number of species).

In the second row of figure (1.8) we show that this decrease in stability for increasing delay T also happens in the parameter-space of matrix A, where we fix the values of the growth vector $\vec{k}$.

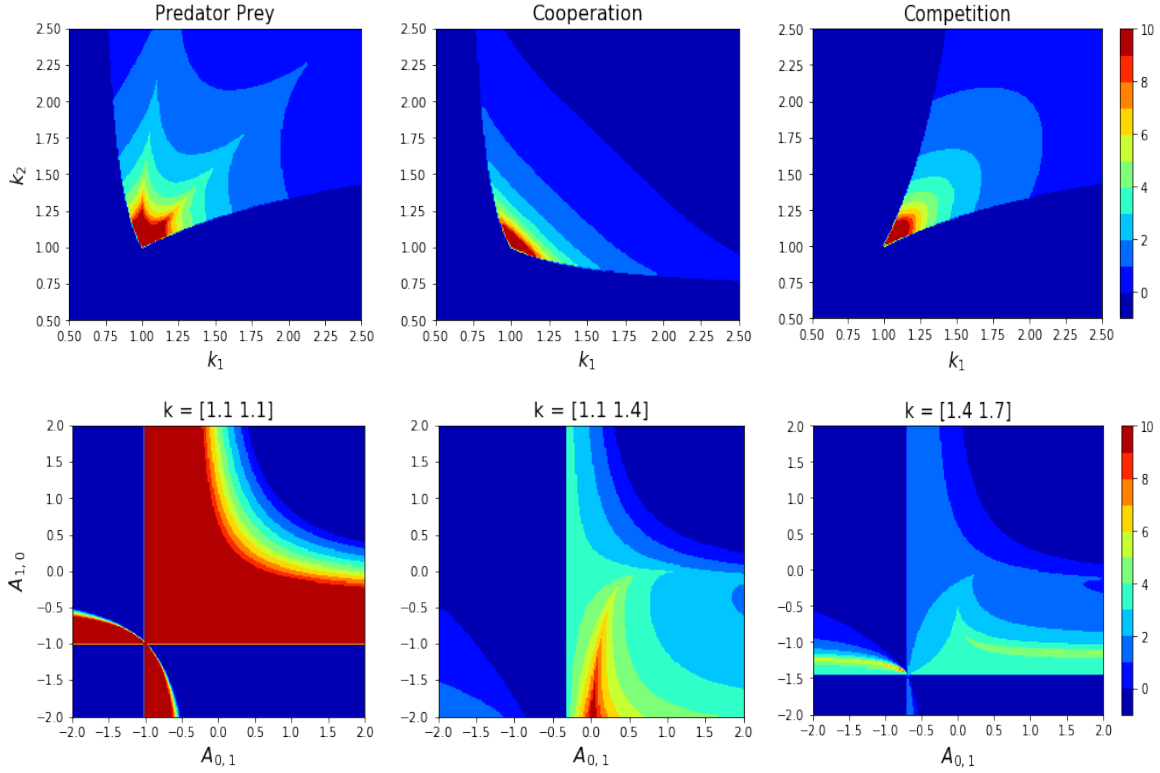

Figure 1.8: *Change on the Stability-Surface diagram in the parameter space of $\vec{k}$ and A for fixed values of A and $\vec{k}$ when we increase the delay T. The color-bars are referred to the parameter T therefore increasing T means going from blue to red.*

After the analytical study, we verified that the same conclusions hold also from the numerical point of view, i.e. we computed the trajectories for a given set of parameters and verified that they do not diverge (they either converge to the equilibrium or oscillate in a self-sustained way). Therefore we made the same mapping of the parameter space to find the different stability-surfaces diagrams for different delays. We obtain very similar results to the analytical Stability-Surfaces. However we also find some important differences, shown in figure (1.9).
From one hand, we numerically confirm that the presence of the delay never stabilizes the non-delayed system, as the Stability-Surface diagram for $T = 0$ remains the

same in both the numerical and the analytical results and that the stability region decreases when we increase the delay. On the other hand, however, we numerically find that the observed decrease in stability is less pronounced than what was expected from the analytical theory. This difference is due to the fact that the formula (1.20), which we use to infer the stability of the equilibria, is able only to predict the solutions which converge to the equilibrium, i.e. the ones with $|z| < 1$. However, there are also several solutions which does not converge to the predicted equilibrium, but still remain stable. For instance all the sustained oscillations and cycles around the equilibrium point will never converge to it, but neither they will diverge to infinity.

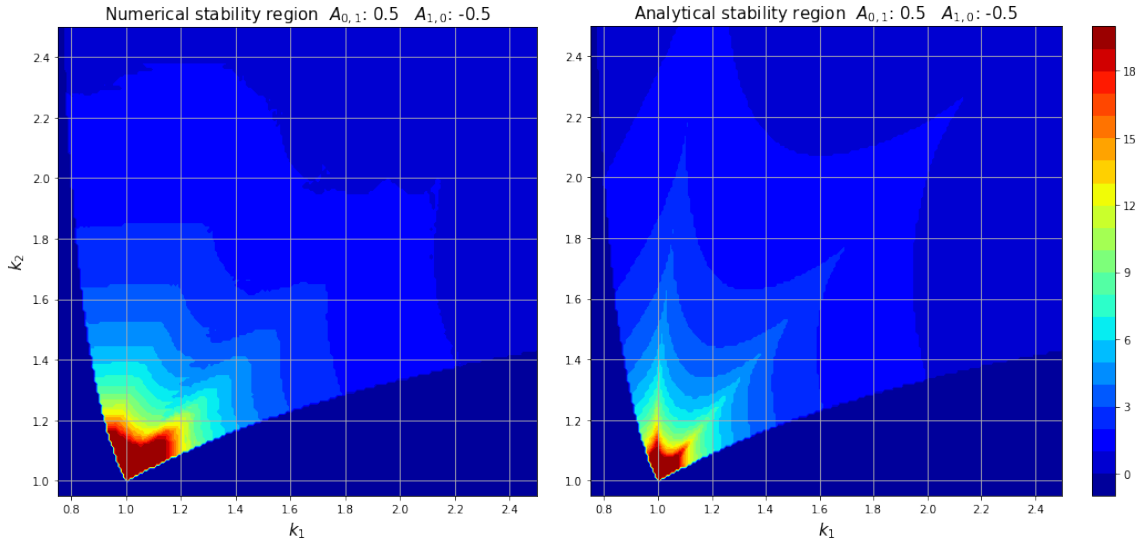

Figure 1.9: *Comparison between the Stability-Surfaces diagram, for different delays, in the parameter-space of $\vec{k}$ in a predator-prey system, computed numerically and analytically. Again the color-bar refers to the parameter T therefore increasing T means going from blue to red.*

Next, after we have established that the delay does not improve the stability of the system, we want to explore how it changes the behavior of the solutions. As we have seen in the previous figure, there is not a negligible part of the parameter-space giving oscillating solutions that are both non-converging and non-diverging. Therefore our objective is to characterize this particular type of solutions.
First of all, we consider the bifurcation diagrams for the two species that is characterized by four parameters (two growth parameters $\vec{k}$ and two off-diagonal terms in the matrix A). Therefore, to have a complete bifurcation diagram, we should vary all the four parameters together; this is obviously impossible to represent graphically, thus we considered a single exemplifying case. Indeed, we fix the matrix A as a cooperative matrix and we change the growth parameters to be $\vec{k} = (1, a)$, where now a is thus the only value that we are varying.
In figure (1.10) we show the resulting bifurcation diagram. We observe that the solutions are again characterized by a trajectory converging to the equilibrium followed, when the parameter a is high enough, by a stable oscillating part which can show also signs of chaoticity in the solutions. Similar results are obtained by using different types of Community matrices A and different values of the growth parameter.

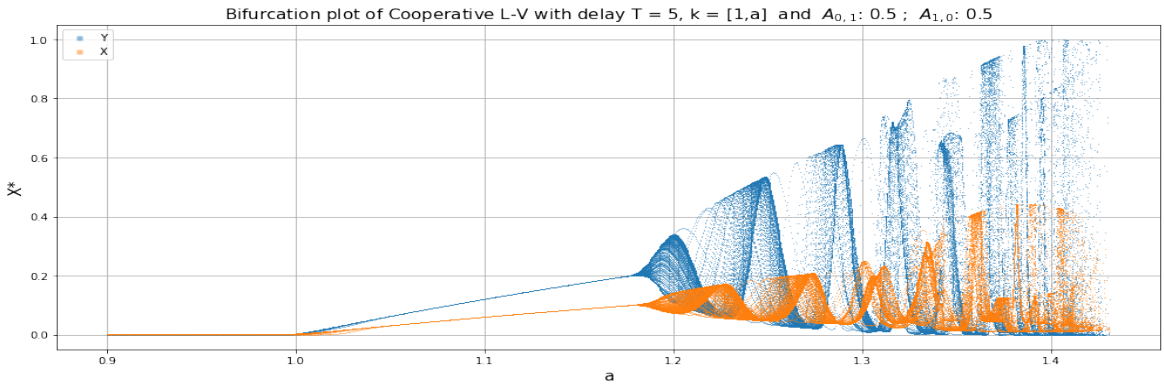

Figure 1.10: *Bifurcation diagram of the system with a Cooperative Community matrix A, a growth rate in the form $\vec{k} = (1, a)$ and the fixed delay $T = 5$. Here we varied the parameter a obtaining the bifurcation diagrams of the 2 species.*

In figure (1.11) we also show how the range of convergence and the range of stable sustained oscillations in the space of the parameter a changes as a function of the delay T for the same type of system described above. We observe that the increase of the delay squeezes both the stability ranges to 1 in the limit $T \to \infty$. Indeed, the lower limit of the stability is exactly $a = 1$ (as shown in the Stability-Surfaces figures) because for $a < 1$ the solutions die out to zero. In the first plot of figure (1.11) we show how the upper limit of these regions scales as a function of the delay T, while in the second plot, we show how the width of the oscillating region decreases, as expected, with T.

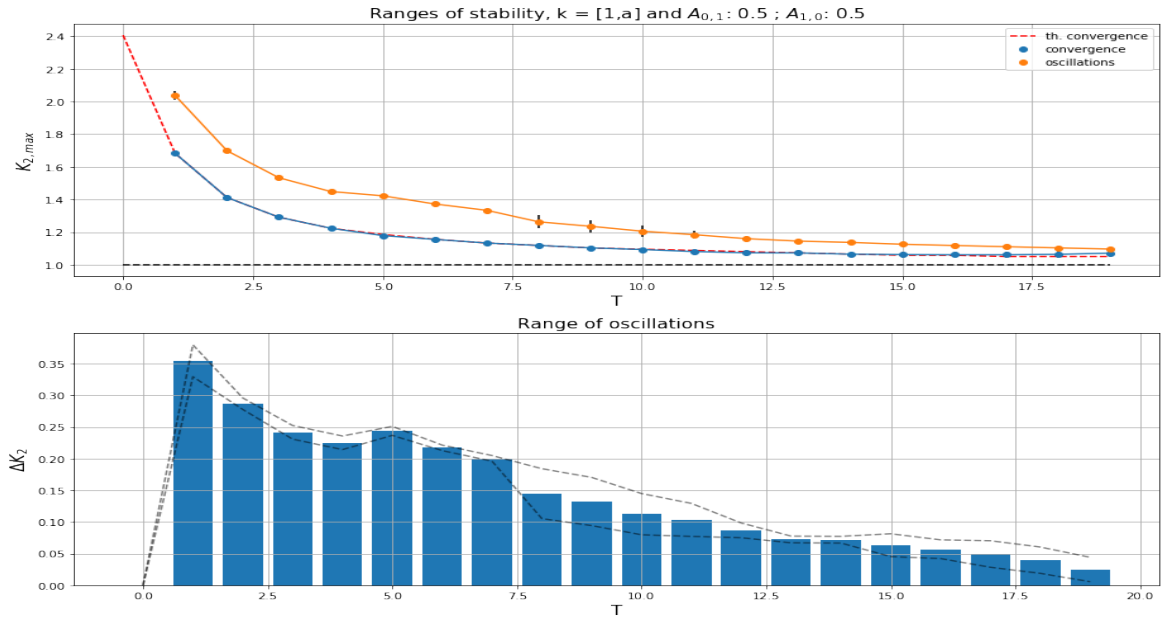

Figure 1.11: *Average (over 10 different realizations of the initial conditions) of the upper limit of the converging range (blue) and of the oscillating range (orange) as a function of the delay T for the bifurcation diagram in figure (1.10). In the second figure we show how the average width of the oscillating region (the region between the blue and the orange lines) changes as a function of the delay; the black dashed lines are the 1σ confidence intervals of the results.*

We did the same numerical analysis for also the other interaction types in the Community matrices A obtaining always similar results.

Now we want to characterize the behavior of the oscillating solutions, in particular we are interested on how the variation of the delay changes the typology of these solutions; for instance we observe that when the delay is increased enough, the solutions from stable oscillating ones become chaotic oscillating ones. In figure (1.12) we show some examples of chaotic solutions originated from the same parameters giving rise also to converging solutions or stable oscillating ones, but when the delay is smaller. We can infer their chaoticity by observing their behavior in the phase space plot, as the trajectories form space-filling curves, i.e. they tend to fill completely the phase space. Later we will present also some other ways to measure the chaoticity of a solution.

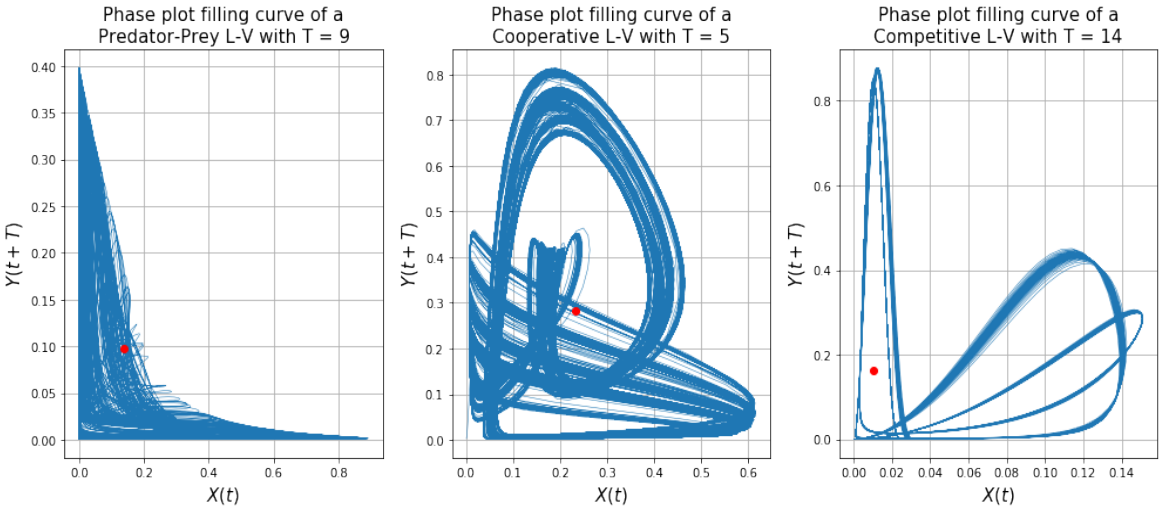

Figure 1.12: *Representation on the phase space of some solutions of the L-V equations with delay for the three different types of Community matrices: predator-prey, cooperative and competitive. They are filling curves in the sense that they fill all the phase space.*

Next we show how the presence of the delay increases strongly the variability of the solutions of a typical Lotka-Volterra system. We compute and show the trajectories of the population dynamics in their phase-space representation and also the distribution of their values for an exemplifying case. In figure (1.13) we have selected some random values for the parameters of a two-species predator-prey Lotka-Volterra system, but so that they give a stable, i.e. converging, solution in the non-delayed case. We observe that, when we add the delay to the system, the behavior of the solutions changes completely: for small enough delays the solutions are still converging (damped oscillations) to the equilibrium, but when the delay is large enough the solutions start to oscillate in a sustained way (in these last cases the analytical formula is not able anymore to predict the stability as we can see in the figure).

The oscillating behavior can be subdivided in two different features: non-chaotic periodic oscillations and chaotic aperiodic oscillations. In fact, we can see in figure (1.13) that, in the beginning the oscillations have a fixed periodicity (see also the regularity of the corresponding distribution of their values), but when the delay surpasses a specific threshold, they become chaotic and aperiodic (the distributions indeed are not regular anymore).

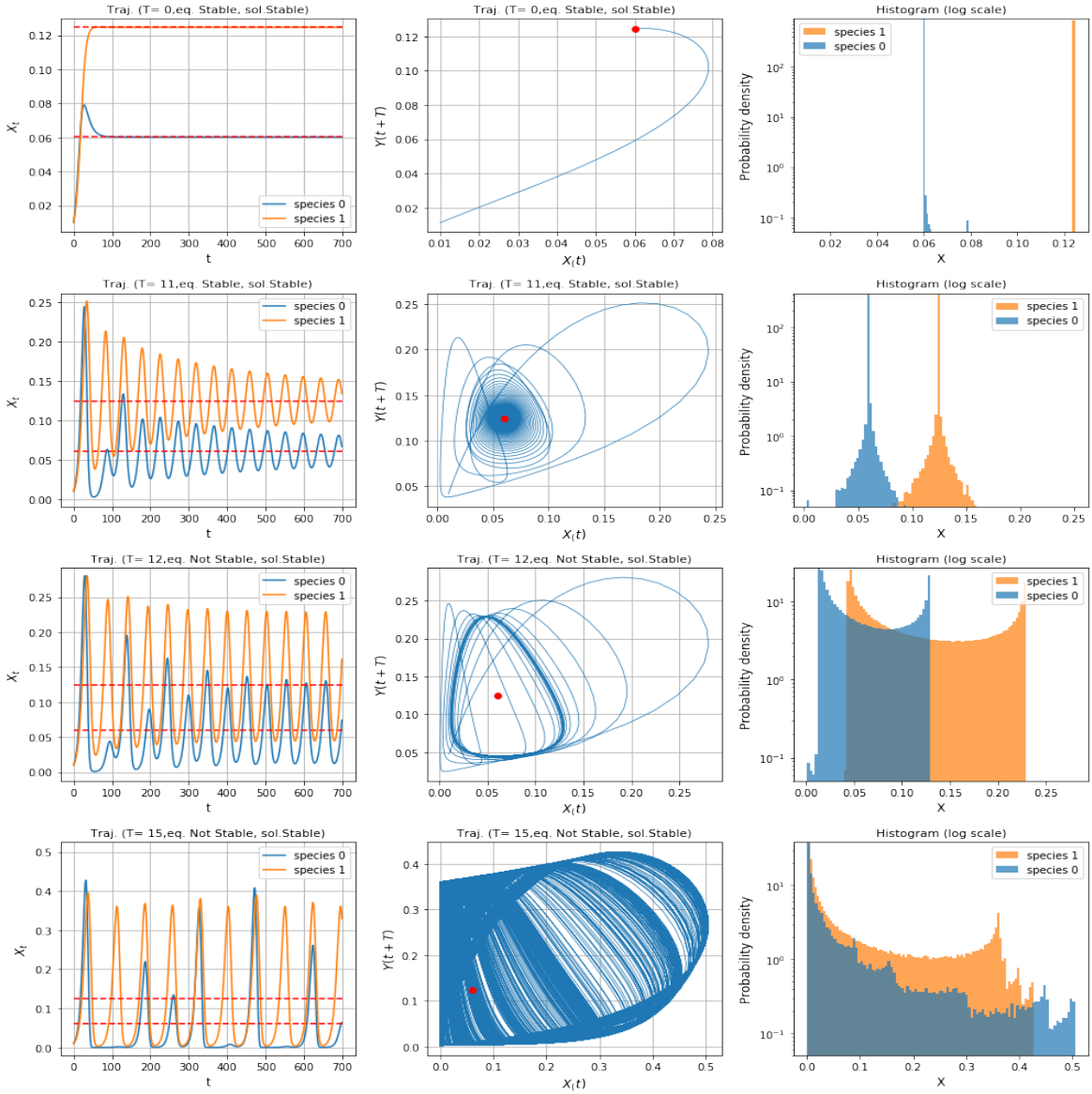

Figure 1.13: *Study of some sample solutions, with different delay intensities, of the two-species Lotka-Volterra predator-prey system; the parameters $\vec{k}$ and A are sampled such that the non-delayed solution (first row) is analytically stable, i.e. converging. For each value of the delay we represent: the time evolution of the trajectories, their evolution on the phase space and the distribution of their values after enough iterations. Each trajectory is also labeled by "Stable" or "not Stable" as obtained both from the analytical results and the numerical ones.*

We conclude this section by presenting some other methods that can be used to discern the chaotic nature of a given oscillating trajectory. These methods, unlike what we have used in the above analysis, are quantitative and allow us to characterize precisely the typology of the oscillating solutions.

The first method is the computation of the power spectral density of the solutions. This quantity describes how the power of a time-dependent signal is distributed over the various frequencies (or periodic components) that constitute it [19]. Given a signal $x(t)$ we define its power spectral density as

$$P(\omega) = \lim_{T\to\infty} \mathbb{E}\Big[|\tilde{x}(\omega)|^2\Big] = \lim_{T\to\infty} \frac{1}{T}\int_0^T \int_0^T \mathbb{E}\Big[x^*(t)x(t')\Big] e^{i\omega(t-t')} dt dt'$$

where $\mathbb{E}$ is the expected value and $\tilde{x}(\omega)$ is the Fourier transform of $x(t)$.
Therefore, if we compute the power spectrum of our solutions, we are able to find the characteristics frequencies of the oscillating time series, if any.

In this case, by observing the power spectrum in figure (1.14), we are able to distinguish between a stable non-chaotic oscillation (which has only a limited number of peaks in the spectrum and one prevailing on the others), and a chaotic aperiodic oscillation (for which the spectrum has an "infinite" number of peaks and none of them prevails predominantly with respect to the others).

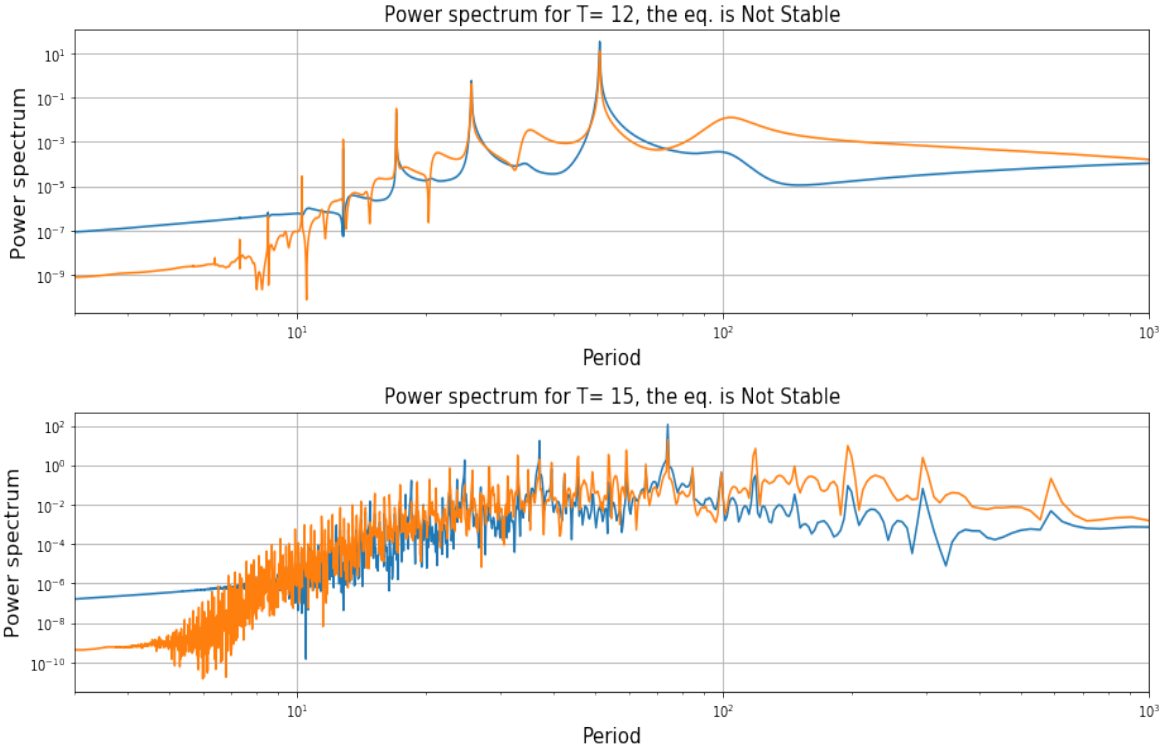

Figure 1.14: *Power Spectral density of the solutions showed in figure (1.13) for two values of the delay, the first is such that the solution is a stable oscillation while the second is a chaotic one. We plotted the power spectrum, in an unusual way, as a function of the periodicity instead of the frequency, because it eases the interpretation of the results. Each plot is also labeled by "Stable" or "not Stable" as obtained from the analytical theory.*

The second method we present is the computation of the maximal Ljapunov exponent of the dynamical system [23]. The Ljapunov exponent is a quantity that characterizes the rate of separation of two trajectories that start with infinitesimally close initial conditions. It is defined in the following way:

$$\lambda = \lim_{t\to\infty} \lim_{|\delta \mathbf{x}_0|\to 0} \frac{1}{t} \ln \frac{|\delta \vec{x}(t)|}{|\delta \vec{x}_0|} \qquad \text{where} \quad \vec{x}(t) \ \text{ is a trajectory with I.C. } \ \vec{x}_0$$

From the definition, we observe that a negative Ljapunov exponent implies that two close trajectories stay close for increasing time. Thus implying stable oscillations. On the contrary, a positive Ljapunov exponent implies that the distance between two infinitesimally close trajectories diverge to infinity when the time increases, thus suggesting chaoticity of our solutions.

In our case we cannot compute analytically the Ljapunov exponent so we will compute it numerically using the method explained by Sprott in [23]. The corresponding results are shown in figure (1.15). We clearly see that the stable oscillations at $T = 12$ have a negative Ljapunov exponent, while the ones at $T = 15$, that we supposed to be chaotic because of the filling curve in phase space and their power spectrum, are indeed chaotic because the Ljapunov exponent is clearly positive.

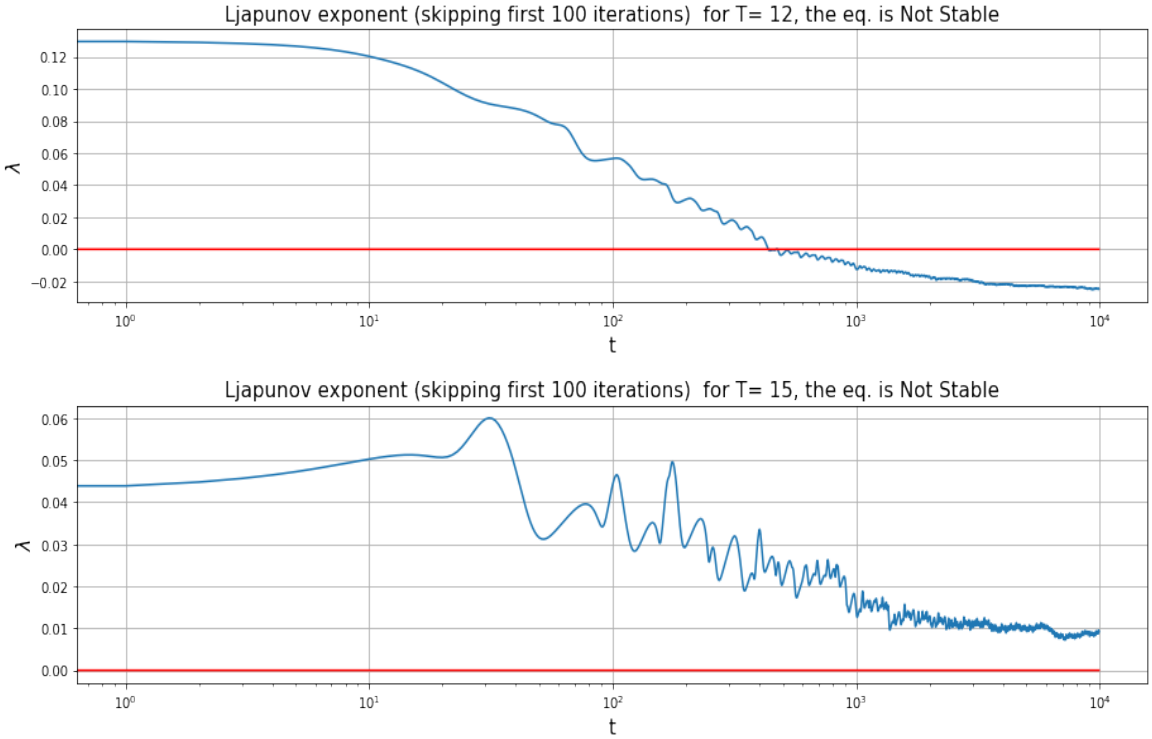

Figure 1.15: *Ljapunov exponent of the system, which trajectories are represented in figure (1.13) for two different values of the delay. The first is such that the solution is a stable oscillation, while the second is a chaotic one. The red line is the x-axis and represents the threshold over which the exponent is positive and the solutions are considered chaotic. Each plot is also labeled by "Stable" or "not Stable" as obtained from the analytical theory.*

CHAPTER 2

RANDOM MATRICES

One of the most important papers in ecology is undoubtedly Robert May's article on the stability of ecosystems [13]. This paper has the merit of introducing for the first time the Random Matrix Theory into the analysis of ecological systems; using some techniques of this theory, which at that time was still developing, He obtained the famous "May's theorem" and formulated in a precise way the famous "Complexity-Stability paradox".
In this chapter we will review his first results and some recent generalizations of them to more complex ecosystems. We will then analyze, using a similar approach, the analog of May's linear equation when the ecosystem is described by a system of ordinary differential equations which depends not only on the populations at the present time, but also on the past populations with a fixed time delay.

2.1 Random matrices without delay

We model a simple ecological system with a generic autonomous ordinary differential equation where $\vec{x}$ is the vector of the populations (or densities) of the S species and $\vec{F}$ is the mapping function which depends exclusively on the population densities. To study the solutions of the system near their equilibrium x^*, given by: $F(\vec{x}^*) = 0$, we will use local asymptotic stability analysis. The first step consists in the linearization of the equations near x^* which results in the linear system:

$$\frac{d\vec{x}}{dt} = \vec{F}\big(\vec{x}(t)\big) \qquad \Rightarrow \qquad \frac{d\vec{y}}{dt} = A \cdot \vec{y}(t) \qquad \text{with:} \qquad \vec{y} = \vec{x} - \vec{x}^* \quad A_{i,j} = \left.\frac{\partial F_i(\vec{x})}{\partial x_j}\right|_{\vec{x}^*} \tag{2.1}$$

Here the $(S \times S)$ matrix A is the Jacobian matrix of the function $\vec{F}$ with respect to the vector $\vec{x}(t)$ computed at the equilibrium point $\vec{x}^*$, in ecology this particular matrix is called "Community matrix".

The purpose of Linear Stability Analysis is to discover whether the system is able to damp or extinguish infinitesimal perturbations of the solutions near the equilibrium. In addition, the stability of the equilibrium is described by the eigenvalues of the Community matrix. For our purposes, we will assume that all the eigenvalues are hyperbolic, namely they all have nonzero real part. When all eigenvalues have negative real parts the equilibrium is stable, however if at least one eigenvalue has positive real part the equilibrium is unstable, because the solutions diverge at least along one direction (only from a local point of view) if subjected to an infinitesimal perturbation.
This method is clearly excellent to inspect the stability of solutions in the sense of discovering the conditions under which they converge monotonically to the equilibrium. However this technique is not strong enough to study the instability region, i.e. where the solutions do not converge to the equilibrium, (and so to infer the instability of the solutions) because it takes into account only the linearized system and doesn't consider the influence of non-linear terms which generally play an important role in the unstable case.
When the Community matrix has at least a positive eigenvalue, the Linear Stability Analysis tells us that the equilibrium is locally unstable, but we cannot use this to infer anything on the global stability. For instance, the solutions in the vicinity of the equilibrium could diverge to infinity or instead they could persist with limit cycles or even chaotic attractors.
Another limitation of the Linear Stability Analysis is that the local stability is defined only on a certain basin of attraction, i.e. only the solutions which are in a neighborhood of the equilibrium follow the properties we discovered, in many cases indeed the basin of attraction is difficult to estimate analytically.

Next, we want to characterize more accurately the Community matrix of a generic ecological system, indeed one of its main properties is that its entries are always real values because $\vec{F} \in \mathbb{R}$. This means that the trace is a real number and therefore all the eigenvalues must either be real or pairs of conjugate complex numbers:

$$Tr[A] = \sum_i \lambda_i(A) \in \mathbb{R} \quad \Rightarrow \quad \lambda(A) = a \;\; ; \;\; \lambda(A) = a \pm ib \quad \text{with} \quad a, b \in \mathbb{R}.$$

Therefore, if we plot the eigenvalues of the matrix on the complex plane we obtain a set of points which is symmetric with respect to the real axis. The stability of the equilibrium is uniquely determined by the real part of the rightmost eigenvalue(s): if that is (are) negative, then the equilibrium is stable, otherwise it is unstable.

It is theoretically possible to compute the Jacobian matrix directly by deriving the function $\vec{F}$. In many cases this function is not known, because ecosystems include an incredible number of interactions and it is not possible to measure them all.
The technique used to make a valid model for all these cases, which was introduced by May[13], relies on disregarding completely the computation of the Jacobian and

considering directly the Community matrix which is assumed to be a random matrix. We can indeed generate the interactions between the species, i.e. the entries of the matrix, by sampling them from a probability distribution which has some fixed parameters like, for instance, the first 2 moments, then we construct the matrix by choosing a precise structure or also its sparseness. Finally we observe that, using this method, instead of knowing the dynamics of the complete ecological system, which is given by $\vec{F}$, we just need to know some of its more descriptive and meaningful parameters and the structure of the food web (or in general the structure of the network of interactions).

2.1.1 May's theorem

In 1972, Robert May writes his celebrated article: "Will a Large Complex System be Stable?" [13] where he introduced for the first time the idea of using random matrices instead of real Community matrices to describe ecological systems. He was also able to obtain a stability criterion. In the next paragraphs we will briefly explain it.

To begin with, May supposed the Community matrix to be a random matrix with connectance C, which means that with probability $(1 - C)$ the entry $A_{i,j}$ is zero, instead with probability C it is sampled from a probability distribution with zero mean and variance σ^2: $A_{i,j} \sim P(0, \sigma)$. The presence of a connectance term implies the sparsity of the matrix and this is necessary to have a meaningful description of the ecosystem; in fact in any ecological system a single species on average interacts only with few others and not with all of them.
In addition, the diagonal entries of the matrix generally are chosen to be constant negative values $A_{i,i} = -d$. This choice is necessary for species to be self regulating, indeed this is the analogue of setting a carrying capacity that binds each population in the ecosystem.

Later on, May investigated whether a linear system of type (2.1), with Community matrix sampled with the method we described above, is stable or not. This translates directly into the analysis of the distribution of the eigenvalues of the random matrix.
May concludes that, for large dimensions S of the random matrix, the probability that any matrix drawn from the ensemble will almost certainly correspond to a stable system, indicated as $P(S, C, \sigma)$, tends to 1 if the variables respect the following stability criterion:

$$P(S, C, \sigma) \to 1 \qquad \Longleftrightarrow \qquad \sigma\sqrt{SC} < d. \tag{2.2}$$

He also presents 2 important corollaries:

1 If 2 ecological systems with the same size have $\sigma_1^2 C_1 \simeq \sigma_2^2 C_2$, then they have a similar stability character. Therefore, if the species of one system have more interactions (bigger connectance), then they must have weaker interactions in

order to have a corresponding "level of stability".

2 May noticed that the structure of the Community matrix also plays an important role. For instance, unstable systems which have a simple random community matrix can become stable if the interactions are rewired into smaller blocks.

This important paper gave rise to the Diversity-Stability debate showing that, using this mathematical formulation, an increase on the complexity/diversity of the ecosystem (defined mathematically by $\sigma\sqrt{SC}$), which is provoked by the increase of S, C, σ, leads to a resulting decrease of stability instead of an increase of that, like what the empirical observations suggest us.

2.1.2 Generalizations of May's theorem

In his paper May explains that his intuition, suggested by the analogy with the Central Limit Theorem, on the distribution of eigenvalues and consequently the criterion for the stability of the system, was inspired by Wigner's work: the "Semi-Circular law" which was valid only for symmetric matrices and by the contemporary work on non-Hermitian matrices by Metha and Ginibre. The final proof that justifies May's stability criterion was ultimately provided by Tao et al. [24] with the so called "Circular law" which states:

> *Given a $(S \times S)$ random matrix M, with i.i.d entries (i.e. independent and identically distributed) which have zero mean, unit variance and finite higher moments, the spectral distribution of the matrix $M/\sqrt{S}$, when $S \to \infty$, converges to a uniform distribution on the unit disk centered on the origin of the complex plane.*

In addition we notice that this law doesn't depend on the probability distribution of the entries of the matrix. Indeed, like for the Central Limit Theorem, the Circular law is universal because it depends only on the first and second moments of the distribution (mean and variance).

Starting from the simple Circular law, we can now abstract it to more complex random matrices obtaining first May's stability criterion and then, by relaxing even more assumptions, also some important generalizations of May's criterion. We will reproduce here the results of Allesina et al. [18] starting from the simple case of the Circular law in which the matrix M has:

$$\max\left[Re[\lambda(M)]\right] \sim \sqrt{S}.$$

First of all we will relax the constraint of unit variance on the i.i.d. entries of the matrix. If we suppose that its entries have a fixed variance σ^2, we can rescale it and return back to the original matrix by dividing the entries by σ, this means that now we have:

$$\max\left[Re[\lambda(M)]\right] \sim \sigma\sqrt{S}.$$

Next we relax the condition that all the entries must be sampled from a given distribution. Indeed, we can also consider matrices which are sparsely connected, i.e. the entries are zero with probability $1-C$ and sampled from the original distribution with probability C. In this case the variance becomes $\sigma^2 \to (1-C)\cdot 0 + C\cdot\sigma^2 = C\sigma^2$, thus we get:

$$\max\left[Re[\lambda(M)]\right] \sim \sigma\sqrt{SC}.$$

In addition we can consider the effect of the diagonal entries on the distribution of the eigenvalues of the matrix M. We know indeed that the diagonal of the matrix determines the mean of its eigenvalues thanks to the relation: $Tr[M] = \sum_i M_{i,i} = \sum_i \lambda_i(M)$. We can intuitively conclude that the sum of a fixed value $-d$ to all the diagonal elements of M shifts to the left the distribution of eigenvalues along the negative direction of the real axis. We also show this in an analytical way: if we compute the eigenvalues of the modified matrix $M \to M - d\mathbb{1}$ we obtain the characteristic equation: $det(M - d\mathbb{1} - \lambda\mathbb{1}) = 0$, this can be solved easily by substituting $(\lambda + d)$ with another variable obtaining finally $\lambda_i = -d + eig_i(M)$ which is the actual shifted eigenvalues.
We finally get the same eigenvalue with maximal real part obtained by May (if we impose that it is less than zero we get again the stability criterion 2.2):

$$\max\left[Re[\lambda(M)]\right] \sim \sigma\sqrt{SC} - d.$$

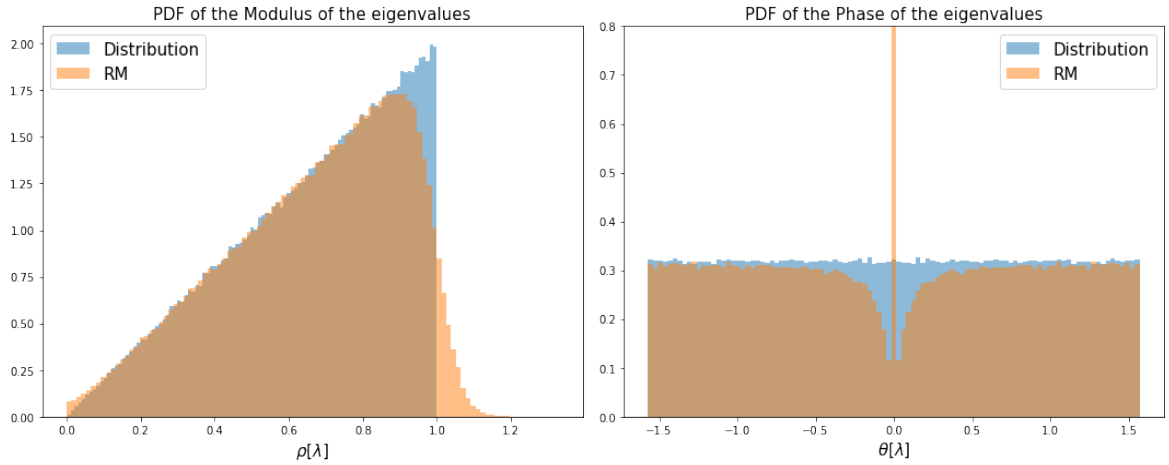

Figure 2.1: *Comparison between the probability distribution function of the Modulus and the Phase of the eigenvalues of a Random matrix with* $S = 100$, $C = 1$, $\sigma = 0.1$ *and the same quantities computed for eigenvalues sampled from a uniform distribution in the circle of radius one and center* $(0, 0)$.

In figures (2.1,2.2) we have shown the main differences between a typical uniform distribution of points on the unit disk and the distribution of the eigenvalues of 10^4 randomizations of the random matrix $M/\sqrt{S}$. We observe that the eigenvalues are not all exactly inside the unit circle, because the dimension of the matrix and the number of randomizations is not infinite, instead the border of the distribution is smoothed. The width of the smooth border decreases for increasing dimensions S until it becomes a precise step function at $S \to \infty$.

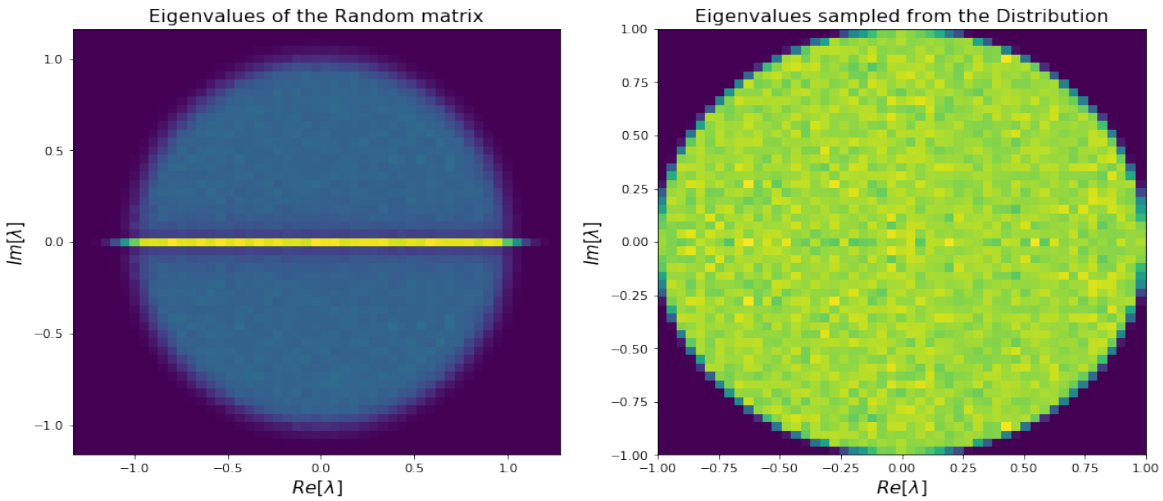

Figure 2.2: *Comparison of the eigenvalues distributions on the complex plane obtained using the two different methods described above (diagonalization of a random matrix and sampling from a uniform distribution). In both the figures we computed the distributions by taking the average over* 10^4 *random matrices.*

Another interesting thing is that there are a lot more eigenvalues on the real axis, i.e. $\theta(\lambda) = 0, \pi$, with respect to the generic uniform distribution on the disk. This behavior can be explained only by some non-trivial theorems on the convergence of the eigenvalues in the Random Matrix Theory, which we won't explain in this work. The proof is based on 2 main concepts: the eigenvalues must be either real or pairs of conjugate complex numbers and also a non-zero fraction (C) of the matrix entries are identically zero.

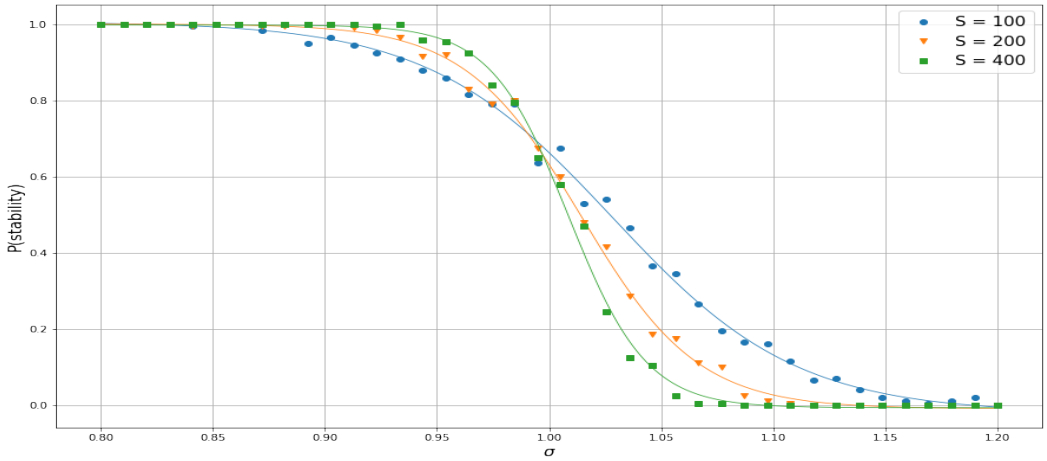

Figure 2.3: *Probability of stability of random matrices with different dimensions* S *as a function of* σ*. All matrices have* $C = 0.5$ *and diagonal* $d = -\sqrt{SC}$ *such that the critical point is* $\sigma = 1$ *and the stability criterion reduces to* $\sigma < 1$*. We computed the Probability by taking 200 randomizations for each combination* $(\sigma,\ S)$*. The solid lines are the best fitting logistic curves.*

Moreover in figure (2.3) we show how the Probability of stability of a Random matrix changes when we increase some parameters (in this case σ). The Probability of stability has been computed as the ratio between the number of stable matrices and the total number of randomizations (200). We observe clearly the decrease on the width of the transition region of the Probability of stability for increasing dimensions of the matrix; ideally the plot at $S \to \infty$ becomes a step function.

Origins of random matrices: the Wigner distribution

The first analytical description of the distribution of eigenvalues of a random matrix was determined by Wigner; his "Semi-Circular law" gives the probability distribution of the eigenvalues of a symmetric random matrix M. Here we present a brief explanation of Wigner's Semi-Circular law taken from [7].
First we define the joint probability density function of all the eigenvalues of the symmetric matrix M; the particular form of this function was discovered in the prehistory of the Random Matrix Theory and we won't present here its proof:

$$p(x_1 \dots x_S) = Z^{-1} \exp\Big(-\frac{1}{2}\sum_{i=1}^{S} x_i^2 \Big) \prod_{j<k} |x_j - x_k| \qquad Z = \text{normalization constant.}$$

The first thing we notice by looking at the distribution is that the exponential term prevents the eigenvalues to stray too far from zero. The factors with absolute value suppress all the configurations in which two eigenvalues are too close. This repulsion factor makes the eigenvalues strongly non-independent because each of them feels the presence of all the others and it is repelled from them.
Starting from this function we can derive the probability density function of sampling a single eigenvalue of M. This is clearly the marginalized pdf $p(x)$ and we can show that in the following way:
We first define a counting function which allows us to compute how many eigenvalues of M are in any given range $[a, b]$:

$$n(x) = \frac{1}{S}\sum_{i}^{S} \delta(x - x_i) \qquad \text{then:} \qquad \int_a^b n(x)dx = \text{ fraction of eigenvalues in } [a, b].$$

Then for any random matrix M, $n(x)$ is a random measure on the real line and, if we take its average over all possible realizations of eigenvalues $\{x_1 \dots x_S\}$ of M, we obtain the distribution of a single eigenvalue of the matrix which is indeed:

$$\langle n(x) \rangle = \int\int p(x_1 \dots x_S) n(x) d\vec{x} = \frac{1}{S}\sum_{i}^{S} \int p(x_1 \dots x_S)\delta(x - x_i) d\vec{x} := p(x).$$

The previous equivalence can be proven immediately by using the fact that $p(x_1 \dots x_S)$ is symmetric over exchange of variables.
Finally we just assert that in the limit of the dimensions of the matrix going to infinity it is possible to compute the marginalized pdf and this gives exactly the "Semi-Circular" probability density of the single eigenvalue:

$$p_{SC}(x) = \lim_{S\to\infty} \sqrt{S} p(\sqrt{S}x) = \frac{1}{\pi}\sqrt{2 - x^2} \qquad \text{with} \quad p(x) := \int\int p(x, x_2 \dots x_S) dx_2 \cdots dx_S$$

This result is the precursor of Random Matrix Theory and of the complete "Circular law" proved in [24]. By applying the same procedures used in the previous section we are able to compute also in this case the maximal eigenvalue of the symmetric matrix M with dimensions $(S \times S)$, variance σ, connectance C, and diagonal elements $-d$

which turns out to be:

$$\max\left[\lambda(M)\right] \sim \sigma\sqrt{2SC} - d \qquad \text{with:} \quad \lambda(M) \in \mathbb{R}. \tag{2.3}$$

Non-zero mean case

We can assess now the effect of having a non-zero mean of the probability distribution from which we sample the matrix elements. We get in fact that the expectation value of the non-diagonal entries of M becomes now: $\mathbb{E}[M_{i,j}] = (1-C)\cdot 0 + C\cdot\mu = C\mu$ while the variance of the non diagonal entries also changes becoming:
$V = \mathbb{E}[M_{i,j}^2] - \mathbb{E}^2[M_{i,j}] = (1-C)0 + C(\sigma^2+\mu^2) - C^2\mu^2 = C(\sigma^2 + (1-C)\mu^2)$.
Next we compute the expectation value of the row sum of any row of matrix M obtaining:

$$\mathbb{E}\big[\sum_j M_{i,j}\big] = -d + \sum_{j\neq i}\mathbb{E}[M_{i,j}] = -d + (S-1)C\mu \qquad \forall i.$$

The independence of the row sum on the index i means that the vector $\vec{1}$, in the limit $S\to\infty$, becomes an eigenvector of matrix M with eigenvalue given by the expectation value of the row sum.
Now we can compute both the radius of the disk in which the eigenvalues are distributed, which is $\sqrt{SV}$, and also its new center by taking the mean of all the eigenvalues except the row sum. We can do this by subtracting the row sum from the sum of all eigenvalues, i.e. the trace $Tr(M) = -dS$, and dividing the result by $(S-1)$, we get then that the new center of the disk is: $(-d - C\mu,\ 0)$.
Finally, given all the previous results, we obtain that the eigenvalue with maximal real part is, depending on the magnitude of μ, either the row sum or the one given by the radius of the disk:

$$\max\left[Re[\lambda(M)]\right] \sim \max\left[\sqrt{SV} - d - C\mu,\ \ -d + (S-1)C\mu\right] = \max\left[\sqrt{SV},\ SC\mu\right] - d - C\mu. \tag{2.4}$$

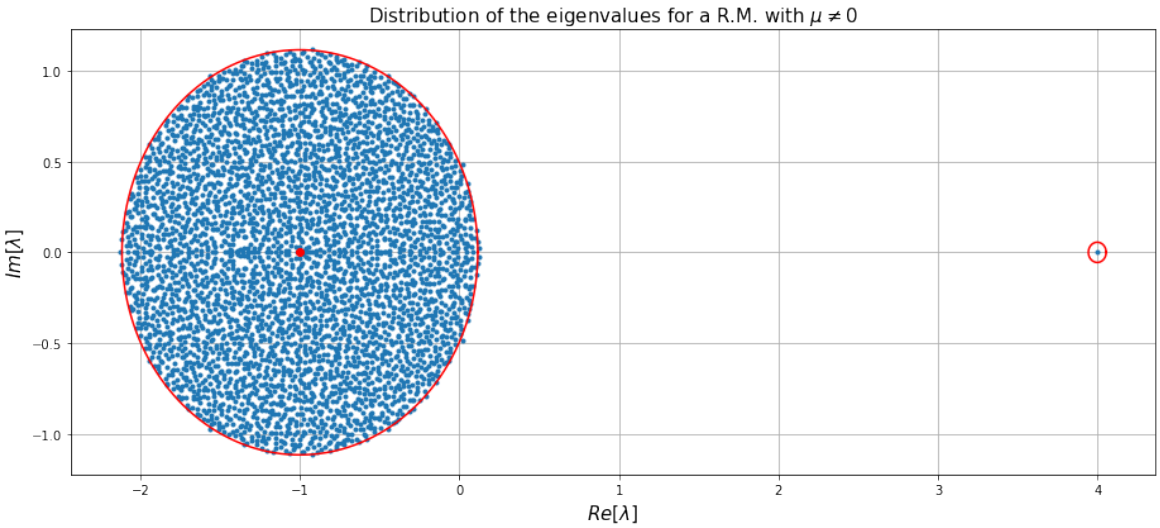

Figure 2.4: *Distribution of the eigenvalues of a random matrix with entries sampled from a distribution with non-zero mean and:* $S = 4000,\ C = 0.025,\ \sigma = 0.1,\ \mu = 0.05,\ d = -1$. *The isolated point in* $(4, 0)$ *is the row sum eigenvalue which we computed above.*

Elliptic law

Finally we can relax also some constraints on the structure of the Community matrix and on the correlation between the entries. In fact, up to now we have considered all the entries of M to be i.i.d. without any correlation between $M_{i,j}$ and $M_{j,i}$. We know indeed that in ecosystems there are often pairwise interactions like predator-prey, mutualistic or competitive, so the entries $M_{i,j}$ and $M_{j,i}$ must be correlated in some way. For example, in the predator-prey case the two entries must have opposite signs, i.e. the predator population grows (+) when interacting with preys which instead decrease (−), while in the mutualistic or in the competitive one they have the same signs (respectively positive and negative). This means that instead of sampling each coefficient independently from the others, we should sample them in pairs $(M_{i,j},\ M_{j,i})$ from a bivariate distribution $P(x, y)$ which has some correlation $\rho = \mathbb{E}[xy]$. This allows us to formulate the "Elliptic law", proposed in [9], which is a generalization of the "Circular law" for coefficients sampled from bivariate distributions:

> *Let M be a $(S \times S)$ matrix with i.i.d off-diagonal coefficients sampled in pairs from a bivariate distribution with zero marginal means, unit marginal variances, finite higher moments and correlation ρ. The spectral distribution of the matrix $M/\sqrt{S}$, when $S \to \infty$, converges to a uniform distribution on the ellipse with horizontal semi-axis $a = 1 + \rho$, vertical semi-axis $b = 1 - \rho$ and center on the origin of the complex plane.*

Like we did for the Circular law, we are able to generalize the Elliptic law for partially connected matrices with non-zero marginal means, non unit variances (arbitrary covariance matrix) and with constant diagonal elements $-d$. For instance, we consider here the general case of a matrix M with:

$$(M_{i,j},\ M_{j,i}) = \begin{cases} -d & \text{when} \quad i = j \\ (0,0) & \text{with probability } (1-C) \\ \sim P(\vec{\mu}, \Sigma) & \text{with probability } C \end{cases} \qquad \text{and} \quad \vec{\mu} = \begin{pmatrix} \mu \\ \mu \end{pmatrix} \quad \Sigma = \begin{pmatrix} \sigma^2 & \tilde{\rho}\sigma^2 \\ \tilde{\rho}\sigma^2 & \sigma^2 \end{pmatrix}$$

We obtain then the following statistics for the off-diagonal coefficients:

$$\mathbb{E}[M_{i,j}] = C\mu \quad \mathbb{V}ar[M_{i,j}] = C(\sigma^2 + (1-C)\mu^2) \quad \rho = \frac{\mathbb{E}[M_{i,j}M_{j,i}] - \mathbb{E}^2[M_{i,j}]}{\mathbb{V}ar[M_{i,j}]} = \frac{\tilde{\rho}\sigma^2 + (1-C)\mu^2}{\sigma^2 + (1-C)\mu^2}.$$

Each off-diagonal entry of the matrix now has the same mean value μ, so like for the previous case we expect the row sum to be an eigenvalue with value $(-d + (S-1)C\mu)$. Also we notice that again the ellipse is centered in $(-d - C\mu,\ 0)$ and has horizontal semi-axis: $\sqrt{SV}(1+\rho)$.
Finally we conclude that the eigenvalue with maximal real part is:

$$\max\left[Re[\lambda(M)]\right] \sim \max\left[\sqrt{SV}(1+\rho),\ SC\mu\right] - d - C\mu. \tag{2.5}$$

Some numerical examples

We now present some examples of the distribution of eigenvalues of particular random matrices with high dimensions. The four types of random matrices we consider here and also in the next sections are the ones proposed by Allesina [17]:

- *Symmetric matrix*: is the most simple random matrix, its eigenvalues are real and distributed according to Wigner's distribution with stability condition (2.3).

- *Random matrix*: generic random matrix where the entries are sampled from a univariate distribution and the eigenvalues follow the stability condition obtained by May (2.2).

- *Predator-Prey matrix*: random matrix in which the entries are sampled from a bivariate distribution with negative correlations, this means that the coefficients $(M_{i,j},\ M_{j,i})$ have opposite signs, the predator has a positive one, while the prey a negative one. The stability condition is (2.7).

- *Mixed matrix*: random matrix in which the entries are sampled from a bivariate distribution with positive correlations, this means that the coefficients $(M_{i,j},\ M_{j,i})$ have same signs, if the signs are positive the interaction between the 2 species is mutualistic while if they are negative the interaction is competitive. The stability condition is (2.7).

To construct the predator-prey random matrices and the mixed matrices we use a method which allows us to sample the entries from a distribution with fixed sign of the random variables; therefore instead of sampling them from the selected pdf we will sample them from the pdf of the absolute value of the random variable. Thus if $P(x)$ is the probability distribution, for the predator-prey case we will sample one interaction strength from the distribution of $|x|$ and the other from the distribution of $-|x|$; for the mixed case we will sample the entries either both from the distribution of $|x|$ or both from the distribution of $-|x|$ (with the same probability of choosing each sign).
This is analogous to sampling the entries from a bivariate distribution where the correlations ρ of the predator-prey matrix and the mixed matrix are:

$$\rho_{pp} = \frac{\mathbb{E}[|x|]\mathbb{E}[-|x|]}{\sigma^2} = -\frac{\mathbb{E}^2[|x|]}{\sigma^2} = -\frac{2}{\pi} \qquad \rho_m = \frac{\mathbb{E}[\pm|x|]\mathbb{E}[\pm|x|]}{\sigma^2} = \frac{\mathbb{E}^2[|x|]}{\sigma^2} = \frac{2}{\pi}. \quad (2.6)$$

The last passage in the equations above can be explained in the following way: considering that the distribution from which we sample the entries is now relevant, because obviously different distributions have different correlations, we choose to use a Gaussian distribution with zero mean and therefore we compute $\mathbb{E}[|x|]$ as :

$$\mathbb{E}[|x|] = \int_{-\infty}^{\infty} \frac{|x|}{\sqrt{2\pi\sigma^2}} \exp\Big(-\frac{x^2}{2\sigma^2}\Big)dx \ = \ \sqrt{\frac{2\sigma^2}{\pi}} \int_0^{\infty} 2ye^{-y^2}dy \ = \ \sqrt{\frac{2\sigma^2}{\pi}}.$$

Finally, using (2.5), the stability criteria of these two types of matrices become:

$$\text{Predator-Prey:} \quad \sigma\sqrt{SC} \leq \frac{d\pi}{\pi - 2} \qquad \text{Mixed:} \quad \sigma\sqrt{SC} \leq \frac{d\pi}{\pi + 2}. \tag{2.7}$$

We observe that the distribution of the eigenvalues of both the matrices will be an ellipse with center $(-d, 0)$ and semi-axes: $a = \sigma\sqrt{SC}(1 - 2/\pi)$ and $b = \sigma\sqrt{SC}(1 + 2/\pi)$. However for the predator-prey matrix the ellipse has a smaller horizontal semi-axis, while for the mixed matrix the smaller semi-axis is the vertical.
Finally, in figure (2.5) we show the distributions of the eigenvalues of the four different types of matrices that we listed above. The first two follow the Semi-Circular and the Circular law, while the last two are perfectly described by the Elliptical law.
Furthermore, we are able to assess the role of the magnitude of the interaction strengths. In fact, σ provides information only on the average interaction strength while $\mathbb{E}[|x|]$ describes their magnitude and takes into account also the presence of weak interactions. Therefore, by using distributions with different $\mathbb{E}[|x|]$ (for example in a uniform distribution this has a bigger value than in a Gaussian one, even though σ is the same), we can increase or decrease the stability of the system. Indeed if we consider (2.6), it is clear that if we choose a distribution with higher interaction strength $\mathbb{E}[|x|]$ we actually increase the stability of the predator-prey system (and decrease it for the mixed case). If we use weaker interactions, the predator-prey system is destabilized while the mixed system gets more stable.

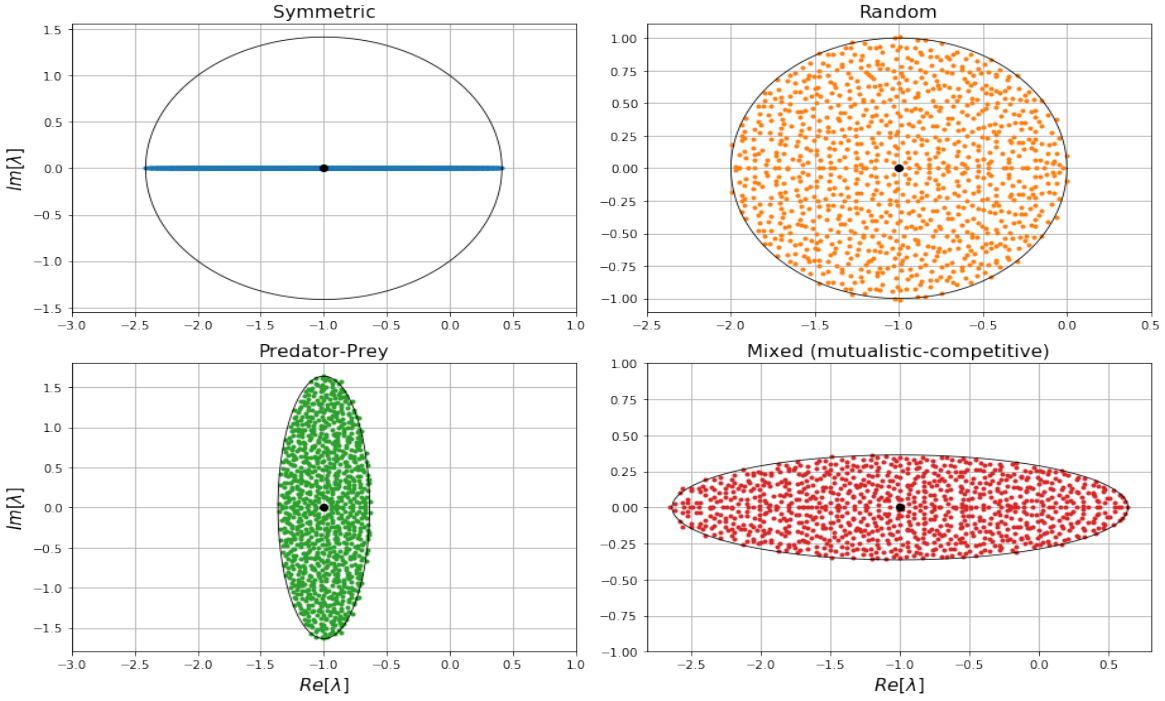

Figure 2.5: *Distributions of the eigenvalues of different types of random matrices with entries sampled from a distribution with zero mean and all with:* $S = 1000,\ C = 0.1,\ \sigma = 0.1,\ d = -1$.

Next we want to study how the stability of these matrices changes with respect to their parameters, by considering the various stability criteria. In fact we already know from the theory that there is a stability transition in the system, because for increasing values of the parameters, it passes from a stable state to an unstable one.

The transition point is predicted analytically by the stability criteria. In figure (2.6) we can clearly see the phase transition of each different type of matrix. Indeed by increasing the parameters σ and C we get that the eigenvalue with maximal real part passes from the left to the right of the imaginary axis and the system becomes unstable.

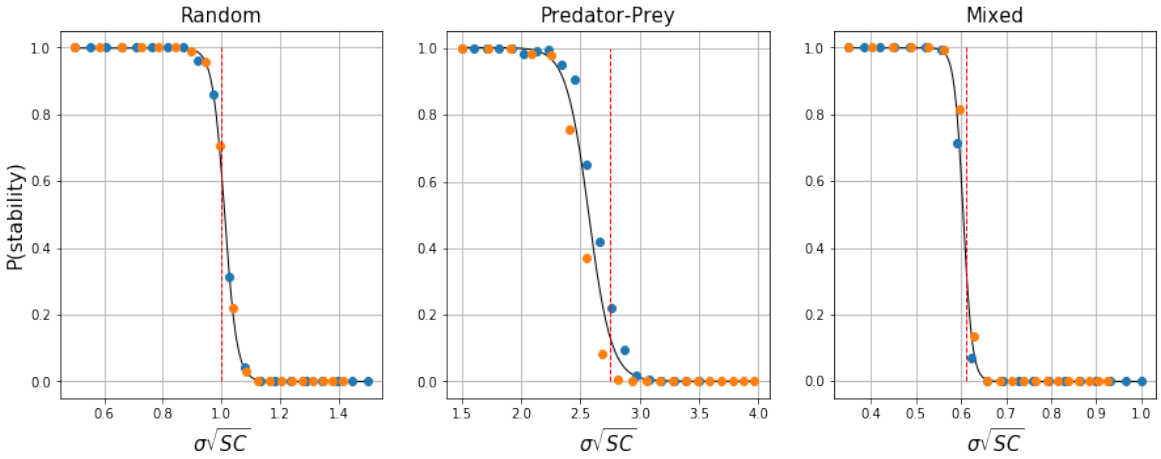

Figure 2.6: *Probability of stability of the 3 types of random matrices as a function of the complexity $\sigma\sqrt{SC}$ (using 200 randomizations for each type); we consider matrices with fixed dimension ($S = 250$), the blue points are referred to matrices with fixed $C = (0.1, 0.1, 0.1)$ and variable σ while the orange ones are referred to matrices with fixed $\sigma = (0.1, 0.3, 0.07)$ and variable C. The black lines are the best fitting logistic curves for all the dataset while the red dashed lines are the transition point predicted by the theory.*

In these figures we computed the probability of stability as the ratio between the number of stable matrices and the total number of randomly generated matrices (in this case we generated 200 random matrices for each choice of parameters); clearly the transition is well represented by a logistic curve of Verhulst type (1.1).

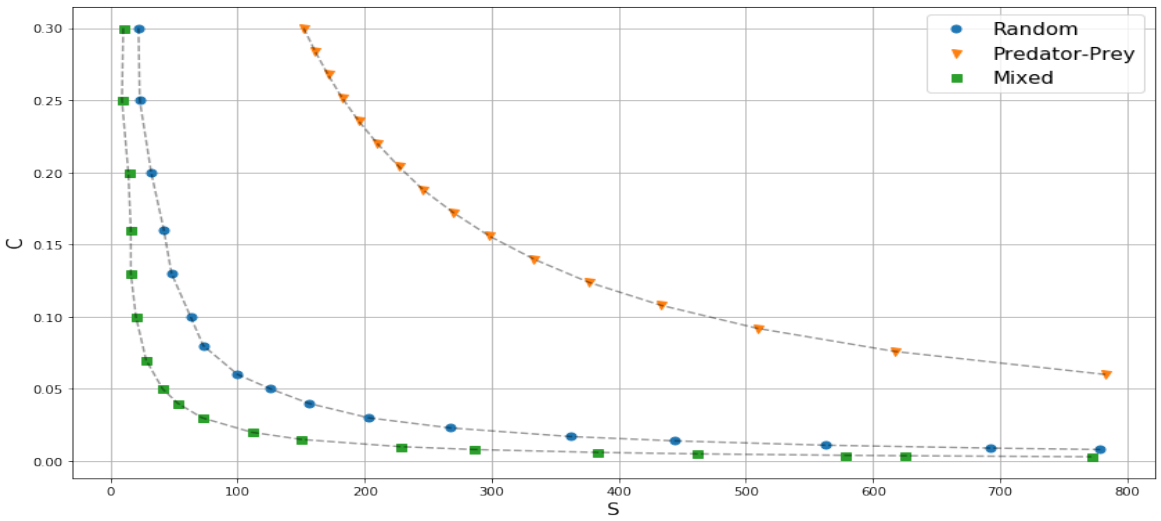

Figure 2.7: *Stability criteria for the three different random matrix types fixing $\sigma = 0.4,\ d = -1$.*

In the end we investigated also the relation between the dimension of the matrix S and its connectance C by fixing the parameters σ, d and, by varying C in a certain range of values, compute for each value of C the maximal dimension $S \in \mathbb{N}$ of the matrices such that the system has probability of stability bigger than one half (which

means that at least half of the sampled matrices are stable). It is possible to see in figure (2.7) that the dependence between the 2 parameters is $S \propto C^{-1/2}$ like we obtained in the analytical stability criterion.

Other improvements of the model

In conclusion, there is still room for improvements in the description of the ecosystems by using different types of random matrices. Indeed we can use the fact that the Community matrices should represent the actual network of interactions between the various species. In the section above we generalized the description of the random Community matrix by increasing its fundamental parameters and relaxing some of its main constraints, but none of these actions really changed the structure of the network. We always had an unstructured matrix, which is equivalent to a completely random graph.
The idea of using more structured random matrices originates from the evidence that Community matrices built from empirical food webs have an intrinsic structure, for instance they represent nested or scale free networks, generally it is possible that they are more stable than the randomly built ones, because they are more realistic. Therefore, the last and most complex restriction to relax is the constraint on the structure of the network (i.e. the Community matrix). Indeed we can generate the different interactions still in a random way, but including also some insights or knowledge on the structure of the network. For example, the Community matrices could be block or nested matrices or, instead of a random graph, they could represent a graph with a power law distribution of the interactions, i.e. a scale free network, or finally we could also use the so called niche and cascade models to create more realistic systems.
All these different structures of the Community matrix have been explored already, even if not exhaustively enough, by Allesina [18], who obtained some counter-intuitive results. He found out that generating more realistic matrices in this way generally hampers the stability, giving systems which are less stable than the unstructured ones; this problem generally is explained by the fact that the community matrix is only an approximation near the equilibrium, while the network structure should emerge in the original differential equation.
In our work we will not explore these characteristics of the system, but we will concentrate onto unstructured random matrices like the ones we used in the section above.

2.2 Random matrices with delay

In order to introduce the effect of past populations into the modeling of the ecological systems, we will consider the following system of autonomous ordinary differential equations, in which the mapping function depends also on the previous populations according to a fixed time delay T. Like before $\vec{F}$ is the mapping function and $\vec{x}$ is the vector of the populations (or densities) of the S species.
We continue our analysis of the time delayed ecological systems using a simple DDE, i.e. delay differential equation, which has the following form:

$$\frac{d\vec{x}}{dt} = \vec{F}\big(\vec{x}(t), \vec{x}(t-T)\big).$$

Our principal objective is to examine how the solutions of the delayed system behave near their equilibrium $\vec{x}^*$, given by: $\vec{F}(\vec{x}^*, \vec{x}^*) = 0$. To perform this analysis, we will first expand the equations near $\vec{x}^*$, obtaining the linear system of DDEs:

$$\frac{d\vec{y}}{dt} = \; A \cdot \vec{y}(t) \; + \; B \cdot \vec{y}(t-T) \qquad \text{with:} \qquad \vec{y} = \vec{x} - \vec{x}^*. \tag{2.8}$$

This new system of DDEs is correct up to the first order of approximation, so we are able to explore the stability of the solutions near the equilibrium $\vec{x} = \vec{x}^*$ (i.e. $\vec{y}^* = 0$), with $|\vec{y}| << |\vec{x}^*|$.
Here A and B are the $(S \times S)$ Jacobian matrices of the map $\vec{F}$ differentiated with respect to the populations $\vec{x}(t)$ and $\vec{x}(t-T)$ and computed at the equilibrium point $\vec{x}^*$. These are the Community matrices which, along with the delay parameter and the initial conditions, characterize uniquely the system.

As for the non-delayed case, we could calculate the Community matrices directly by differentiating the function $\vec{F}$, but often we don't really know its exact form. To avoid this problem, we use May's idea and consider the Community matrices as random matrices which we will sample from a probability distribution that depends only on a smaller set of parameters (like mean, variance, etc.).

2.2.1 Stability using the Ljapunov function method

The first and most simple method we can use to study the stability of the solutions near the equilibrium ($\vec{y}^* = 0$) of the linearized DDE is the so called Ljapunov function method; this method allows us to investigate under what conditions on A and B, the trivial solution of (2.8) is asymptotically stable, independently on the delay T. This technique clearly will give us only some sufficient conditions for stability. In fact, being independent on the delay, they are not strong enough for a fine study of the transition from a stable to unstable state, therefore, if we want to get finer conditions, we need to refine the method (we will do it in the section below).
A generic function $L(t) = L(y(t))$ is a Ljapunov function for a system of ordinary differential equations if, and only if, the following conditions are satisfied:

- $L(y) > 0 \quad \forall y \neq 0$ it is positive for any value of y which is not the equilibrium.
- $L(y = 0) = 0$ it goes to zero in the equilibrium point.
- $\frac{d}{dt}L(t) \;=\; \vec{\nabla}L(y)\dot{\vec{y}} \;\leq 0 \quad \forall \vec{y}(t)$ the function is monotonically decreasing in time for any trajectory near the equilibrium, i.e. any solution of (2.8).

Therefore, if the conditions prescribed above are satisfied, we can conclude that the equilibrium is globally asymptotically stable; instead if they are satisfied only locally near the equilibrium then that is only locally asymptotically stable.
Now we define the Ljapunov function we will use in our system as:

$$L(t) = \; y^2(t) \; + \; \alpha \int_{t-T}^{t} y^2(s)ds \; = \; \vec{y}^T(t)\vec{y}(t) \; + \; \alpha \int_{t-T}^{t} \vec{y}^T(s)\vec{y}(s)ds \qquad \text{with:} \quad \alpha > 0. \tag{2.9}$$

The first two conditions are easy to verify from the definition of the function L, while the third inequality is not elementary and it is not always verified because it depends on the matrices A, B. Therefore if we impose the third constraint, we get a condition on the matrices, or on their eigenvalues, for the stability of the equilibrium.
Thus we will rewrite the third constraint in a simpler way, which includes also the matrices A, B; by using the following notation for the variables, $\vec{y} = \vec{y}(t)$ and $\vec{y}_T = \vec{y}(t - T)$, we obtain:

$$\frac{d}{dt}L(t) \;=\; \vec{y}^T\dot{\vec{y}} + \dot{\vec{y}}^T\vec{y} + \alpha\vec{y}^T\vec{y} - \alpha\vec{y}_T^T\vec{y}_T = \; \vec{y}^T(A + A^T + \alpha\mathbb{1})\vec{y} + \vec{y}^T B\vec{y}_T + \vec{y}_T^T B^T\vec{y} - \alpha\vec{y}_T^T\vec{y}_T$$

$$= \begin{pmatrix}\vec{y}^T & \vec{y}_T^T\end{pmatrix}\begin{pmatrix}A + A^T + \alpha\mathbb{1} & B \\ B^T & -\alpha\mathbb{1}\end{pmatrix}\begin{pmatrix}\vec{y} \\ \vec{y}_T\end{pmatrix} = \; \vec{z}^T W\vec{z} \qquad \text{with:} \qquad \vec{z} = \begin{pmatrix}\vec{y} \\ \vec{y}_T\end{pmatrix}.$$

We rewrote the inequality by using a bilinear form in $\vec{z}$ so we can now modify it by eliminating the anti-symmetric parts of the matrix W (because obviously in a bilinear form only the symmetrical part "survives") obtaining finally the inequality:

$$\frac{d}{dt}L(t) = \vec{z}^T W_s\vec{z} \;\leq\; 0 \qquad \text{with:} \quad W_s = \begin{pmatrix}A + A^T + \alpha\mathbb{1} & (B + B^T)/2 \\ (B + B^T)/2 & -\alpha\mathbb{1}\end{pmatrix}. \tag{2.10}$$

Next, knowing that W_s is a symmetric matrix and it is always possible to diagonalize it, we are able to rewrite the inequality (and bound it) in a simpler form in which we use only the maximum eigenvalue of the matrix:

$$\frac{d}{dt}L(t) \;=\; \vec{z}^T W_s\vec{z} \;\leq\; \max\big[eig(W_s)\big]z^2 \;\leq 0.$$

We then obtain that the Ljapunov function is surely monotonically decreasing, i.e. the equilibrium is globally asymptotically stable (obviously this is not a double implication but only a sufficient condition), if the maximum eigenvalue of the symmetric matrix W_s is negative for a fixed $\alpha > 0$ that we can choose freely.

Next we make some observations on the matrix W_s:

- The matrix is symmetric so all the eigenvalues must be real numbers.

- The trace of the matrix is such that $Tr\big[W_s\big] = Tr\big[A + A^T\big] = 2Tr\big[A\big]$.

- We know that if the trace of the matrix W_s is positive then there must exist at least a positive eigenvalue so we easily see that the equilibrium can be stable only if $Tr\big[A\big] < 0$ otherwise it's necessarily unstable.

We now want to rewrite the matrix W_s in another way that allows us to compute more precise inequalities; we will use the so called "Block LDU decomposition" to rewrite W_s as the product of 3 matrices (a Lower triangular, a Diagonal and an Upper triangular block matrices) by calculating the so called Schur complement of W_s. This method can be found in many linear algebra's books, like for instance [27].
First of all we define the two symmetric matrices $\widetilde{A} = (A + A^T)$ and $\widetilde{B} = (B + B^T)/2$ and the first Schur complement of matrix W_s: $C_1 = \widetilde{A} + \alpha\mathbb{1} + \widetilde{B}^2/\alpha$, this allows us to rewrite the matrix W_s as the following product of matrices:

$$W_s = \begin{pmatrix} \widetilde{A} + \alpha\mathbb{1} & \widetilde{B} \\ \widetilde{B} & -\alpha\mathbb{1} \end{pmatrix} = \begin{pmatrix} \mathbb{1} & -\widetilde{B}/\alpha \\ 0 & \mathbb{1} \end{pmatrix} \begin{pmatrix} C_1 & 0 \\ 0 & -\alpha\mathbb{1} \end{pmatrix} \begin{pmatrix} \mathbb{1} & 0 \\ -\widetilde{B}/\alpha & \mathbb{1} \end{pmatrix} = M^T \widetilde{W}_s M.$$

Using this we are finally able to rewrite the inequality with the change of basis $\vec{w} = M\vec{z}$ obtaining:

$$\frac{d}{dt}L(t) = \vec{w}^T \widetilde{W}_s \vec{w} \;\leq\; 0 \qquad \text{with:} \quad \widetilde{W}_s = \begin{pmatrix} \widetilde{A} + \alpha\mathbb{1} + \widetilde{B}^2/\alpha & 0 \\ 0 & -\alpha\mathbb{1} \end{pmatrix}. \tag{2.11}$$

We can now expand the starting inequality by using the following chain of inequalities:

$$\vec{w}^T \widetilde{W}_s \vec{w} \;=\; \vec{w}_1^T C_1 \vec{w}_1 \;-\; \alpha \vec{w}_2^T \vec{w}_2 \;\leq\; \vec{w}_1^T C_1 \vec{w}_1 \;\leq\; \big(\alpha + \lambda_{max}(\widetilde{A}) + \frac{1}{\alpha}\lambda_{max}(\widetilde{B}^2)\big)\vec{w}_1^T \vec{w}_1 \;\leq\; 0.$$

Here in the last relation we used the Weyl's inequality which allows us to substitute the maximal eigenvalue of a matrix with the sum of the maximal eigenvalues of the matrices that make it up obtaining: $\lambda_{max}(C_1) \leq \alpha + \lambda_{max}(\widetilde{A}) + \frac{1}{\alpha}\lambda_{max}(\widetilde{B}^2)$, this procedure is possible only for Hermitian matrices.
Now, considering that $\alpha > 0$, we get the inequality in terms of the eigenvalues of the matrices A and B:

$$\alpha^2 + \alpha\lambda_{max}(\widetilde{A}) + \lambda_{max}(\widetilde{B}^2) \;\leq\; 0 \qquad \Rightarrow \qquad \lambda_{max}(\widetilde{A}) \;<\; 0$$

$$-\lambda_{max}(\widetilde{A}) - \sqrt{\lambda_{max}(\widetilde{A})^2 - 4\lambda_{max}(\widetilde{B}^2)} \leq 2\alpha \leq -\lambda_{max}(\widetilde{A}) + \sqrt{\lambda_{max}(\widetilde{A})^2 - 4\lambda_{max}(\widetilde{B}^2)}$$

$$\begin{cases} \lambda_{max}(\widetilde{A}) \;<\; 0 \\ \lambda_{max}(\widetilde{A})^2 \geq 4\lambda_{max}(\widetilde{B}^2) \end{cases} \qquad \Rightarrow \qquad \lambda_{max}(\widetilde{A}) \;\leq\; -2\sqrt{\lambda_{max}(\widetilde{B}^2)}.$$

Finally, using the notation $\lambda_{|max|}(M)$ for the absolute value of the eigenvalue of maximal magnitude of the matrix M, we are able to write the stability condition:

$$\lambda_{max}(A + A^T) \;\leq\; -\lambda_{|max|}(B + B^T) \qquad \Rightarrow \qquad \exists\, \alpha > 0 \;\text{ such that: }\; \frac{d}{dt}L(t) \;\leq\; 0. \tag{2.12}$$

This relation can be useful to compute the stability inequality in terms of the matrices A and B but obviously it give us only a sufficient condition for the stability which is not too stringent.

A new Stability criterion

If we apply the previous inequality to a linearized system in which the matrices (A,B) are random matrices we obtain a sort of generalization of May's theorem for the delayed case.
We consider random matrices with shape $(S \times S)$, connectance C, diagonal entries $M_{ii} = -d$ and non-diagonal entries $M_{ij} \sim P(0, \sigma)$ randomly sampled from a distribution with zero mean and variance σ^2 . For the Semi-Circular law both the matrices $\widetilde{A} = A + A^T$ and $\widetilde{B} = B + B^T$ have eigenvalues distributed with a semi-circular probability distribution (in the $S \to \infty$ limit) inside the portion of the real axis enclosed by the disks with center in $(-2d, 0)$ and radius $r = 2\sigma\sqrt{2SC}$.

By using the Semi-Circular law we can now estimate the maximal eigenvalues of $\widetilde{A}$ and $\widetilde{B}$ and insert them inside the inequality (2.12) obtaining:

$$\lambda_{max}(\widetilde{A}) \;=\; -2d_A + 2\sigma_A\sqrt{2SC_A} \;\leq\; -2|d_B| - 2\sigma_B\sqrt{2SC_B} \;=\; -\big|\lambda_{|max|}(\widetilde{B})\big|.$$

With some manipulations and using the following definition of the complexity $\chi_\alpha = \sigma_\alpha\sqrt{S_\alpha C_\alpha}$ we finally get the new stability relation:

$$\sqrt{2}\big(\chi_A + \chi_B\big) \;=\; \sqrt{2S}\big(\sigma_A\sqrt{C_A} + \sigma_B\sqrt{C_B}\big) \;\leq\; d_A - |d_B| \quad \Rightarrow \quad \exists\, \alpha > 0 \;\big|\; \frac{d}{dt}L(t) \;\leq\; 0.$$

By observing this inequality it's evident that every time we introduce a delay into the system we are increasing its instability (according to this formula), in fact now, in the delayed case, χ_A has a smaller upper limit on the values that give stability (without delay we had $\chi_A \leq d_A$).
Besides, now, to increase the stability of the delayed system is necessary to decrease (in absolute value) the shift on the diagonal of the B matrix or, like for the non-delayed case, to reduce the complexity of both the matrices.

Finally we notice that the proposed generalization of May's stability criterion to the delayed system is not as powerful as the original, the non-delayed one, because in this case we have more strict conditions which allow for stability with a probability $P(stable) = 1$ given any value of S. Indeed, this criterion is not able to describe all the cases in which the system is stable, in fact it can pick only a small subset of those ones, giving us only some sufficient conditions.
Instead, the original Circular law provides necessary and sufficient conditions, being a lot more inclusive, because it is able to determine all the values of the variables which give a stable ecosystem. This lack of specificity is due to the series of approximations we used on the computation of our final inequality, like for instance the Weyl inequality, and also to the limited power of the Ljapunov function method.

As a final remark we notice that this new criterion is able to determine only the subset of values of the parameters under which the system is stable for any delay T, therefore it misses all those cases in which the stability is delay-dependent.

2.2.2 Other stability criteria

Here we present briefly some other stability criteria present in literature which are explained in detail on the book of Gopalsamy [8].
First of all we define the two principal quantities we are going to use in the following calculations, the matrix norm and the associated matrix measure (logarithmic norm):

$$\|A\| = \max_j \sum_i |A_{i,j}| \qquad \mu(A) = \lim_{h\to 0^+} \frac{\|\mathbb{1} + hA\| - 1}{h} = \max_j \Big[A_{j,j} + \sum_{i\neq j} |A_{i,j}|\Big].$$

A different Delay-independent Stability theorem

In his book Gopalsamy presents an alternative Ljapunov function method with respect to the one we used in the previous section, indeed he proposes the following Ljapunov functional:

$$L(t) = \sum_i \Big[\ |y_i(t)| + \sum_j |B_{i,j}| \ \Big(\int_{t-T}^{t} |y_j(s)| ds \Big) \ \Big].$$

Then, using this functional it is possible to show that the trivial solution $\vec{y}(t)$ of (2.8) is asymptotically stable, whatever the size of the delay T is, when the matrices A, B respect the following constraints:

$$\mu(A) < 0 \quad \text{and } B \text{ is small enough:} \quad \|B\| < -\mu(A). \tag{2.13}$$

Rozhkov and Popov theorem

Let's consider the system (2.8) in the case of zero delay, in this case we obtain $\dot{\vec{y}}(t) = (A+B)\vec{y}(t)$. If the solution of this new system is asymptotically stable and if we let two positive constants M, α to satisfy:

$$\|e^{(A+B)t}\| \leq Me^{-\alpha t} \quad \text{with:} \quad M \geq 1,\ \alpha > 0.$$

Then, the trivial solutions of (2.8) with non-zero delay are asymptotically stable if the delay is small enough to satisfy the following inequality:

$$T \cdot M\big(\|A\| + \|B\|\big)\|B\| \ < \ \alpha.$$

Khusainov and Yun'kova theorem

Let's consider again the system (2.8) in the case of zero delay, the non delayed case gives us the system $\dot{\vec{y}}(t) = (A+B)\vec{y}(t)$. If the solution of this system is asymptotically

stable and C is a real symmetric positive definite matrix which satisfies:

$(A+B)^T C+C(A+B) = -\mathbb{1}$ with: $\lambda_{max}(C), \lambda_{min}(C) =$ max and min eigenvalues of C.

Then also the trivial solution of (2.8) is asymptotically stable for all delays $T < T_0$ with T_0 defined as:

$$T_0 = \Big(2(\|A\| + \|B\|)\|CB\|\Big)^{-1}\Big(\lambda_{min}(C)/\lambda_{max}(C)\Big)^{1/2}.$$

Finally we notice that in this last theorem it is difficult to compute C for given A, B and since we need the maximum and minimum eigenvalue of C to find the maximal delay for stability (T_0) this technique is not useful for high dimensional systems like the ones we treat here.

Furthermore, all the stability theorems which we presented in this section don't give us a stability criterion as strong as May's law, where the stability was directly linked to the parameters of the random matrices ($S,\ C,\ \sigma,\ d, \dots$). Instead here we get only sufficient conditions by means of bounds. Therefore we will need to use a different method which allows us to obtain the eigenvalues of the system.

2.2.3 Linear Stability Analysis and eigenvalues of the system

A more precise and useful way to study the solutions of the linearized system near its equilibrium $\vec{y}^* = 0$ is to use the so called Linear Stability Analysis. This method relies on using solutions of the form $\vec{y}(t) = e^{\lambda t}\vec{v}$, where $\vec{v}$ is a vector of constants which depends on the initial conditions and the parameter $\lambda \in \mathbb{C}$ is an effective eigenvalue of the system. Even though the parameter λ is not a real eigenvalue, because the characteristic equation is not an eigenvalue equation, we will make an exception on the notation and call it eigenvalue or λ parameter for brevity.
If we insert the hypothesized solution into the system of DDEs, we obtain a characteristic equation for λ which gives us all possible solutions of the system near the equilibrium; if we obtain that all the λ parameters have negative real part, then the solutions must be obviously stable, because in that case: $\vec{y}(t \to \infty) \to \vec{0}$.
Now we apply this method to (2.8) and we obtain the following characteristic equation:

$$\lambda\vec{v} = A\vec{v} + e^{-\lambda T}B\vec{v} \quad \Leftrightarrow \quad det\big(A + e^{-\lambda T}B - \lambda\mathbb{1}\big) = 0. \tag{2.14}$$

The equation for the determinant is not solvable unless we consider matrices A and B which have the same base of eigenvectors. This means that they must be simultaneously diagonalizable, i.e. they are commuting matrices. Considering that we are using random matrices, this is never the case. In fact, especially in the limit of large S, random matrices never commute; therefore this method will be useful only in the cases when either one of the matrices is zero or else one of them is a multiple of the identity (and so it can commute with any other matrix). Thus, if we use matrices A, B such that $\big[A,\ B\big] = 0$, we obtain the following equation for the

eigenvalues (where $a,\ b$ are eigenvalues respectively of A and B and correspond to the same eigenvector):

$$\lambda \ = \ a \ + \ e^{-\lambda T} b \quad \longrightarrow \quad (\lambda - a) T e^{(\lambda - a)T} = b T e^{-aT} \quad \longrightarrow \quad \lambda = a + \frac{1}{T} W(bTe^{-aT}). \tag{2.15}$$

Here we solved the last equation using the Lambert W function, also called "product-log" which is a multivalued function defined by the equation:

$$W(z)e^{W(z)} = z \qquad \text{where:} \quad W(z) = f^{-1}(z) \quad \text{with:} \quad f(z) = ze^{z}.$$

It is now possible to study the sign of the maximum "eigenvalue" λ of the system to find out if it gives a stable equilibrium or not. By imposing all eigenvalues λ to be negative we obtain the following relation between the eigenvalues of the two Community matrices a, b and the delay T, this must be satisfied for all the eigenvalues of A and B and it can select a range of values for the delay such that the equilibrium is stable:

$$Re\big[\ W(bTe^{-aT})\ \big] \ \leq \ -aT \qquad \forall a, b.$$

Moreover it is clear that this relation is not solvable analytically in the most general case when $a, b, T \neq 0$ because the Lambert W function cannot be expressed in terms of elementary functions.
For instance in the case $a = 0$, i.e. the case in which there is no matrix A but instead the system depends only on the delayed populations, the characteristic equation becomes:

$$\lambda e^{\lambda T} - b = 0 \quad \longrightarrow \quad ze^{z} + \gamma = 0 \quad \text{with:} \quad z = \lambda T \quad \gamma = -bT = \rho e^{i\theta}.$$

The solutions of the equation above have been proven by Bellman and Cooke [3] to have always a negative real part if the following constraints are satisfied:

$$Re[z] < 0 \quad \Leftrightarrow \quad Re[\gamma] > 0 \quad \wedge \quad \pi/2 - |\theta| > \rho.$$

From these inequalities we retrieve the stability conditions for the parameter λ of the actual system which are now expressed in terms of the delay T and the eigenvalues of matrix B:

$$Re[\lambda] < 0 \quad \Leftrightarrow \quad Re[b] < 0 \quad \wedge \quad \pi/2 - |\theta| > \rho T \quad \text{with:} \quad b = -\rho e^{i\theta}. \tag{2.16}$$

Finally, this result implies that the solutions of a system with delay are stable only when some conditions are satisfied: first, the equilibrium of the system without it, i.e. the one with $T = 0$, have stable solutions. Second, the magnitude of the delay must be less than a given value, which depends on the modulus and phase of all the eigenvalues of the system, otherwise the solutions are unstable.

In addition, if we want to apply the same theorem to systems with a non-zero matrix A we get some hard non-linear equations which still haven't been solved analytically so it is actually easier to study that problem from a numerical perspective.

In figure (2.8) we studied numerically the expression in (2.15) to discover which are the values that the eigenvalues of B can assume such that the system remains stable, i.e. the eigenvalue λ with maximal real part is negative, for different delays T. We considered the two main cases, when the matrices A and B commute:

1 when $A = 0$ and so all its eigenvalues are $a = 0$.

2 when $A = -\mathbb{1}$ and so all of them are $a = -1$.

We discovered that, when there is no matrix A, the eigenvalues of B must all have a negative real part otherwise the parameter λ has positive real part. This means that the system must be already stable in the non-delayed case. In addition the stability region decreases in extent for larger delays. Therefore, the system remains stable if it decreases its complexity ($\propto \sigma\sqrt{SC}$), i.e. the radius of the distribution of the eigenvalues decreases. This result is exactly in line with the analytical description of equation (2.16).

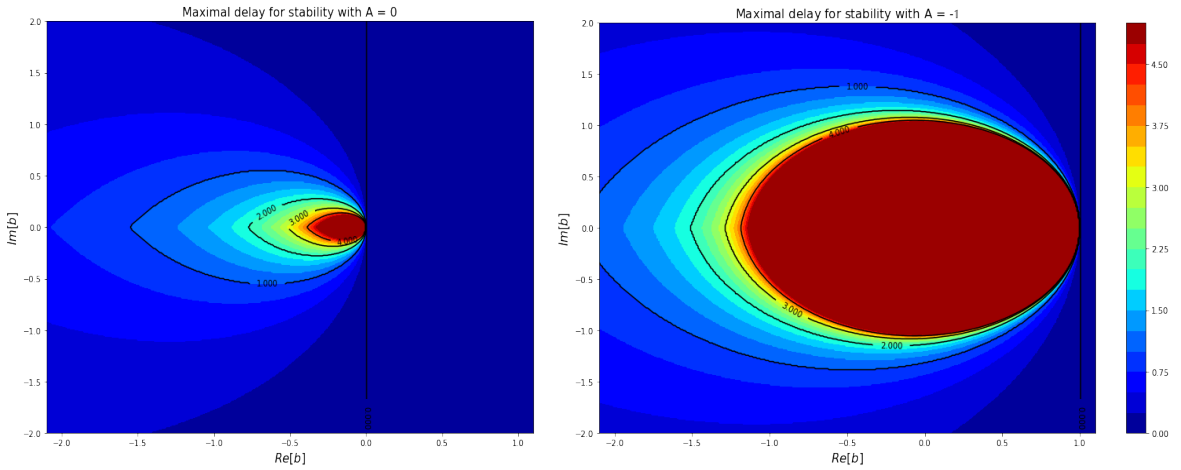

Figure 2.8: *Range of values which the eigenvalues of B can assume such that the eigenvalue $\lambda(T)$ of the system remains with negative real part (different color means different delay T). We considered the 2 cases when the eigenvalues of A are either all $a = 0$ or all $a = -1$. Here the color-bars refer to T, therefore increasing the delay means going from blue to red.*

Instead when we have a matrix $A = -\mathbb{1}$ we get a -1 shift to the left (even though is not a rigid translation) of all the eigenvalues of B which now must be absolutely smaller than 1, this means that now the matrix B doesn't need anymore the term $-d$ on the diagonal to shift the center of the distribution. In addition to that, like in the other case, the "stability-zone" decreases in extent for larger delays, but unlike before, the distribution of the eigenvalues of B can be located in a larger area where they have the same stability properties.

As a final remark, by observing both figures, we notice that Community matrices B which have eigenvalue distributions stretched along the horizontal direction are generally more stable (or at least stable for higher delays) with respect to matrices in which the eigenvalues are distributed more in the vertical direction. This means that mixed (mutualistic-competitive) random matrices are often more stable, or stable for larger delays, with respect to predator-prey ones.

2.2.4 Distribution of the eigenvalues

Using the equations obtained from the Linear Stability Analysis it is now possible to compute the "eigenvalues" of the linearized delayed system. In particular, using (2.15), we are able to compute the eigenvalues of any system in the form $\dot{\vec{x}} = A\vec{x}(t) + B\vec{x}(t-T)$ in which the matrices $A,\ B$ commute. Indeed we are able, in analogy with the methods used in the non-delayed case, to study the system with the random matrices technique by sampling the entries of the two community matrices $A,\ B$ from some probability distribution.
First of all we will start with a system which has only the delay term, i.e. the system $\dot{\vec{x}} = B\vec{x}(t-T)$ in which the Community matrix B is a random matrix. Then we can study a more general case in which the matrix A is a multiple of the identity matrix, i.e. $A = -d\mathbb{1}$, and B is again a random matrix. This last example is indeed the most complex case we are able to study using the aforementioned method. In fact it is impossible to sample two random matrices which are simultaneously diagonalizable (i.e. they commute) because, from their their definition, the probability of such an event is almost zero when S is large enough. Therefore if the two matrices don't commute, we cannot compute the eigenvalues of the system, using that technique, because the characteristic equation (2.14) is not solvable for $S \gg 1$.

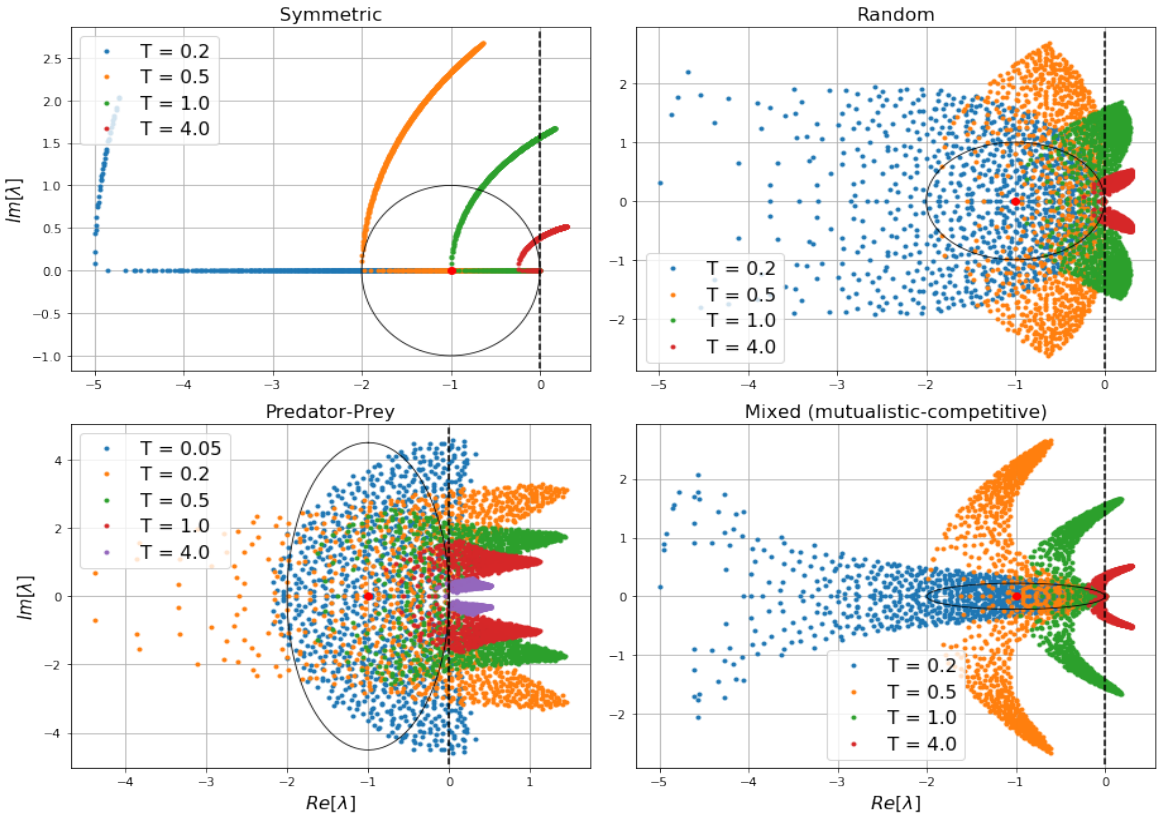

Figure 2.9: *Distributions of the eigenvalues of the system with $A = 0$ and B of 4 different types of random matrices with entries sampled from a distribution with zero mean and with: $S = 1000,\ C = 0.1,\ \sigma = 0.1\gamma,\ d = -1$; here we have chosen different σ values such that the transition point of the non-delayed system remain the same for all the 4 types of matrices: $\gamma = \left(\ 1/\sqrt{2},\ 1,\ \pi/(\pi-2),\ \pi/(\pi+2)\ \right)$. We also computed the eigenvalues for different delays T (different colors); also the black solid lines represent the borders of the distribution of eigenvalues in the non-delayed case.*

Starting from the linearized system $\dot{\vec{x}} = B\vec{x}(t-T)$ we are able to compute the eigenvalues when the matrix B is a random matrix obtaining the figure (2.9).
We are able to distinguish the distribution of the eigenvalues of the system with only the delay term for the four main types of Community matrices B. We observe that in all of them, except for the predator-prey type, the rightmost eigenvalue remains the same with respect to the non-delayed case, i.e. the one on the real axis, only if the delay remains under a certain threshold. When the delay exceeds that threshold the rightmost eigenvalue changes, it becomes one of the values in the "wings" of the distribution with a non-zero imaginary part and its real part starts to grow for increasing delays until the system becomes unstable.
Unlike that, in the predator-prey matrices the presence of the delay always destabilize the system. In fact we can see that even for small delays the rightmost eigenvalue has always a positive real part and a non-zero imaginary part (so it isn't a point on the real axis anymore). In addition, we notice also that there is a maximum for the real part of the rightmost eigenvalue: when the delay increases too much its real part starts to decrease.

Instead, if we start from the linearized system $\dot{\vec{x}} = -d\mathbb{1}\vec{x}(t) + B\vec{x}(t-T)$ we can compute the eigenvalues when the matrix B is again a random matrix obtaining figure (2.10).

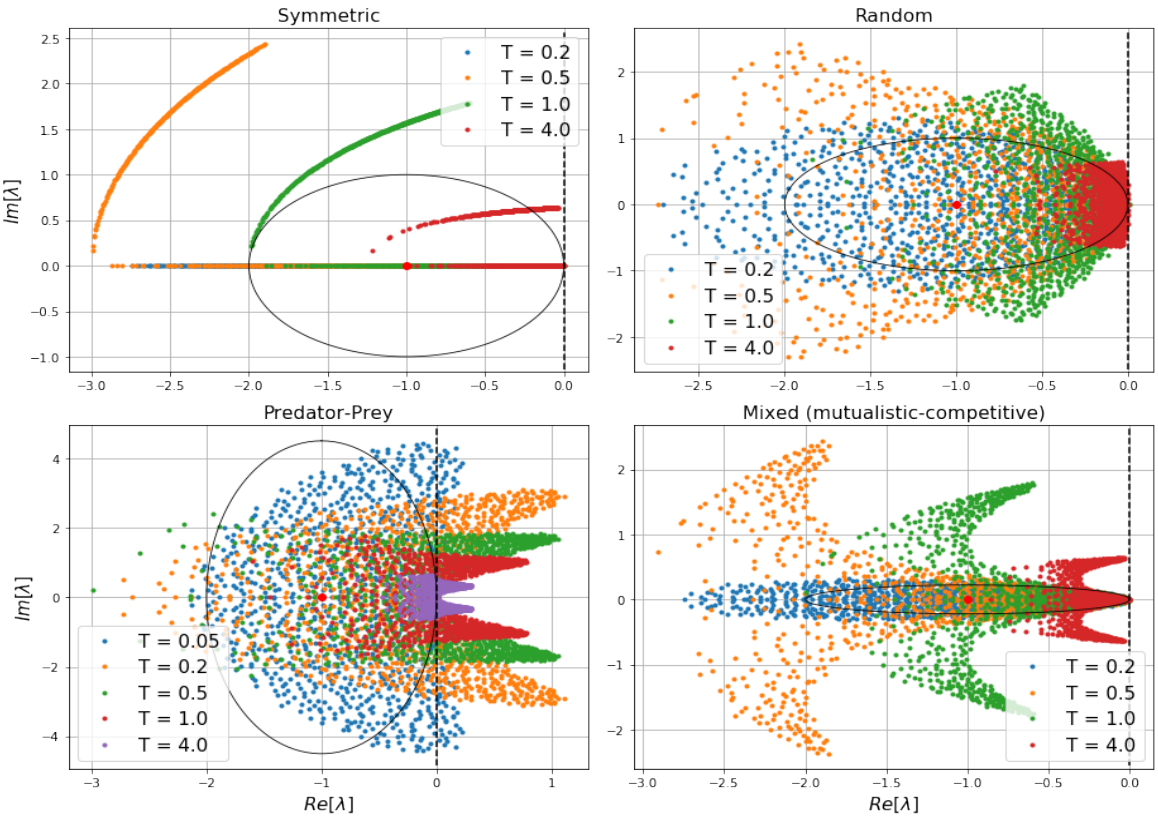

Figure 2.10: *Distributions of the eigenvalues of the system with $A = -\mathbb{1}$ and B of 4 different types of random matrices with entries sampled from a distribution with zero mean and with: $S = 1000,\ C = 0.1,\ \sigma = 0.1\gamma,\ d = 0$; here we again have chosen different σ values for the same reason of the previous figure: $\gamma = \left(\ 1/\sqrt{2},\ 1,\ \pi/(\pi-2),\ \pi/(\pi+2)\ \right)$. We also computed the eigenvalues for different delays T (different colors); also the black solid lines represent the borders of the distribution of eigenvalues in the non-delayed case.*

We observe the distribution of the eigenvalues of the system with both the delay term and the non delayed one for the four main types of Community matrices B and a fixed matrix $A = -\mathbb{1}$. Like in the previous case we again have that the predator-prey system is always destabilized by any positive delay. In contrast, the other three types of matrices are always stable for any value of delay if the non-delayed system is already stable. Therefore the presence of the delay doesn't change the situation, indeed the rightmost eigenvalue remains the one on the real axis and is not modified by the introduction of some delay, also none of the other eigenvalues exceed the imaginary axis, thus the system remains stable.
Here for example we are considering a distribution constructed in such a way that, in absence of delay, the system defined by $A + B$ is exactly at the transition point (a circle tangent to the imaginary axis from the left) and, if we slightly increase S, C or σ, the maximal eigenvalue becomes positive. Including the delay we notice that the situation remains the same and the system is again exactly at the transition point. This result can be explained easily by observing figure (2.8); in fact, we observe that there the region which give stable solutions remains approximately the same for any delay $T > 4$. Therefore, if all the eigenvalues of B are distributed inside that region, the system remains stable for any T.

Eigenvalue distribution when both A and B are random matrices.

We introduce now an alternative method to compute the eigenvalues of the system $\dot{\vec{x}} = A\vec{x}(t) + B\vec{x}(t-T)$ when both matrices $A,\ B$ are random matrices which don't commute, hence the characteristic equation (2.14) cannot be solved in the same way. Starting from the linearized system, instead of substituting a solution in the form $\vec{x}(t) = e^{\lambda t}\vec{v}$ and computing the parameter λ independently of the vector $\vec{v}$, we now consider $\vec{v}$ to be either an eigenvector of matrix A, denoted with $\vec{a}$, or an eigenvector of matrix B, denoted with $\vec{b}$. We obtain then two possible new characteristic equations for the eigenvalue λ:

$$\lambda\vec{a} \;=\; a\vec{a} \;+\; e^{-\lambda T}B\vec{a} \qquad \text{or} \qquad \lambda\vec{b} \;=\; A\vec{b} \;+\; be^{-\lambda T}\vec{b}. \tag{2.17}$$

Next, if we multiply both sides of each equation by the transposed eigenvector $\widetilde{a}$ or $\widetilde{b}$ and isolate λ, we get the following equations:

$$\begin{cases} \lambda\vec{a}^2 \;=\; a\vec{a}^2 \;+\; e^{-\lambda T}\widetilde{a}B\vec{a} \\ \lambda\vec{b}^2 \;=\; be^{-\lambda T}\vec{b}^2 \;+\; \widetilde{b}A\vec{b} \end{cases} \longrightarrow \begin{cases} \lambda \;=\; a \;+\; e^{-\lambda T}\big(\widetilde{a}B\vec{a}\big)/\vec{a}^2 \\ \lambda \;=\; e^{-\lambda T}b \;+\; \big(\widetilde{b}A\vec{b}\big)/\vec{b}^2 \end{cases}$$

Finally using the Lambert W function we obtain a formula for the eigenvalue $\lambda(T)$ in both cases:

$$\lambda(T) \;=\; \begin{cases} a \;+\frac{1}{T}W(\rho_b T e^{-aT}) & \text{using } \vec{a} \text{ and:} \quad \rho_b = \sum_{i,j} B_{i,j}\vec{a}_i\vec{a}_j \;/\; \sum_i \vec{a}_i^2 \\ \rho_a + \frac{1}{T}W(bTe^{-\rho_a T}) & \text{using } \vec{b} \text{ and:} \quad \rho_a = \sum_{i,j} A_{i,j}\vec{b}_i\vec{b}_j \;/\; \sum_i \vec{b}_i^2 \end{cases} \tag{2.18}$$

In conclusion, we are now able again to compute the eigenvalue distribution of the system, even though the two matrices don't commute. We just need to compute the

eigenvectors of one of the two Community matrices and project the other matrix onto its eigenspace by computing ρ_i. We can freely choose between the two methods obtaining different results for the eigenvalues λ.
Furthermore, the technique that we proposed gives completely different distributions if we use eigenvectors of one matrix instead of the ones of the other. This difference on the distributions still does not have an explanation and should be studied more deeply in future investigations.

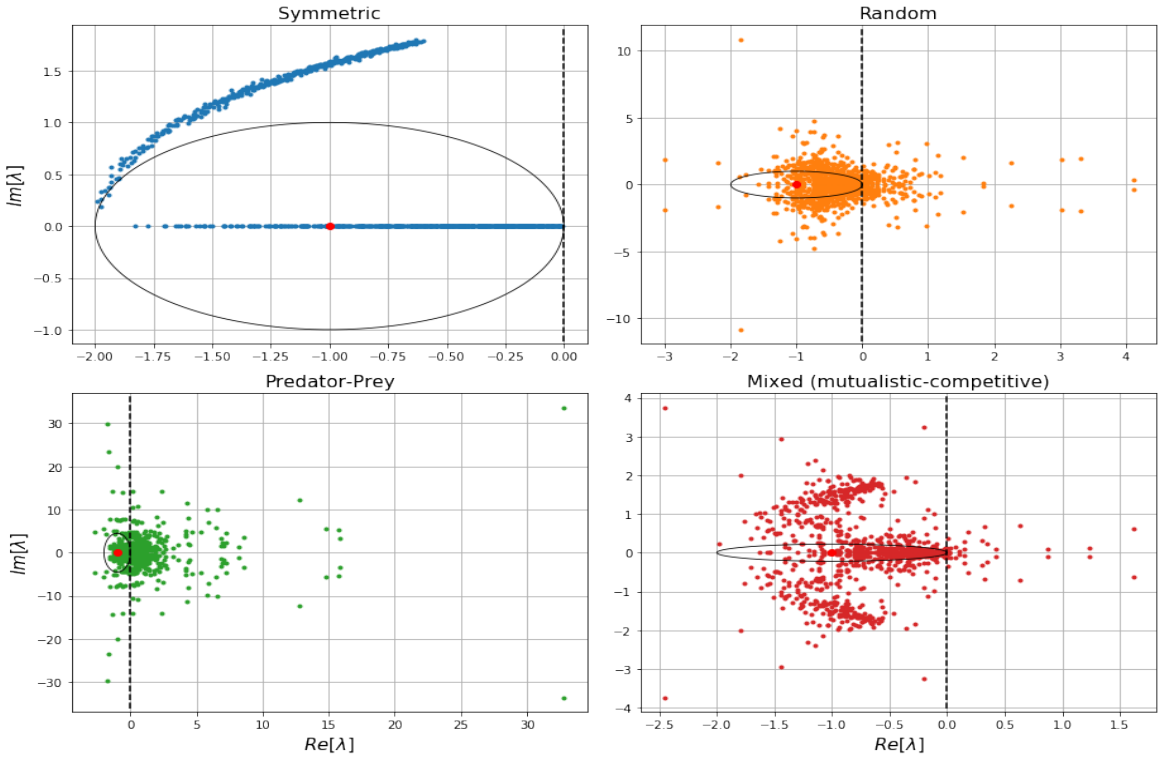

Figure 2.11: *Distributions of the eigenvalues of the system with both A and B random matrices of the 4 different types, the entries of both of them are sampled from a distribution with zero mean and with: $S = 1000,\ C = 0.1,\ \sigma = 0.1\gamma,\ d_A = -1,\ d_B = 0$; here we again have chosen different σ values for the same reason of the previous figure: $\gamma = \left(1/\sqrt{2},\ 1,\ \pi/(\pi-2),\ \pi/(\pi+2)\right)$. We computed the eigenvalues for a fixed delay $T = 1$ and we used the eigenvectors of matrix B for the calculations; again the black solid lines represent the borders of the distribution of eigenvalues in the non-delayed case.*

In figure (2.11) we show that, when both A and B are random matrices, the "radius" of the eigenvalue distribution grows, while, at the same time, the eigenvalues disperse widely in the complex plane, i.e. the shape of the distribution is not fixed anymore. In addition, an important number of eigenvalues have a large positive real part which utterly destabilize the system.
Moreover, we observe that, when both matrices are symmetric random matrices, the distribution is really similar to the one of the system with $A = 0$ (the only difference now is that the eigenvalues with non-zero imaginary part are distributed in a larger area) and the stability of the system can be described in the same way.
Finally, we can explain the increase in the number of eigenvalues with a large modulus by simply observing that, now that we are using also the eigenvectors of the random matrices to compute the parameter λ, the "randomness" of the system increases a lot with important effects also on the distribution.

2.2.5 Maximal real part of eigenvalues vs. S and T

We study now, with more specificity, the behavior of the eigenvalue with maximal real part of the linearized system. This analysis is more important with respect to the actual study of the whole eigenvalue distribution because the stability of the system depends uniquely on the rightmost eigenvalue. Therefore we are going to study its behavior for two different systems: the one which has only the delay part, i.e. with $A = 0$, and the one with the partial influence of the non delayed term, i.e. with $A = -d\mathbb{1}$. The matrix B will be again a random matrix of the four main types we described before (symmetric,completely random, predator-prey, mixed). Then we will consider also the case in which both A and B are random matrices even though, as we discovered in the previous section, in that situation the distribution of eigenvalues is a lot more difficult to characterize.
Note: in the following sections we will refer to the eigenvalue with maximal real part as the "maximal" or "rightmost" eigenvalue for brevity.

Maximal eigenvalue vs. size S

The first relation we investigate is the dependence between the real part of the rightmost eigenvalue and the dimensions of the Community matrix. In this section we have set the parameters of the random matrices such that the transition which leads to instability in the non-delayed case happens at $S \approx 1000$ for each type of matrix (as we can see from the black dashed lines in the following figures). We obtained the resulting plots by taking the average of the maximal eigenvalues of 10 different randomizations of B with the same parameters.

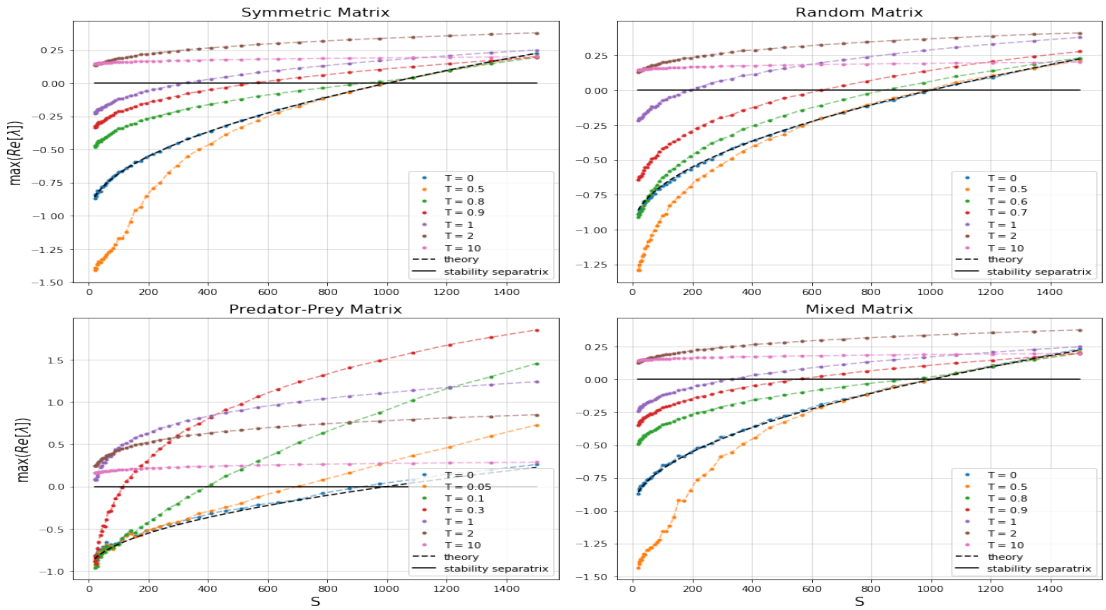

Figure 2.12: *Maximal real part of the eigenvalues of the system vs. size of the matrices; with $A = 0$ and B of 4 different types of random matrices with entries sampled from a distribution with zero mean and with: $C = 0.1$, $\sigma = 0.1\gamma$, $d = -1$; here we have again $\gamma = \left(1/\sqrt{2},\ 1,\ \pi/(\pi-2),\ \pi/(\pi+2)\right)$. We computed the eigenvalues for different delays T (different colors); also the black dashed line represent the distribution of eigenvalues in the non-delayed case while the black solid line the transition point to instability.*

In figure (2.12) we show the behavior of the maximal eigenvalue for increasing S values in the case when $A = 0$. We observe that, again, when the delay is small enough (later we will see that it is when $T \lesssim 0.5$), the transition point from stability to instability, i.e. the intersection with the black solid line, doesn't change with respect to the non-delayed case for all the three types of matrices with exception of the predator-prey one. Then, increasing the delay, the transition point shift to smaller values of S until it reaches the point where the delay is high enough that the system remains unstable for any value of S.
In the predator-prey system we observe plainly what we inferred from the distributions in the previous section. For increasing delays the transition point shifts always to smaller S values (until the system remains unstable for any S) and it doesn't exist a range of delay values which leaves the transition point unchanged like in the other three cases. Indeed, as we can see in the figure, the effect of the delay is a lot stronger on the predator-prey system with respect to the others. Also, the relation between the rightmost eigenvalue and the size S of the ecosystem changes a lot with respect to the non delayed case, even for small delays.

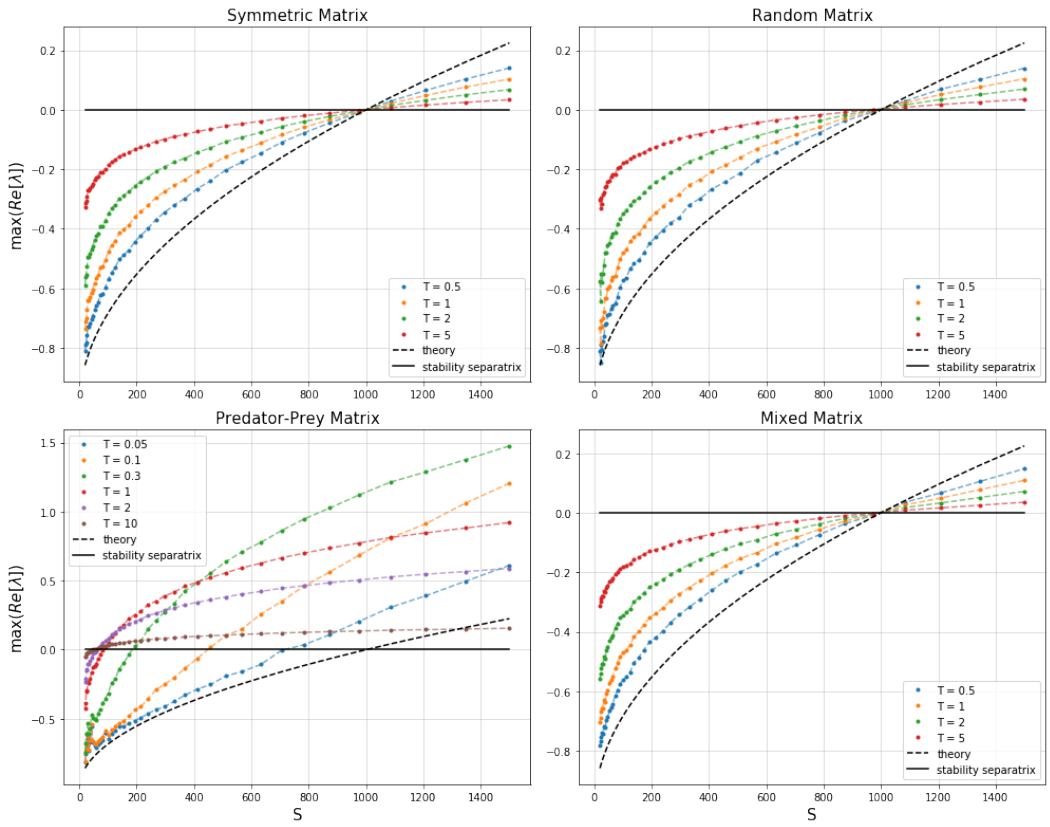

Figure 2.13: *Maximal real part of the eigenvalues of the system vs. size of the matrices; with $A = -\mathbb{1}$ and B of 4 different types of random matrices with entries sampled from a distribution with zero mean and with: $C = 0.1$, $\sigma = 0.1\gamma$, $d = 0$; here we have again $\gamma = \left(1/\sqrt{2},\ 1,\ \pi/(\pi-2),\ \pi/(\pi+2)\right)$. We computed the eigenvalues for different delays T (different colors); also the black dashed line represent the distribution of eigenvalues in the non-delayed case while the black solid line the transition point.*

Furthermore, in figure (2.13) we show the relation between the real part of the rightmost eigenvalue and the dimension of the matrix in the case when $A = -\mathbb{1}$. In contrast with the previous case we observe that here in all systems, with exception

to the predator-prey one, the transition point remains always the same and it is not influenced by the delay. In fact, for different delays the dependence between the maximal eigenvalue and S changes but it doesn't influence the point in which the maximal eigenvalue assumes a positive real part which depends only on S.
The predator-prey system instead doesn't change its behavior with the introduction of the matrix A and the relation between its rightmost eigenvalue and S remains more or less the same as the $A = 0$ case.
The main difference between the system with $A = 0$ and the one with $A = -\mathbb{1}$ is that in the last one there is always a transition point independently on the delay. Thus, even for high delays the transition point is either the same or, in the predator-prey case, shifted to smaller S values.

In addition, we can analyze the relation between the eigenvalue with maximal real part and the other parameters that determine the random matrix, like, for instance, the connectance C or the standard deviation σ. The results which we obtain from that are extremely similar to the ones we obtained in figures (2.13) and (2.12) so we won't include those here. In fact, we already know that the radius (or the semi-axis) of the distribution of the eigenvalues of a random matrix is proportional to the complexity term: $\sigma\sqrt{SC}$. Therefore the procedure to study the dependence of the maximal eigenvalue on S is equivalent to the one for C and σ.

Finally, the dependence of the maximal real part of the eigenvalues on the dimensions of the matrix (but also on σ and C) is not described anymore by a power law like in the non-delayed case. In fact, if we make a log-log plot we get that the dependence is not linear. Indeed the mutual dependence is a lot more complex and it is more similar to a Poly-logarithmic function (which is exactly what we expect from the expansion of the Lambert function).

Maximal eigenvalue vs. delay T

Now, we investigate how the real part of the rightmost eigenvalue of the system depends on the time delay T. Again we have set the parameters C, σ, d such that the non delayed system has a transition to instability at $S = 1000$. Here we explore the dependence on T for some matrices with size S bigger and smaller than the transition value 1000. Also, like before, we have taken averages over 10 randomizations of B.

In figure (2.14) we show the dependence of the eigenvalue with maximal real part on the delay T, when the system has $A = 0$ and so the only Community matrix is the one associated to the delayed term.
The first thing we notice is the graph of the case $S = 1000$ which is the one in which the non-delayed system is on the transition point (the maximal eigenvalue is zero). We see clearly the presence of a "transition" time delay T_{tr} such that, the rightmost eigenvalue remains the same for all $T < T_{tr}$. Therefore this value T_{tr} is a sort of Höpf bifurcation point which separates all the stable to the unstable cases. Like before the predator-prey system makes an exception because, for any delay (even

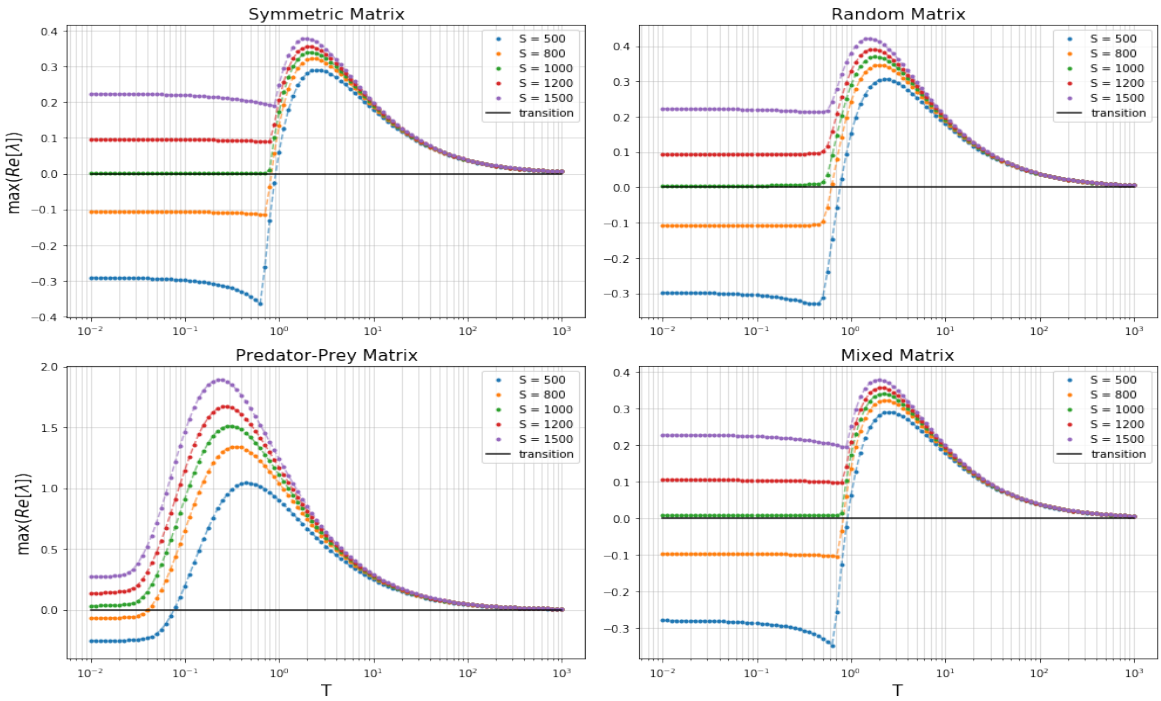

Figure 2.14: *Maximal real part of the eigenvalues of the system vs. delay T; with $A = 0$ and B of 4 different types of random matrices with entries sampled from a distribution with zero mean and with: $C = 0.1,\ \sigma = 0.1\gamma,\ d = -1$; here we have again $\gamma = \left(1/\sqrt{2},\ 1,\ \pi/(\pi-2),\ \pi/(\pi+2) \right)$. We computed the eigenvalues for different dimensions S of the community matrices (different colors); also the black solid line represent the transition point.*

$T \ll 1$), the rightmost eigenvalue has a bigger real part with respect to the one of the non-delayed case.

This sudden change on the real part of the rightmost eigenvalue can be easily explained by observing how the distribution of the eigenvalues changes for increasing delays. In fact, when the delay reaches T_{tr}, the stability region for the eigenvalues of B, represented in figure (2.8), become smaller than the region in which they are distributed. Therefore, the system becomes unstable, indeed the eigenvalues on the "wings" of the distribution become the rightmost ones crossing the imaginary axis, and for increasing T their real part increase proportionally.

Instead, when we use Community matrices which are not on the transition point of the non-delayed system, i.e. when $S \neq 1000$, we have different behaviors of the maximal eigenvalue.

If $S > 1000$ the non-delayed system is already unstable and the presence of the delay cannot stabilize it (but we still have a region of T values where the maximal eigenvalue remains unchanged). Instead, if $S < 1000$, i.e. the non-delayed system is stable and under the threshold of transition, we have again a range of T values in which the rightmost eigenvalue doesn't change or it even decreases. Then at some value of delay the eigenvalue starts to grow and reaches the transition point where the system becomes unstable. There, unlike the $S = 1000$ case, there is no range of T values such that the maximal eigenvalue remains in the transition line, but instead it crosses that on a single point.

Moreover we observe that, as we expected from the analytical models, if the non-delayed system is stable already, i.e. $S \leq 1000$, there is a maximal value of the delay

under which the system with delay remains stable and over which the rightmost eigenvalue has a positive real part.
In addition we notice also two other important features present in all cases. First, when T increases to infinity the maximal eigenvalue tends to zero, this is due to the fact that the whole distribution gets compressed to a point in the origin in the limit $T \to \infty$. This is clear when observing the expression of $\lambda(T)$. Using the asymptotic behavior of $W(z)$, presented in Eq. (2.20), which states that $W(z)$ diverges slower than $\log(z)$ as $z \to \infty$, we get:

$$\lim_{T\to\infty} |\lambda(T)| = \lim_{T\to\infty} \frac{|W(bT)|}{T} \lesssim \lim_{T\to\infty} \frac{|\log(bT)|}{T} = 0$$

Second, there is always the presence of a peak in the maximal eigenvalue for a given value T in all the four different types of matrices, after that the rightmost eigenvalue decreases for increasing delays. Also, the delay T_{max} associated to the peak cannot be computed analytically but only numerically.

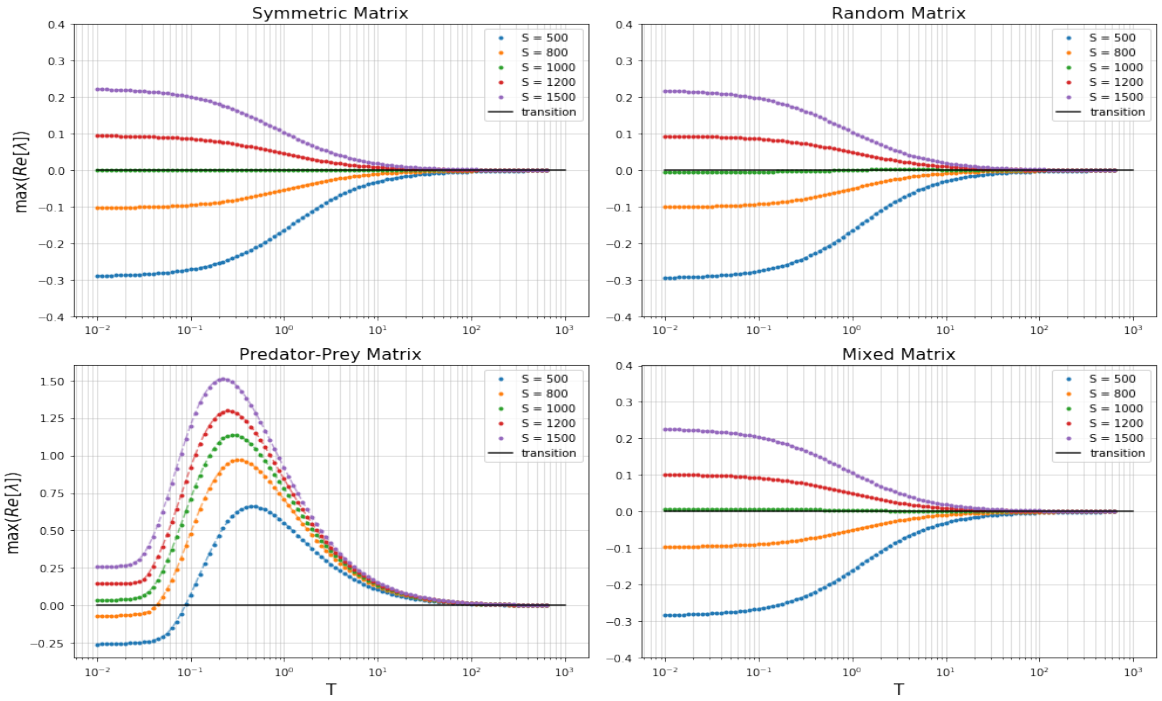

Figure 2.15: *Maximal real part of the eigenvalues of the system vs. delay T; with $A = -\mathbb{1}$ and B of 4 different types of random matrices with entries sampled from a distribution with zero mean and with: $C = 0.1,\ \sigma = 0.1\gamma,\ d = 0$; here we have again $\gamma = \left(1/\sqrt{2},\ 1,\ \pi/(\pi-2),\ \pi/(\pi+2)\right)$. We computed the eigenvalues for different dimensions S of the community matrices (different colors); also the black solid line represent the transition point.*

In figure (2.15) we show the dependence of the eigenvalue with maximal real part on the delay T when the system has $A = -\mathbb{1}$ and the only random matrix is the Community matrix B. It is easier to interpret these graphs by observing the distributions of the eigenvalues. In fact, with exception of the predator-prey system, the other systems have all the same behavior: when they are on the transition point the delay doesn't destabilize them (horizontal line) while, if they are not, the maximal eigenvalue tends to zero in the $T \to \infty$ limit, growing for $S < 1000$ and decreasing for

$S > 1000$ (the proof is analogue to the one for $a = 0$).
Moreover, the behavior of the predator-prey system remains the same as the case $A = 0$. Indeed, the fact that the terms -1 are on the diagonal of A instead of B doesn't change the behavior. The only difference is that now the system is a lot more damped and thus, the maximal eigenvalue assumes smaller values in the peak of the graph. This evidence can be connected to the observation we did in figure (2.8). There, in fact, we noticed that the behavior of a system with a predator-prey matrix (which has a distribution elongated on the vertical direction) is similar in the two cases.

Maximal eigenvalue when both A and B are random matrices

In conclusion, as an example, we show in figure (2.16) how the real part of the rightmost eigenvalue scales with the size S of the system when both the Community matrices A and B are random matrices and the eigenvalue is computed using the technique (2.18). The maximal eigenvalue now can vary a lot and, to have a better resolution, we need to change the scale of both axes. Thus we have chosen a log-log plot where, considering that under the transition point the maximal eigenvalue is negative, we plotted in the y-axis the real part of the rightmost eigenvalue +1 (therefore the line that marks the transition is the horizontal line at $y = 1$).

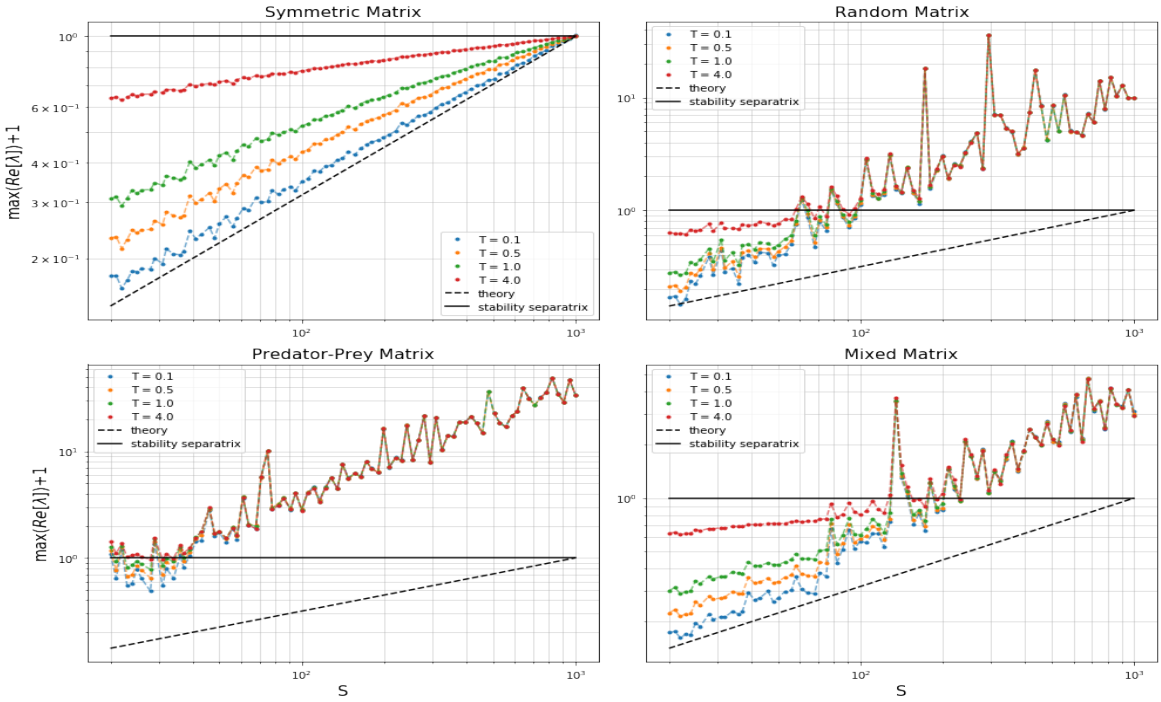

Figure 2.16: *Maximal real part of the eigenvalues of the system* $(+1)$ *vs. size of the matrices; with* A *and* B *random matrices of the same type with entries sampled from a distribution with zero mean and with:* $C = 0.1,\ \sigma = 0.1\gamma,\ d_A = -1,\ d_B = 0$ *; here we have again* $\gamma = \left(1/\sqrt{2},\ 1,\ \pi/(\pi-2),\ \pi/(\pi+2) \right)$ *and we computed the eigenvalues using the eigenvectors of matrix* B*. We computed the eigenvalues for different delays* T *(different colors); also the black dashed line represent the distribution of eigenvalues in the non-delayed case while the black solid line the transition point.*

Here we observe easily what we noticed by studying the eigenvalue distribution: the situation is clearly a lot more disordered and with exception of the symmetric matrices

where the rightmost eigenvalue has a very similar behavior to the case with $A = 0$, the maximal eigenvalue of the other types of matrices grows in a more complicated way. Indeed the transition point which separates the stable to the unstable cases cannot be identified with precision. Moreover this system is clearly a lot more unstable with respect to the one where only B was a random matrix. Furthermore, observing the distributions, we notice that for increasing S the rightmost eigenvalue changes a lot: it is not the same one which increases smoothly in magnitude but instead it hops to different values giving the plot in figure.
Another thing we notice is that while, before the transition, the real part of the eigenvalue has a strong dependence on the delay, for higher S, after the transition value, the magnitude of the delay has a weak influence on the maximal eigenvalue.

2.2.6 Scaling laws of the eigenvalues.

Subsequently, we explore the behavior of the eigenvalues of the system, given by equation (2.15), in some limiting cases or particular ranges, for example: when the argument of the Lambert function $W(z)$ is near zero, when it reaches infinity and most importantly near the transition point where the system changes from stable to unstable.
The reason for this analysis is that it doesn't exist an explicit formula for the Lambert W function .Thus we are able to obtain some "scaling laws" of the eigenvalues with respect to the parameters of the system only in particular cases. For instance when it is possible to get an approximate formula by computing an expansion of the Lambert function.

Different expansions of the Lambert function.

To compute $\lambda(T)$, we need an expansion of the function $W(z)$ near some point z_0. We will use the Lagrange inversion formula which states:

> *Let's consider* $a, z_0 \in \mathbb{C}$ *and assume that* $f(w) = z,\ f(a) = z_0$ *with* $|w-a| < \delta$, $|z - z_0| < \varepsilon$ *for* $\delta, \varepsilon > 0$ *and* $f'(a) \neq 0$*; if* $f(w)$ *is analytic at* $w = a$ *then* $f(w) = f(a) + \sum_{n=1}^{\infty} f_n (w - a)^n$*.*
> *We define now its inverse as* $z \to z_0$ *to be* $g(z) = a + \sum_{n=1}^{\infty} g_n (z - f(a))^n$*.*
> *The goal is to compute the Taylor coefficients* g_n *of the inverse function given that we know the original function* $f(w)$*. Lagrange's theorem shows that the relation between the two of them is the following:*

$$g_n = \frac{1}{n!} \frac{d^{n-1}}{dw^{n-1}} \Big(\frac{w-a}{f(w) - f(a)} \Big)^n \Big|_{w=a} \qquad \text{for} \quad n = 1, 2, \dots$$

Using the result above we are able to compute the power expansion near the point $z = f(w = 0) = 0$ of the inverse function of $f(w) = we^w$ which is the actual definition of the Lambert W function. Indeed we obtain:

$$W(z) = \sum_{n=1}^{\infty} \frac{(-n)^{n-1}}{n!} z^n \quad \text{as } z \to 0 \qquad \text{it converges for } |z| < e^{-1}. \tag{2.19}$$

Next, we are interested on the asymptotic behavior of the eigenvalues in the limit when the argument of the function W go to infinity. We need to know the asymptotic behavior of $W(z)$ as $z \to \infty$. We obviously cannot use the Lagrange inversion formula, because the function is not analytic as $z \to \infty$, therefore we will assume $z \in \mathbb{R}$ and make the following observations:

- $W(z)$ must diverge as $z \to \infty$, otherwise $W(z) = c \;\Rightarrow\; c \cdot e^c < \infty \;\Rightarrow\; z < \infty$.
- $W(z)$ must diverge slower than any power of z, otherwise $W(z) = z^\alpha$ with $\alpha > 0$ gives that $z^\alpha e^{z^\alpha} \to \infty$ faster than any power of z.
- $W(z)$ must diverge also slower than $\ln(z)$, otherwise $W(z) = \ln(z)$ gives that $z \ln(z) \to \infty$ faster than z.

It is possible to show that the asymptotic behavior of $W(z)$ in the limit $z \to \infty$ is:

$$W(z) = \ln(z) - \ln\big(\ln(z)\big) + \frac{\ln\big(\ln(z)\big)}{\ln(z)} + o\left(\frac{\ln\big(\ln(z)\big)}{\ln(z)}\right) \qquad \text{as} \quad z \to \infty. \tag{2.20}$$

Indeed the proof of this result is fairly simple and is presented in pag. 19 of [5]. Finally we notice that using the Lagrange inversion formula with a different approach, similar to the one used in [5], we are able to get an expansion of $W(z)$ near the branching point $z^* = -e^{-1}$. This series has a bigger radius of convergence with respect to the power series expansion (2.19), therefore it is valid both for higher values of z and for z near zero.

$$W(z) = -1 + \varphi(z) + \frac{1}{6}\varphi^2(z) - \frac{1}{72}\varphi^3(z) - \frac{7}{2160}\varphi^4(z) + \frac{7}{5760}\varphi^5(z) + O\big(\,|z + \frac{1}{e}|^3\,\big). \tag{2.21}$$

Where we used the function: $\varphi(z) = \ln\left(1 + \sqrt{2e(z + 1/e)}\right)$.

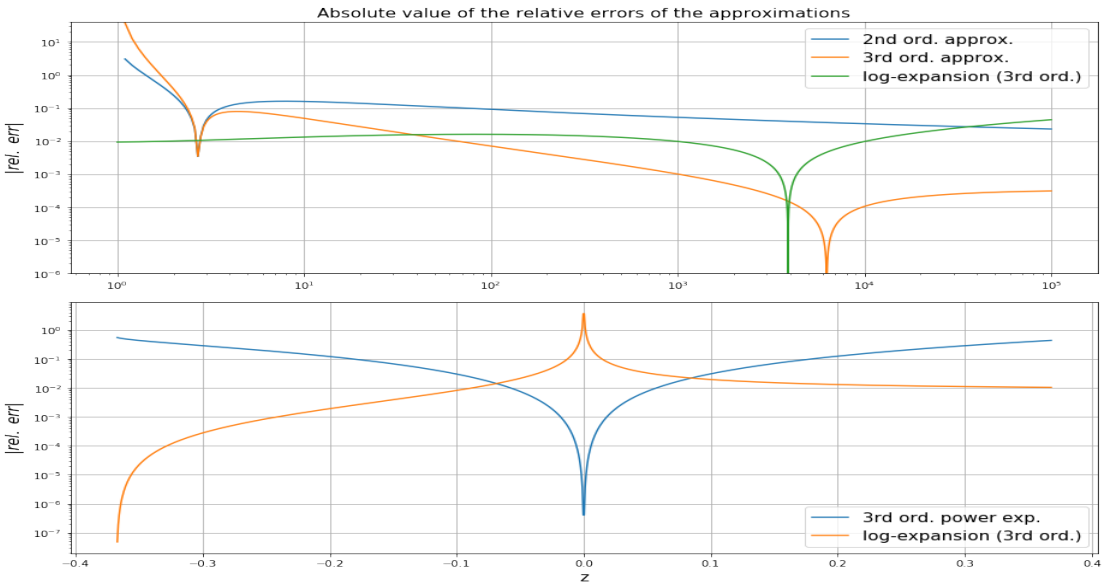

Figure 2.17: *Absolute value of the relative error of each different approximation of $W(z)$ with respect to the real $W(z)$. In the first figure are represented the approximations valid for great values of z which are the 2nd and 3rd order (2.20) and the third order (2.21). In the second there are the approximations of $W(z)$ near $z = 0$, i.e. the 3rd order power expansion (2.19) and again the 3rd order (2.21).*

In figure (2.17) we present the absolute value of the relative error of each series expansion of $W(z)$ with respect to the actual function $W(z)$; we can clearly see in which region each approximation is better than the others. In particular, the power expansion (2.19) is obviously useful only near $z = 0$ while the approximation given by (2.20) is the most precise in the limit $z \to \infty$. The best expansion series to study the transition region (which can happen for different values of z but still small enough ones) is certainly the logarithmic expansion (2.21) near $z = e^{-1}$ because it has a bigger radius of convergence and it describes well the function $W(z)$ both for negative and positive z-values.
Finally we add that the cuspidal points in (2.17), in which the relative error decreases a lot, are just the intersections between the approximations of $W(z)$ and the actual function. Therefore in that case the relative error, as definition, goes to zero.

Scaling of the eigenvalues

The key step now is to decide which expansion we should use. We already studied which one is the best for each range of values of $z \in \mathbb{R}$ in figure (2.17) but we need to find out when the approximation $z \in \mathbb{R}$ is meaningful and when it is not.
First of all we observe that, using the expansion (2.21) instead of the exact expression of $W(z)$ to compute the parameter $\lambda(T)$ from the eigenvalues of A and B, we obtain nearly the same results. Indeed using the third order on φ of the expansion the two results are already indistinguishable one from the other.

Next we want to obtain a scaling law for the eigenvalue with maximal real part, by using some approximation of $W(z)$, as a simple function of the parameters S, C, d, σ, T. We first need to identify which eigenvalues of A and B lead to the total eigenvalue $\lambda(T)$ with maximal real part and this is not always an easy task. For instance in all the cases in which the eigenvalue $\lambda(T)$ with maximal real part is on the real axis (or at least in its vicinity) then we immediately know (numerically) that it is associated to the eigenvalue with maximal real part of the matrix B which is given by the Circular/Elliptical law. However this is not always the case, in other instances the eigenvalue with maximal real part has a non-null imaginary part, for example it could belong to the "wings" of the distribution on the complex plane like we can see in some of the cases with higher delay (or generally in all the predator-prey systems) in figure (2.9).
Thus we will consider now all the cases in which $\max\big(Re[\lambda(T)]\big)$ is on the real axis and then, because $W(z)$ is a monotonic increasing function when $z \in \mathbb{R}$, this is directly associated to the maximal eigenvalue of B:

$$\max\big(Re[\lambda(T)]\big) = a + \frac{1}{T} W\Big(Te^{-aT} \max\big(Re[b]\big)\Big).$$

In the next examples we will use always $\max\big(Re[b]\big) = b_{max} = -d + \sigma\sqrt{SC}$ which is the eigenvalue with maximal real part of the random matrix B in the generic Circular law. We can obviously consider also all the other types of matrices by using for b_{max} the different expressions obtained in the generalization of May's criterion to the

other types of matrices.

First, by substituting the expression obtained in (2.19) into (2.15) we obtain a power expansion, valid for small values of the argument, of the function $\lambda(T)$ which gives the eigenvalues of the system with respect to a, b which are the eigenvalues of the 2 Community matrices:

$$\lambda(T) = a + \sum_{n=1}^{\infty} \frac{(-n)^{n-1}}{n!} b^n T^{n-1} e^{-naT} \qquad \text{for:} \quad |b|T < e^{Re[a]T-1}$$

Given this expansion is possible to study the behavior of the eigenvalues, in particular their real parts, in the limit of small delay when the constraint is always respected. We obtain the first terms of the expansion which are:

$$\lambda(T) = a + be^{-aT} - b^2 T e^{-2aT} + o\big(Te^{-2aT}\big) \qquad \text{for:} \quad |b|T < e^{Re[a]T-1}$$

Now considering that in the case in which $A = 0$ we have $b_{max} = -d + \sigma\sqrt{SC}$ we obtain the following maximal eigenvalue of the system:

$$\max\big(Re[\lambda(T)]\big) = b_{max}\big(1 - b_{max}T + o(b_{max}^2 T^2)\big) \qquad \text{for:} \quad |b_{max}|T < e^{-1}$$

Therefore, knowing that the system is stable when $\max\big(Re[\lambda(T)]\big) < 0$, if the non-delayed system is stable, i.e. $b_{max} < 0$, the system with small delay will always be stable if the condition $|b_{max}|T \ll 1$ is met.

Next, given the equation (2.20), we are able to describe the asymptotic behavior of the eigenvalues of the system, when the size S goes to infinity, by substituting it again in (2.15). First of all we consider the case in which $A = 0$, therefore the eigenvalue with maximal real part (using the third order of the approximation) will be:

$$\max\big(Re[\lambda(T)]\big) = \sim \frac{1}{T}\ln\left(\frac{\sigma T\sqrt{SC}}{\ln\big(\sigma T\sqrt{SC}\big)}\right) + \frac{1}{T}\frac{\ln\big(\ln\big(\sigma T\sqrt{SC}\big)\big)}{\ln\big(\sigma T\sqrt{SC}\big)} \qquad \text{for} \quad S \gg \frac{1}{C}\Big(\frac{1+dT}{\sigma T}\Big)^2$$

Instead, in the case in which $A = -d\mathbb{1}$ and $\max\big(Re[b]\big) = \sigma\sqrt{SC}$ we obtain:

$$\max\big(Re[\lambda(T)]\big) \sim \frac{1}{T}\ln\left(\frac{\sigma T\sqrt{SC}}{dT + \ln\big(\sigma T\sqrt{SC}\big)}\right) + \frac{1}{T}\frac{\ln\big(dT + \ln\big(\sigma T\sqrt{SC}\big)\big)}{dT + \ln\big(\sigma T\sqrt{SC}\big)} \qquad \text{for} \quad S \gg \frac{1}{C}\Big(\frac{e^{-dT}}{\sigma T}\Big)^2$$

Therefore, if the parameters of the system respect the constraint, i.e. the limiting case when the dimension of the matrix is very large, the maximal eigenvalue of the system scales sub-logarithmically, instead of scaling as a power law like in the non-delayed case.

Finally, to describe the transition region in a better way we can use (2.21) where we define:

$$\varphi = \begin{cases} \ln\left(1+\sqrt{2e(\sigma T\sqrt{SC}-dT+1/e)}\right) & \text{when } A=0 \text{ and } b_{max}=-d+\sigma\sqrt{SC} \\ \ln\left(1+\sqrt{2e(\sigma T\sqrt{SC}e^{dT}+1/e)}\right) & \text{when } A=-d\mathbb{1} \text{ and } b_{max}=\sigma\sqrt{SC} \end{cases}$$

Thus we get: $\max\left(Re[\lambda(T)]\right) \sim a + \frac{1}{T}\left(-1+\varphi+\frac{1}{6}\varphi^2-\frac{1}{72}\varphi^3-\frac{7}{2160}\varphi^4+\frac{7}{5760}\varphi^5+\cdots\right)$

Furthermore, if we want to study the scaling of the eigenvalues in all the cases in which the rightmost eigenvalue is not on the real axis we will need first to obtain an expression which describes them in an analytical way in terms of the parameters of the random matrix ($S,\ C,\ \sigma,\ d, \ldots$). This task obviously is not easy and we still don't know a technique to compute them analytically.

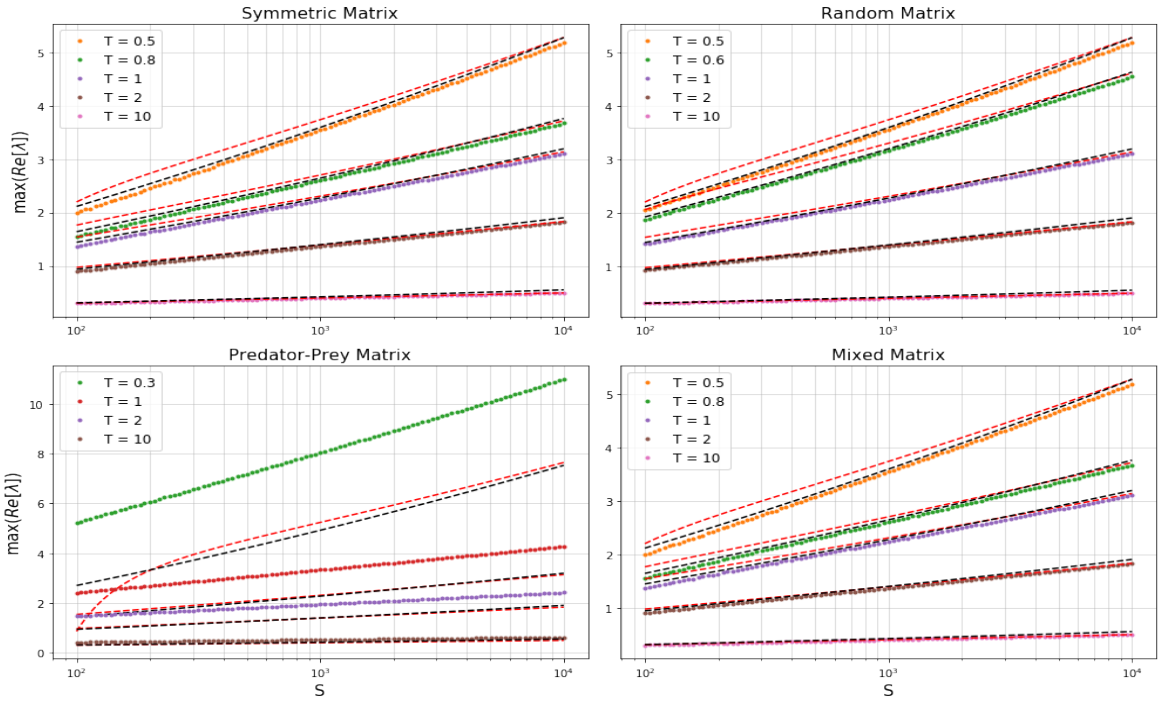

Figure 2.18: *Scaling of the eigenvalue with maximal real part with respect to the dimension S of the matrix in the asymptotic limit. We used a system with $A=0$ and B random matrix with $C=0.5,\ \sigma=1,\ d=1$. In addition we included the asymptotic behaviour predicted by the 2 expansions: the red dashed lines represent (2.20) while the black ones (2.21). We also computed the eigenvalues for different delays T (different colors)*

In figure (2.18) we show the scaling of the real part of the rightmost eigenvalue with respect to the dimensions of the matrix in the limit when the argument of $W(z)$ is high enough, i.e. $z \gg 1$, and the maximal eigenvalue is on the real axis. To study the asymptotic behaviour, which is far from the transition point (in this case is at $S \approx 10$), we have chosen high values of C and σ.
We observe that in this limit the expansion given by (2.21) is still the best one (only for really high values of S the other expansion is better) and more importantly, only for the predator-prey Community matrices, we are not able to describe the scaling of the eigenvalues by using this expansion. Indeed in all other cases the rightmost eigenvalue of the system is always associated to the eigenvalue with maximal real

part of matrix B (which is the one on the real axis) even for high delays. This is due to the fact that when we are far enough from the transition point, and so $b_{max} > 1$, the complex eigenvalues on the "wings" of the distribution are not big enough to surpass the one on the real axis. The predator-prey case, as we already explained, obviously cannot be described through the given expansions because the rightmost eigenvalue is always (even when $b_{max} \gg 1$) associated to an eigenvalue with non-null Imaginary part, which is on the "wings" of the distribution, and we are not able to compute it analytically.

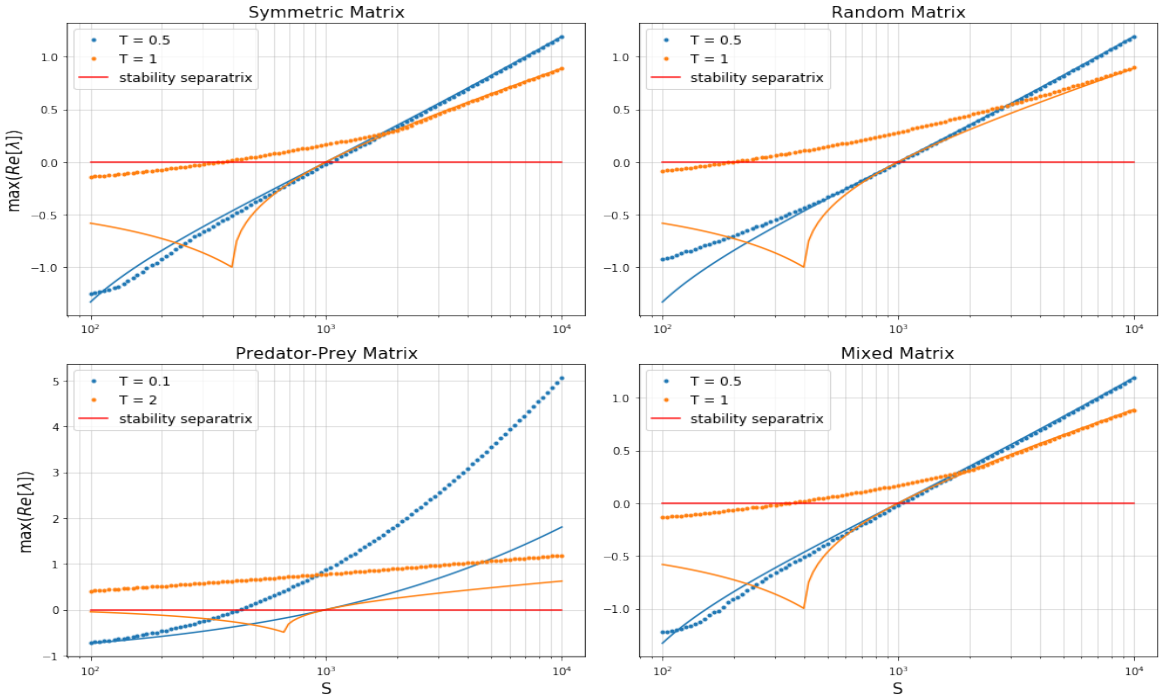

Figure 2.19: *Scaling of the eigenvalue with maximal real part with respect to the dimension S of the matrix near the transition point ($S = 1000$, represented by the red line). We used a system with $A = 0$ and B random matrix with $C = 0.1,\ \sigma = 0.1,\ d = 1$. In addition we included the scaling predicted by the logarithmic expansion (2.21) represented by the solid lines. We computed the eigenvalues for a couple of meaningful delays T (different colors)*

Finally we present in figure 2.19 the scaling of the eigenvalue with maximal real part with respect to the dimensions of the matrix near the transition point (which now is at $S = 1000$ because we have chosen the parameters C, σ, d on purpose).
Again it is evident that the scaling in the predator-prey system cannot be depicted for any delay, using our approximation, for the same reason we explained before. Instead we can notice that for small enough delays the expansion (2.21) is able to capture the scaling of the real part of the rightmost eigenvalue. We verified numerically that this is not true anymore when the delay is large enough (for instance in the orange points) such that the rightmost eigenvalue changes and instead of being on the real axis it becomes one on the "wings" of the distribution which we aren't able to describe analytically. However, when S is big enough, like we have seen in (2.18), the eigenvalue on the real axis become the biggest one and we are again able to describe the scaling of the eigenvalue with our approximation.

2.2.7 *Delay dependent Community matrix*

Analyzing the collection of analytical and numerical results that we obtained in the previous sections, regarding the eigenvalue distribution of the linear delayed system, the most important result that we get is that generally the delay never improves the stability of the ecosystem but instead in many situations it increases its instability. The main empirical and ecological reason for this hindrance to occur is that we are considering delay-independent Community matrices A and B, instead usually the coefficients that connect the various populations inside the ecosystem should also have a strong dependence on the delay. In particular the strength of the interactions between species, i.e. the variance of the distribution from which we sample the entries of the Community matrices, should decrease for increasing values of delay because, as a common empirical evidence, the further an event is in the past the less it should influence the present behavior of the populations.

To include this improvement on the description of the ecosystem we can start from the mathematical perspective and ask ourselves: "Knowing the characteristic equation of our system, how can we make a uniform translation of the λ parameters to the left direction of the real axis such that the system becomes more stable ?".
The answer is easy, we just need to make the following substitution into equation (2.14): $\lambda \to \lambda + c$ with $c \in \mathbb{R}$ and analyze how this, for a given parameter c, changes the distribution of eigenvalues.
We obtain indeed a different characteristic equation which depends also on the new parameter c (if $c > 0$ then the eigenvalues are shifted to the left, otherwise they are shifted to the right):

$$\lambda\vec{v} \;=\; (A - c\mathbb{1})\vec{v} \;+\; e^{-\lambda T}(e^{-cT}B)\vec{v} \quad \Leftrightarrow \quad det\big((A - c\mathbb{1}) + e^{-\lambda T}(e^{-cT}B) - \lambda\mathbb{1}\big) \;=\; 0.$$

Moreover, to get a uniform translation of the eigenvalues of our system we just need to shift their average by adding a constant value $-c$ to the diagonal of matrix A and then multiplying the Community matrix B by a damping factor which decreases for increasing delays. This operation is perfectly in line with what we had supposed previously from the empirical observations.

Therefore, if we consider now a more generic dependence of the Community matrix B on the delay parameter, we can characterize it just by making the substitution: $B \to f(T)B$ where $f(T)$ is a decreasing positive function of the delay T (it could even be an $(S \times S)$ matrix with each coefficient decreasing for increasing delay). The effect of this scalar multiplicative factor is purely on the variance of matrix B, in fact if $B_{i,j} \sim P(0, \sigma)$ then, from the definition of random variables $f(T)B_{i,j} \sim P(0, f(T)\sigma)$. Therefore we simply decrease the strength of the interactions when the delay increases, this is exactly what we supposed on our empirical observations.
For example, if we choose again $f(T) = e^{-cT}$ and we add $-c\mathbb{1}$ to matrix A we get an exact shift of the eigenvalues of the system as we can clearly see from the next

equation and as we have shown in figure (2.20):

$$\lambda_0 = a + \frac{1}{T}W(bTe^{-aT}) \qquad \longrightarrow \qquad \lambda_{shift} = a - c + \frac{1}{T}W(bTe^{-cT}e^{-(a-c)T}) = \lambda_0 - c.$$

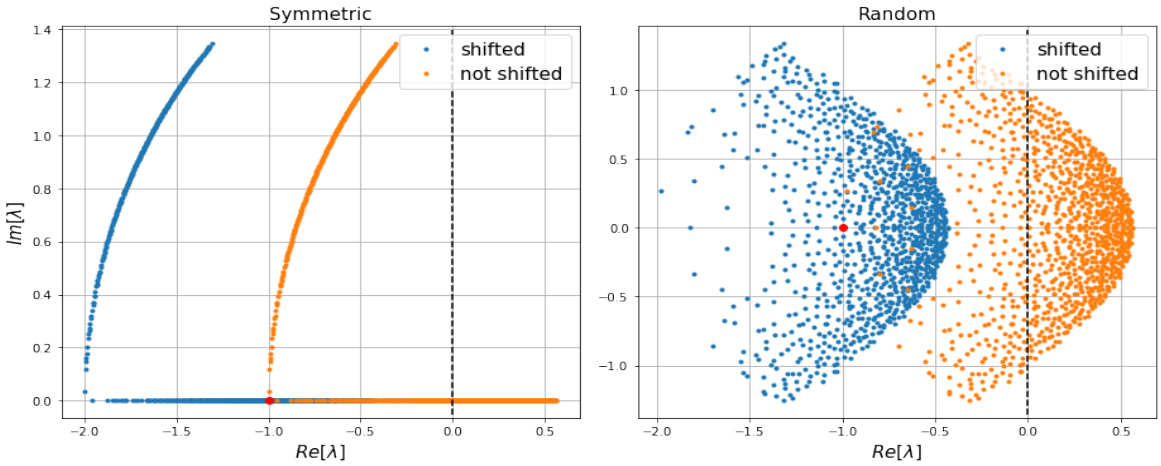

Figure 2.20: *Distributions of the eigenvalues of the system with the shifting function* $f(T)$ *and without it. We have set* $A = -\mathbb{1}$, $f(T) = e^{-T}$ *with* $T = 1$ *and* B *is a random matrix with entries sampled from a distribution with zero mean and with:* $S = 1000,\ C = 0.1,\ \sigma = 0.1,\ d = 0$.

Numerical examples

In addition, we will now present some numerical examples of the distribution of eigenvalues of the system: $\dot{\vec{x}} = A\vec{x}(t) + f(T)B\vec{x}(t-T)$ in which, as stated above, $f(T)$ is a positive monotonically decreasing function of the delay T.

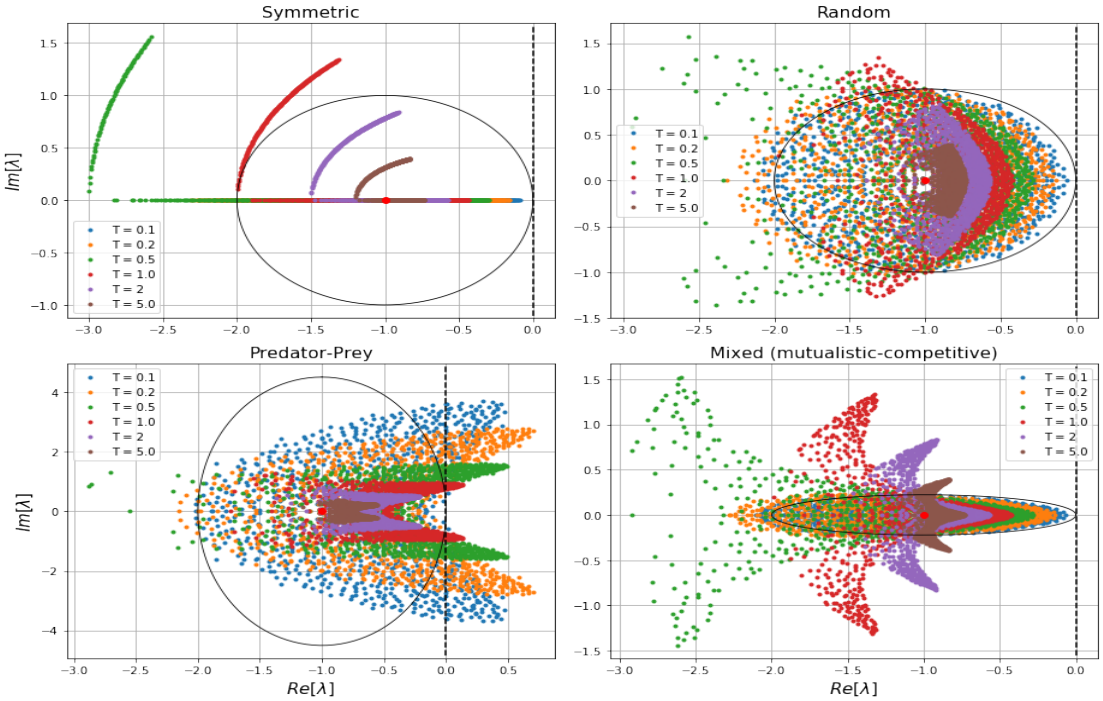

Figure 2.21: *Distributions of the eigenvalues of the system with* $A = -c\mathbb{1}$, $f(T) = e^{-cT}$ *with* $c = 1$ *and where* B *is a random matrix of the 4 different types in the titles with entries sampled from a distribution with zero mean and with:* $S = 1000,\ C = 0.1,\ \sigma = 0.1,\ d = 0$. *We also computed the eigenvalues for different delays* T *(different colors).*

Comparing figure (2.21) with the eigenvalues of the original delayed system (without the $f(T)$ term) represented in figure (2.9) we can see clearly that the effect of the damping term $f(T)$ on the eigenvalue distribution of the matrix, for increasing values of the delay, is to actually shift it to the left part of the complex plane and consequently stabilize the system. We have chosen $A = -c\mathbb{1}$ and $f(T) = e^{-cT}$ which gives, as we have seen before, an exact shift without deformation of the eigenvalue distribution. This is not a compulsory choice, in fact any positive monotonically decreasing function of the delay T would have had the same effect, the only difference is a slight deformation of the eigenvalue distribution for different types of $f(T)$.

Furthermore, in figure (2.22) we can observe the effect of different damping functions $f(T)$ on the distributions of the eigenvalues. Depending on the form of f the resulting distributions are all shifted to the left some more and some less than the others, also their "shape" is deformed in different ways. Therefore we conclude that if the damping function $f(T)$ is a monotonic decreasing function of the delay the effect on the distribution of the eigenvalues is somehow universally the same because it always shift them to the left increasing the stability of the system.

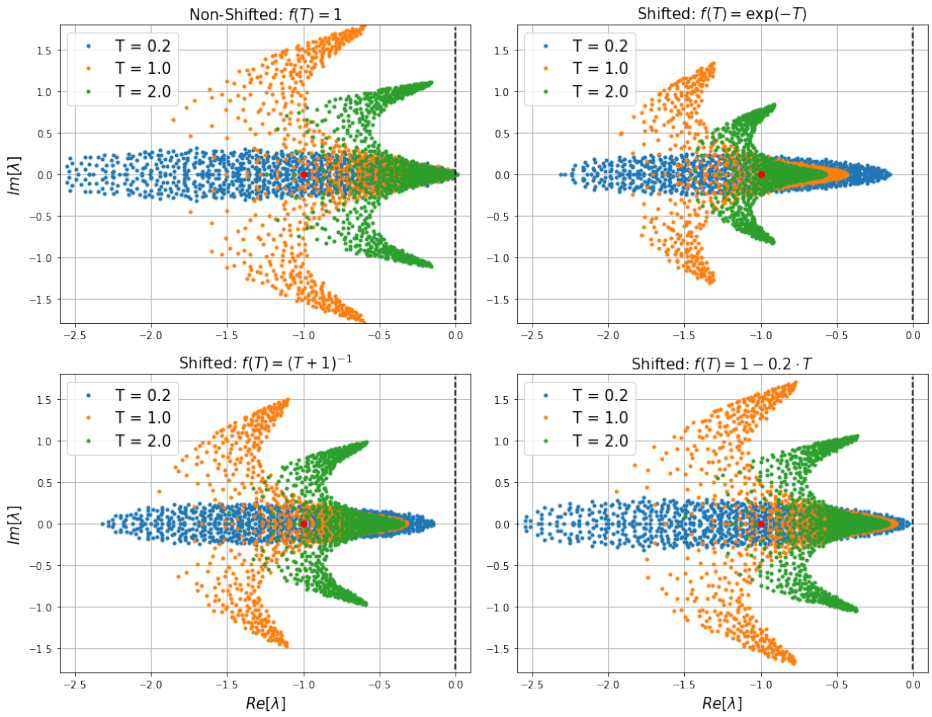

Figure 2.22: *Distributions of the eigenvalues of the system with $A = -\mathbb{1}$, different damping functions $f(T)$, and where B is a random matrix of the Mixed type with entries sampled from a distribution with zero mean and with: $S = 1000,\ C = 0.1,\ \sigma = 0.1,\ d = 0$. We computed the eigenvalues for different delays T (different colors).*

Finally in figure (2.23) we show how the rightmost eigenvalue of the system increases as a function of S. This time the matrix B is not delay-independent anymore, instead, like in the previous figures, we included the dependence on the delay using the damping function $f(T)$.
We observe that the insertion of the delay inside the equations which describe the ecosystem has now a stabilizing effect. Indeed the transition between stability and

instability, if we increase the value of the delay, happens for larger dimensions S of the ecosystem with respect to the non-delayed case. The rightmost eigenvalue of the system, in fact, grows slower for larger values of delay T.
The predator-prey system makes again an exception because of the particular shape of the eigenvalue distribution, but still we observe that, when the delay is high enough, the system is again more stable than the non-delayed case.

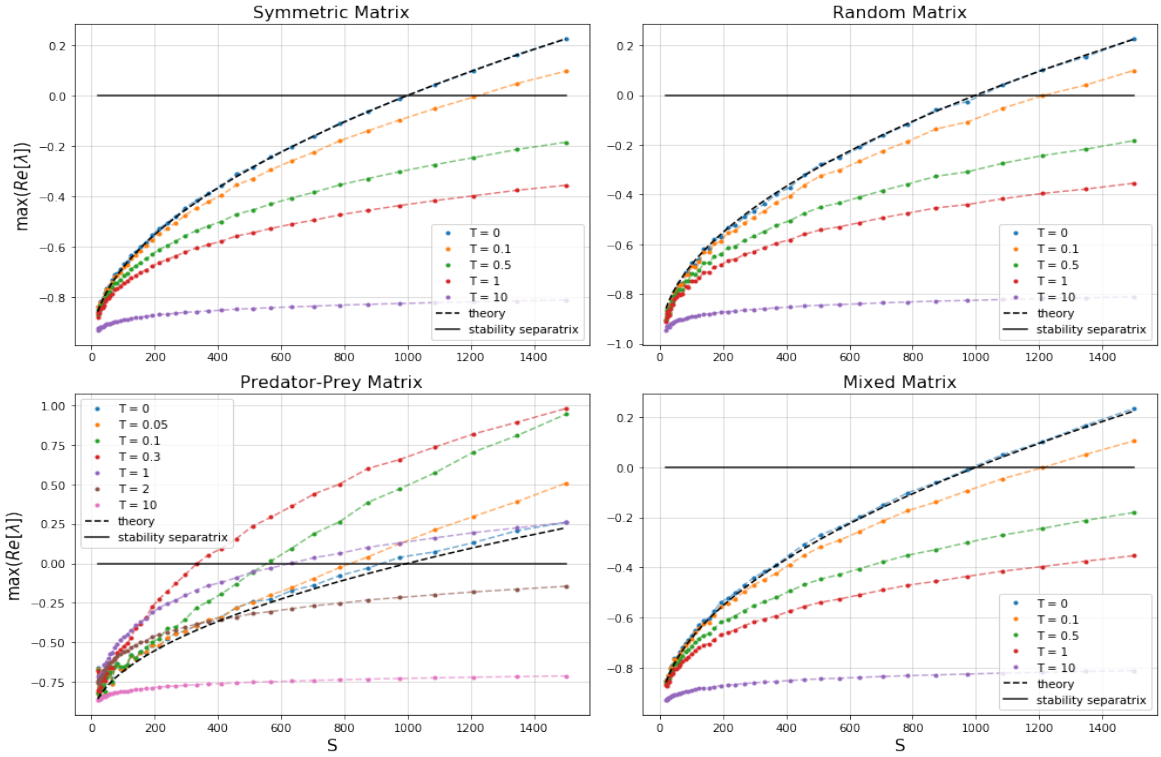

Figure 2.23: *Maximal real part of the eigenvalues of the system vs. size of the matrices; with* $A = -c\mathbb{1}$, $f(T) = e^{-cT}$ *with* $c = 1$ *and where* B *can be the 4 different types of random matrices with entries sampled from a distribution with zero mean and:* $C = 0.1,\ \sigma = 0.1\gamma,\ d = 0$ *; here we have again* $\gamma = \left(\ 1/\sqrt{2},\ 1,\ \pi/(\pi-2),\ \pi/(\pi+2)\ \right)$*. We computed the eigenvalues for different delays* T *(different colors); also the black dashed line represent the distribution of eigenvalues in the non-delayed case while the black solid line the transition point.*

2.2.8 Transition curves

In this final section we show some figures which represent the transition surfaces for the delayed system. In this case the parameter space is the 2 dimensional space of S and T, thus the separatrix is a line instead of a proper surface. Indeed, here we have computed, for different values of the delay, the precise value of the size S of the ecosystem, such that it undergoes the transition changing from stable to unstable. Thus, in the following plots all the points of the plane, i.e. the pairs (S, T), that are below each line, represent a set of parameters that give a stable ecosystem. Instead, the points above it have a positive real part of the rightmost eigenvalue and give unstable solutions.

In figure (2.24) we show the transition curves for the delayed system of equations in which $A = 0$ and the only Community matrix is the Random Matrix B (independent on the delay). First of all, the size S at which the non-delayed system undergoes the

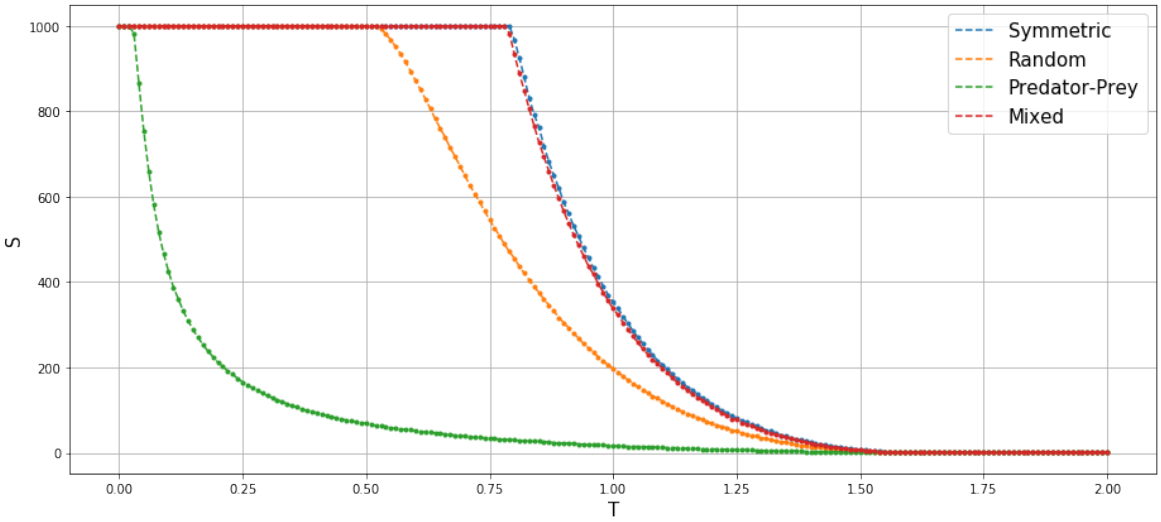

Figure 2.24: *Transition curves for the system with $A = 0$ and B a random matrix of the 4 types. We show the relation between the size S at which the phase transition happens and the delay T of the system. In all the plots we fixed the parameters $C = 0.1,\ \sigma = 0.1,\ d = 1$ and took the average over 100 randomizations.*

transition is chosen to be $S = 10^3$ for all the cases.
Another remarkable thing, is that the Symmetric and the Mixed case have the same transition curves. For both of them the transition-value of the size S remains the same as the non-delayed case until it starts to decrease steeply at the exact value of delay when the eigenvalues on the "wings" of the distributions pass through the imaginary axis destabilizing the ecosystem. In the generic random case instead, the size S starts to decrease for smaller delays more smoothly. The smoothness of this last transition is due to the absence of eigenvalues with non-zero imaginary part which pass the imaginary axis and destabilize the system becoming the rightmost eigenvalue. In fact, now the destabilization is caused by the rightmost eigenvalue on the real axis which shifts to the right for increasing delays. Finally we observe that the transition-value of the size of predator-prey systems starts to decrease already for any $T > 0$ and does it in a steeper way, as we already observed in the previous section.
We will not show here the transition curves of the delayed system with $A = -\mathbb{1}$ and B Random Matrix because we have already seen that the distributions remain formally the same for the predator-prey system while, for the other 3 types, the transition point doesn't change. Therefore, in that case, the curves are just horizontal lines.

In figure (2.25) we show the transition separatrices for the delayed system in which we considered a delay dependence of the Community matrix B.
We observe that the presence of the damping term $f(T) = e^{-T}$ multiplied by the Community matrix changes completely the behavior of the stability-zone in the parameter space. Before in fact the surface below the curves was finite and decreasing for increasing delays, now, when the delay increases, the area underlying the curves is not finite anymore. Indeed we observe that, if the delay is large enough, the transition-values of the size S start to grow exponentially as a function of the delay T (by making a plot with S in logarithmic scale in fact we obtain straight lines).

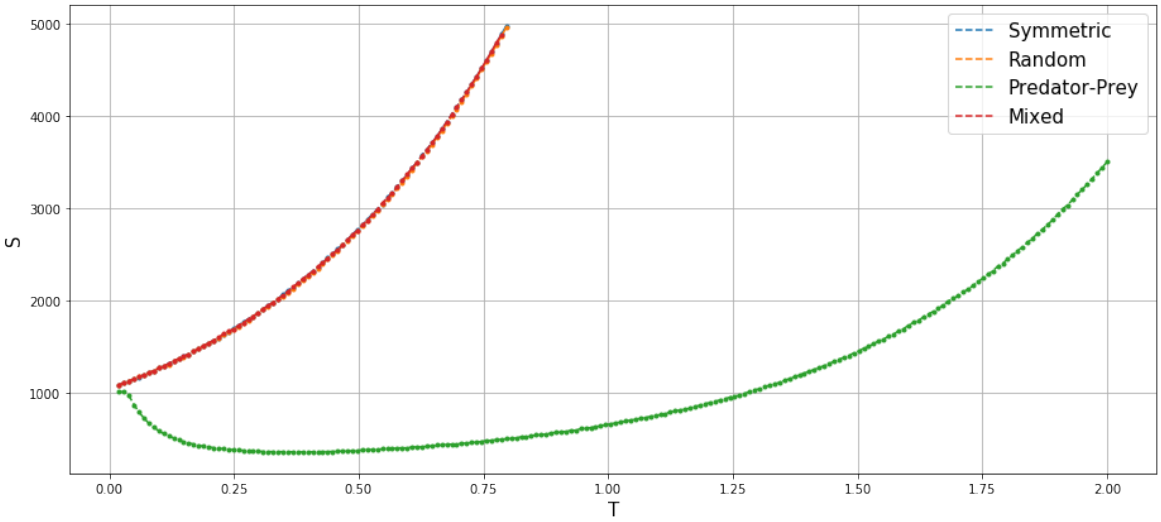

Figure 2.25: *Transition curves for the system with $A = 0$ and B a random matrix of the 4 types multiplied to $f(T) = e^{-T}$. We show the relation between the size S at which the phase transition happens and the delay T of the system. In all the plots we fixed the parameters $C = 0.1,\ \sigma = 0.1,\ d = 0$ and took the average over 100 randomizations.*

We notice also another fundamental thing: in this case the different types of matrices, with exception of the predator-prey one, have all the same behavior, in fact the transition-value of S has exactly the same exponential dependence on T. The predator-prey system instead, for its characteristic construction, is again destabilized for small values of the delay. However when the delay is large enough the exponential factor $f(T)$ is strong enough to stabilize the system and consequently the transition-value of S starts to grow exponentially on the delay like the other cases.
In conclusion, this characteristic behavior of the transition curves of the ecosystems with delay-dependent Community matrices is definitely a feature worth of further studies. In particular, an interesting future development could be to characterize the relation between the transition curves and the damping factor $f(T)$.

CHAPTER 3

CONCLUSIONS

The results that we have obtained in this Dissertation show that the presence of delayed terms in the equations of the dynamics of ecosystems has an important impact on the behavior of the populations. This is a fundamental ingredient which should be taken into consideration in the Complexity-Stability debate.

The first thing that we observe from the results is that in Few-species dynamical systems, like the Logistic and the Lotka-Volterra ones, the delay strongly influences the stability. Indeed often, for large enough values of T, solutions that are stable in the non-delayed case are not stable anymore in the delayed one. This is a direct consequence of the Höpf (or Neimark-Sacker) bifurcation, in the parameter T, which the system undergoes.
Moreover, when the delay doesn't destabilize the solutions, it increases the variability giving rise for instance to chaotic (and then aperiodic) oscillations; this is clear when comparing the bifurcation diagrams of non-delayed and delayed systems.
For these type of DDEs there are already a lot of studies in the literature and there is little space for improvement on our knowledge of their behavior. Probably one of the topics that could be explored more rigorously is whether the presence of the delay can stabilize solutions which otherwise would be unstable. In our analysis we discovered that generally the delay cannot stabilize solutions which are already unstable at $T = 0$. However there exist some particular exceptions, like, for instance, some cases when the Community matrix of the Lotka-Volterra system is Cooperative $(++)$ and has particular values of the off-diagonal terms.

Subsequently, regarding delayed Multi-species ecosystems described by random matrix techniques, we obtained some original and fairly unexpected results.
First of all, we noticed that the use of delayed terms in our description changes completely the distribution of the "effective" eigenvalues $\lambda(T)$ and therefore the stability of the whole ecosystem. Generally what we observe is that the delay does

not destabilize the ecosystem if T is small enough. However, when it reaches some threshold value, there is a Höpf bifurcation and the rightmost eigenvalue crosses the Imaginary axis, destabilizing the system.
Furthermore something that could need further study is the technique used to compute the effective eigenvalues of the linearized system with both A and B Random matrices. Indeed the technique that we proposed gives completely different distributions if we use eigenvectors of one matrix instead of the ones of the other, this result still does not have an explanation.
Moreover, another topic which should be studied more precisely is whether it exists some analytical technique to compute which eigenvalue of the Community matrix B leads to the rightmost "effective" eigenvalue λ. Knowing it, we would be able to predict, analytically, how the rightmost eigenvalue of a delayed ecosystem scales with respect to the parameters (ex. S, C, $\sigma, \dots$) in all the possible cases and therefore infer its stability. In fact, right now we are able to do this only for a subset of all the cases, i.e. when $T < T_{tr}$.

Finally, the most promising result that we have obtained is how the delay, expressed in a particular way, can stabilize ecosystems which would be unstable otherwise. Indeed we discovered that, when the Community matrix depends on the delay (decreasing its variance for increasing delays), unstable systems can become stable. This is our most important contribution to the Complexity-Stability debate.

Bibliography

[1] J. T. Carlton A. Cohen. Accelerating invasion rate in a highly invaded estuary. *Science*, 279:555–558, 1998.

[2] J. B. Rasmussen A. Ricciardi. Extinction rates of north american freshwater fauna. *Conserv. Biol.*, 13:1220–1222, 2000.

[3] R. Bellman and K.L. Cooke. *Differential-Difference equations*. Mathematics in Science and Engineering 6. Academic Press, 1963.

[4] J. Galeano et al. Rethinking the logistic approach for population dynamics of mutualistic interactions. *Journal of Theoretical Biology*, 363:332–343, 2014.

[5] R. M. Corless et al. On the lambert w function. *Adv Comput Math*, 5:329–359, 1996.

[6] M.J. Feigenbaum. Quantitative universality for a class of nonlinear transformations. *J. Stat. Phys.*, 19:25–252, 1978.

[7] P. Vivo G. Livan, M. Novaes. *Introduction to Random Matrices*. SpringerBriefs in Mathematical Physics 26. Springer, 2018.

[8] K. Gopalsamy. *Stability and Oscillations in Delay Differential Equations of Population Dynamics*. Mathematics and Its Applications 74. Springer, 1992.

[9] S. O'Rourke H. Nguyen. The elliptic law. *International Mathematics Research Notices*, 2015:7620–7689, 2015.

[10] A. J. Lotka. Elements of physical biology. *Nature*, 116, 1925.

[11] R. MacArthur M. Rosenzweig. Graphical representation and stability conditions of predator-prey interaction. *American Naturalist*, 97:209–223, 1963.

[12] T. R. Malthus. *An Essay on the Principle of Population as It Affects the Future Improvement of Society, with Remarks on the Speculations of Mr. Godwin, M. Condorcet, and Other Writers*. J. Johnson, 1798.

[13] Robert M. May. Will a large complex system be stable? *Nature*, 238(5364):413–414, 1972.

[14] K. S. McCann. The diversity-stability debate. *Nature*, 405:228–233, 2000.

[15] J.D. Murray. *Mathematical Biology I. An Introduction*. Interdisciplinary Applied Mathematics. Springer, 2002.

[16] S.C. Maitra N.S. Goel and E.W. Montroll. On the volterra and other nonlinear models of interacting populations. *Reviews of Modern Physics*, 43(2 part 1):231–276, 1971.

[17] S. Tang S. Allesina. Stability criteria for complex ecosystems. *Nature*, 483:205–208, 2012.

[18] S. Tang S. Allesina. The stability–complexity relationship at age 40: a random matrix perspective. *Popul Ecol*, 57:63–75, 2015.

[19] D Childers S. Millers. *Probability and random processes*. Academic Press, 2012.

[20] A. Maritan S. Suweis, J. Grilli. Disentangling the effect of hybrid interactions and of the constant effort hypothesis on ecological community stability. *Oikos*, 123:525–532, 2014.

[21] L. E. Sigler. *Fibonacci's Liber Abaci: A Translation into Modern English of Leonardo Pisano's Book of Calculation*. Springer, 2002.

[22] H. Smith. *An Introduction to Delay Differential Equations with Applications to the Life Sciences*. Applied Mathematics. Springer, 2011.

[23] J. C. Sprott. *Chaos and Time-Series Analysis*. Oxford University Press, 2003.

[24] V. Vu T. Tao and M. Krishnapur. Random matrices: universality of esds and the circular law. *Ann Probab*, 38:2023–2065, 2010.

[25] P. F. Verhulst. Recherches mathématiques sur la loi d'accroissement de la population. *Nouveaux Mémoires de l'Académie Royale des Sciences et Belles-Lettres de Bruxelles*, 18:1–42, 1845.

[26] C.H. Zhang X.P. Yan. Hopf bifurcation in a delayed lokta–volterra predator–prey system. *Nonlinear Analysis: Real World Applications*, 9:114–127, 2008.

[27] F. Zhang. *The Schur Complement and Its Applications*. Numerical Methods and Algorithms 4. Springer, 2005.